Growth, photophysiology and photosynthesis of two marine diatoms grown under predictable intra-diel light fluctuations

William Passfield

A thesis submitted for the degree of Doctor of Philosophy in Marine Biology

Department of Biological Sciences

University of Essex

February 2019

Abstract

Natural diatom populations experience variability in irradiance because of several physical processes. Laboratory studies often neglect this and use a static light environment. Consequently, the way dynamic light environments impact growth and photophysiology of diatoms is poorly understood. To address this, several aspects of photophysiology were measured in the diatoms *Thalassiosira pseudonana* and *Phaeodactylum tricornutum* when grown under square-wave (SQ), sinusoidal (SI), and low (LF) and high (HF) amplitude light fluctuations of a 1-hour period each with the same light dose.

Acclimation to increasing light fluctuation amplitude was found to be functionally similar to high light acclimation. Chlorophyll-*a* specific light absorption coefficients, maximum photosystem II electron transport rates (ETR) and the capacity for non-photochemical quenching (NPQ) all increased from SI to HF cultures.

In both species increasing light fluctuation amplitude reduced growth rate. This reduction was greater for *T. pseudonana* than *P. tricornutum.* In HF cultures growth rates were 50% and 62% of those in SQ cultures respectively for the two species. Similar daily ETR between SI and LF cultures of *P. tricornutum* suggested that differences in the photosynthetic efficiency of light utilisation were a poor explanation for the lower growth rates in LF

cultures. Lower growth rate under fluctuating light was instead hypothesised to be caused by greater photodamage and energy investment in photoprotection.

Higher NPQ in *P. tricornutum* reduced net photodamage compared with *T. pseudonana*. However, light harvesting and ETR in *P. tricornutum* appeared to be adapted to a lower light environment than *T. pseudonana*. Higher amplitude light fluctuations also decreased intradiel variability in photoacclimation. This response was greater in *P. tricornutum* and was responsible for this species ability to maintain a consistent daily ETR between SI and LF regimes. This is thought to give *P. tricornutum* a competitive advantage in more dynamic light environments.

Acknowledgements

Firstly, I would like to thank both my supervisors Prof. Richard Geider and Prof. Tracy Lawson. They have provided consistent guidance throughout my PhD when I needed it. Their continual input and support have been instrumental in completing this project. Thanks also to NERC, for funding my PhD.

I am very grateful to the people who have provided support during the experimental part of this project. In particular Dr. Phil Davey, Tania Cresswell-Maynard, Dr Dima Svistunenko, John Green and Dr Dawn Rose. All of whom have provided invaluable technical expertise and knowledge, without which this project could not have been completed. Thanks also to Kevin Oxborough for providing some of the equipment used in this project. I would also like to thank James Fox, Victor Figueroa, and Phil Siegel for working alongside me in the lab, and for acting as a sounding board for many of my ideas.

Last, but by no means least, I am extremely thankful to my friends and family for supporting me emotionally, and occasionally providing much needed distractions during my PhD. I am particularly grateful to my parents, who have put up with me uncomplainingly, and supported me financially, as I wrote and re-wrote this thesis.

Contents

Table I. Table of Abbreviations. Definitions of common abbreviations used in this thesis.

Abbreviation	Definition
ANOVA	Analysis of variance
ATP	Adenosine triphosphate
CDF	Cumulative distribution function
DD- DT	Diadinoxanthin- diatoxanthin cycle
ETR	Electron transport rate (of PSII photochemistry)
FRRF	Fast repetition rate fluorometry
HF	High fluctuations ($\frac{z_{mix}}{z_{eu}} = 1$)
HL	High light (273 µmol m^{-2} s^{-1} mean irradiance)
ICAM	Integrating cavity absorption meter
LED	Light emitting diode
LF	Low fluctuations ($\frac{z_{mix}}{z_{eu}} = 0.5$)
LL	Low light (185 µmol m^{-2} s^{-1} mean irradiance)
NADP+	Nicotinamide adenine dinucleotide phosphate
NPQ	Non-photochemical quenching
NSV	Normalised Stern-Volmer coefficient
OLC	Oxygen light curves
PAR	Photosynthetically active radiation (400-700 nm)
PDF	Probability density function
P-I	Photosynthesis-irradiance (response curve)
PQ	Plastoquinone pool
PSII	Photosystem II
PTFE	Polytetrafluoroethylene
PTOX	Plastoquinone terminal oxidase
Q_A	PSII primary electron acceptor
Q_B	PSII secondary electron acceptor
RCII	PSII reaction centres
ROS	Reactive oxygen species
RUBISCO	Ribulose-1,5-bisphosphate carboxylase/oxygenase
SI	Sinusoidal
SQ	Square-wave
SV	Stern-Volmer coefficient
VAZ	Violaxanthin- antheraxanthin-zeaxanthin cycle
VIF	Variance inflation factor

Table II. Table of symbols. Definitions of symbols used throughout this thesis in order of appearance. Symbols are grouped according to the sets of equations they pertain to.

Symbol	Definition	Units	Group of equations
I_M	Maximum irradiance	µmol m^{-2} s^{-1}	Light regime
LP	Light period/photoperiod	hours	Light regime
Z_{rel}	Mixing depth relative to euphotic depth	m	Light regime
$\frac{z_{mix}}{z_{eu}}$	Mixing depth relative to euphotic depth	dimensionless	Light regime
MP	Mixing period	hours	Light regime
$\bar{I}$	Mean irradiance	µmol m^{-2} s^{-1}	Light regime
I_{Med}	Median irradiance with respect to time	µmol m^{-2} s^{-1}	Light regime
I_{Med}^{D}	Median irradiance with respect to dose	µmol m^{-2} s^{-1}	Light regime
D	Light dose		Light regime
I	Irradiance	µmol m^{-2} s^{-1}	Light regime
$p(I)$	PDF of I within the photoperiod	n/a	Light regime
$P(I)$	CDF of I within the photoperiod	n/a	Light regime
D_{sq}	Light dose in a square-wave light regime	µmol m^{-2} s^{-1}	Light regime
$d(I)$	PDF of I within the light dose	n/a	Light regime
$D(I)$	CDF of I within the light dose	n/a	Light regime
μ	Growth rate	d^{-1}	Growth rate
$[chl]$	Chlorophyll-*a* concentration	mg m^{-3} or µg L^{-1}	Absorption coefficient
A'	Absorbance measured in an ICAM spectrophotometer	dimensionless	Absorption coefficients
A	Absorbance measured over a 1 cm pathlength	cm^{-1}	Absorption coefficients
a_0	Coefficient of ICAM absorbance correction	dimensionless	Absorption coefficients
a_1	Coefficient of ICAM absorbance correction	dimensionless	Absorption coefficients
λ	Wavelength	nm	Absorption coefficients
$a(\lambda)$	Absorption coefficient at wavelength λ	m^{-1}	Absorption coefficients
a^{chl}	Chlorophyll-*a* specific absorption coefficient	m^2 mg chl^{-1}	Absorption coefficients

Table II (continued).

$E(\lambda)$	Irradiance at wavelength λ	µmol m^{-2} s^{-1}	Absorption coefficients
$\bar{a}^{chl}$	Spectrally weighted chlorophyll-a specific absorption coefficient	m^2 mg chl^{-1}	Absorption coefficients
F_o	Dark acclimated PSII minimum fluorescence	arbitrary units	PSII photochemical efficiency
F_m	Dark acclimated PSII maximum fluorescence	arbitrary units	PSII photochemical efficiency
F_v	Dark acclimated PSII variable fluorescence ($F_m - F_o$)	arbitrary units	PSII photochemical efficiency
$\frac{F_v}{F_m}$	Maximum photochemical efficiency of PSII	dimensionless	PSII photochemical efficiency
σ_{PSII}	Dark acclimated PSII effective cross section	nm^2	PSII photochemical efficiency
F'	PSII initial fluorescence under actinic light	arbitrary units	PSII operating efficiency
F'_m	PSII maximum fluorescence under actinic light	arbitrary units	PSII operating efficiency
$\sigma_{PSII}{}'$	PSII effective cross section under actinic light	nm^{-2}	PSII operating efficiency
F'_q	PSII variable fluorescence under actinic light ($F'_m - F'$)	arbitrary units	PSII operating efficiency
$\frac{F'_q}{F'_m}$	PSII photochemical efficiency under actinic light	dimensionless	PSII operating efficiency
ETR	PSII electron transport rate	µmol e^- mg chl^{-1} s^{-1}	PSII ETR
$\bar{a}^{chl}_{act}$	Chlorophyll-*a* specific absorption coefficient spectrally weighted to FRRF and OLC actinic LEDs	m^2 mg chl^{-1}	PSII ETR
ETR_{max}	Light-saturated maximum PSII ETR	µmol e^- mg chl^{-1} s^{-1}	PSII ETR
I_k	Saturation irradiance of PSII ETR	µmol m^{-2} s^{-1}	PSII ETR
b	Curvature parameter of the ETR-irradiance relationship	dimensionless	PSII ETR
α	Initial slope of the ETR-irradiance relationship	µmol e^- [µmol phot]$^{-1}$ m^2 [mg chl]$^{-1}$	PSII ETR
A_e	Absorption efficiency. Ratio of two spectrally weighted chlorophyll-*a* absorption coefficients	dimensionless	Spectral corrections

Table II (continued).

F_0'	PSII minimum fluorescence under actinic light	arbitrary units	NPQ
ΔNSV	Maximum increase in NSV	dimensionless	NPQ
NSV_0	Minimum NSV (often referred to as minimum NPQ)	dimensionless	NPQ
I_{50}	Saturation irradiance for NSV	µmol m^{-2} s^{-1}	NPQ
n	Curvature parameter of the NSV-irradiance response	dimensionless	NPQ
NSV_{max}	Maximum NSV (often referred to as NPQ capacity)	dimensionless	NPQ
P_{gross}	Gross O_2 evolution by photosynthesis	µmol O_2 mg chl^{-1} s^{-1}	OLC
P_n	Net O_2 evolution by photosynthesis	µmol O_2 mg chl^{-1} s^{-1}	OLC
R	O_2 consumption by respiration in the dark	µmol O_2 mg chl^{-1} s^{-1}	OLC
P_{max}	Maximum gross O_2 evolution by photosynthesis	µmol O_2 mg chl^{-1} s^{-1}	OLC
${I_k}^{O_2}$	Saturation irradiance for gross O_2 evolution	µmol m^{-2} s^{-1}	OLC
b^{O_2}	Curvature parameter for the P-I response measured by O_2 evolution	dimensionless	OLC
α^{O_2}	Initial slope of the P-I response measured by O_2 evolution	µmol O_2 [µmol phot]$^{-1}$ m^2 [mg chl]$^{-1}$	OLC
n_{PSII}	PSII photosynthetic unit size	mol RCII [mol chl]$^{-1}$	PSII unit size
$\bar{a}_{PSII}^{chl}$	Chlorophyll-*a* specific light absorption by PSII	m^2 mg chl^{-1}	PSII unit size
$\bar{a}_{FRRF}^{chl}$	Chlorophyll-a specific absorption coefficient spectrally weighted to FRRF excitation LEDs	m^2 mg chl^{-1}	PSII unit size
P_{80}^{I}	80th percentile for the CDF of I within the photoperiod	µmol m^{-2} s^{-1}	
k_i	Rate constant for PSII photodamage	$hour^{-1}$	Photodamage and repair
$F_v/F_{m_{LIN}}$	F_v/F_m measured under gross photoinhibition in the Ragni model	dimensionless	Photodamage and repair

Table II (continued).

$GPiR$	Rate constant for gross photodamage according to the Ragni model	hour^{-1}	Photodamage and repair
$NPiR$	Rate constant for net photodamage according to the Ragni model	hour^{-1}	Photodamage and repair
RR	Rate of PSII repair in the Ragni model	hour^{-1}	Photodamage and repair
k_r	Rate constant for PSII repair	hour^{-1}	Photodamage and repair
$[RCII_i]$	Concentration of damaged PSII reaction centres	undefined	Photodamage and repair
$[RCII_f]$	Concentration of functional PSII reaction centres	undefined	Photodamage and repair
$RCII_i$	Fraction of damaged PSII reaction centres	dimensionless	Photodamage and repair
$RCII_f$	Fraction of functional PSII reaction centres	dimensionless	Photodamage and repair
k_r^{max}	Maximum k_r assuming Michaelis-Menten kinetics as a function of k_i	hour^{-1}	Photodamage and repair
k_i^M	Michaelis constant for k_r assuming Michaelis-Menten kinetics as a function of k_i	hour^{-1}	Photodamage and repair
q_p	Coefficient of PSII photochemical quenching	dimensionless	Target for PSII photodamage
σ_i	Functional target for photodamage	m^2 mol phot^{-1}	Target for PSII photodamage
$\frac{\sigma_{PQ}{}'}{\sigma_i}$	Photochemical charge separations per photodamage incident at PSII	e$^-$	Target for PSII photodamage
Γ	Any parameter indicative of photoacclimation	undefined	

1. Introduction

1.1. Phytoplankton in a dynamic environment

Phytoplankton form the base of almost all marine food webs, and, despite accounting for only approximately 1% of the total global photosynthetic biomass (Falkowski, 1994), are responsible for as much as 50% of the global net primary production (Behrenfeld *et al*., 2001; Field *et al*., 1998). Marine phytoplankton also play a vital role in several biogeochemical cycles, for example the phosphorus cycle (Paytan and McLaughlin, 2007) and the nitrogen cycle (Gruber, 2004). Additionally, primary production by phytoplankton contributes to the biological pump (Ducklow *et al*., 2001). This is a key factor in the control of atmospheric carbon dioxide concentrations, enabling long-term sequestration of carbon in marine reservoirs (Ducklow *et al*., 2001; Falkowski *et al*., 2000). The biological pump has become of significant interest in recent years in the context of climate change and global increases in the atmospheric carbon dioxide concentration (Nishino *et al*., 2011; Passow and Carlson, 2012; Riebesell *et al*., 2007).

Although they play a vital role in numerous marine processes, individual phytoplankton are microscopic, and even motile species are only capable of swimming at very limited speeds (Harvey and Menden-Deuer, 2012; Ross and Sharples, 2007). Diatoms in particular are largely incapable of

swimming (Lauria *et al*., 1999), and although they can move vertically through the water column by modulating their buoyancy are often unable to overcome turbulent vertical mixing (Moreno-Ostos *et al*., 2009). This group accounts for approximately 40% of marine primary production, and up to 70% of primary production in coastal systems (Field *et al*., 1998; Uitz *et al*., 2010), and as a result of their limited motility the movement of diatoms both vertically and horizontally in the water column is largely dictated by the water motion itself (Blauw *et al*., 2012; Hobson and McQuoid, 2001; Lauria *et al*., 1999). Being largely immotile organisms in a dynamic environment, phytoplankton have little control over the environmental conditions they experience, and may experience significant short-term variability in abiotic factors, which exert bottom-up control on rates of primary productivity.

Of the variety of abiotic factors which can limit phytoplankton primary production, light is arguably the most variable on short timescales (minutes to seconds) and is a fundamental requirement of photosynthesis (Wagner *et al*., 2006). Since light intensity decreases exponentially with depth phytoplankton cells may experience changes in light intensity of several orders of magnitude over relatively short timescales (minutes to seconds) as they are mixed vertically through the water column, particularly in more turbid and turbulent environments (e.g. coastal waters). In contrast, nutrient availability in the open ocean tends to vary seasonally (Whitney, 2011), and the existence of microzone boundary layers surrounding individual cells is thought to

modulate short-term spatial variability (Lazier and Mann, 1989; Mitchell *et al*., 1985). Similarly, temperature variability tends to occur seasonally, and the magnitude of spatial and temporal changes is relatively small within the wind mixed layer (Lemos and Sanso, 2006).

1.2. Natural sources and timescales of light variability

Variability in the light environment experienced by phytoplankton occurs as a result of numerous processes and operates on a wide range of magnitudes and timescales.

One of the most predictable sources of variability is the change in irradiance throughout the course of a day from sunrise to sunset (the diel light cycle). On longer timescales seasonal changes in daylength (here daylength and photoperiod are used interchangeably to refer to the light period of a 24 hour light-dark cycle) and in the maximum (i.e. midday) irradiance result in large, predictable differences in the daily light environment throughout the course of a year (Forsythe *et al*., 1995; Mejdoul and Taqi, 2012). Seasonal changes in cloud cover can also cause significant changes in the percentage of solar irradiance reaching the ocean throughout the course of a year (Klein and Hartmann, 1993).

Changes in the light environment also occur as a result of processes that operate on short timescales of tens of minutes to less than a second.

Before light reaches the ocean, attenuation by clouds can cause large scale reductions in the irradiance of up to 90%, and the unpredictable movement of clouds across the sky imposes random fluctuations on light reaching the ocean's surface (Stramska and Dickey, 1998). In the upper few meters of the ocean refraction of light by surface waves creates patches of focussed and defocussed light. These wave-induced fluctuations in irradiance vary in magnitude with wave/wind conditions, and up to five-fold changes in irradiances in less than a second have been reported (Dera and Stramski, 1993). Despite the extreme nature of these variations, light scattering within the water column causes the intensity of wave-induced light fluctuations to decrease rapidly with depth, for example in the open ocean fluctuations can be reduced by half in 20m of water (see table 1 in Stramska and Dickey, 1998). Finally, when considering the whole water column, turbulent mixing processes are thought to impose random changes in irradiance on individual cells as they move vertically. The timescale and magnitude of these changes depends on the turbulence, which in turn is dependent on physical parameters such as temperature (i.e. stratification), depth, and surface wind shear (Falkowski, 1984; Ross and Sharples, 2004).

This study focuses on irradiance fluctuations on timescales and magnitudes consistent with vertical mixing in the water column, and diel variability in solar irradiance.

1.3. Experimental approaches to intra-diel light variability

Variability in irradiance is often ignored in experimental studies, and also in measurements of marine primary productivity. In laboratory experiments cultures are typically grown under an unrealistic square-wave light function (e.g. Granger *et al*., 2004; Interlandi, 2002; Staehr and Sand-jensen, 1997) and estimates of ocean primary productivity from changes in carbon-14 (^{14}C) or oxygen concentration (Williams *et al*., 1983) are often taken from bottles incubated at a single depth or on board a research vessel (e.g. Carpenter *et al*., 2004; Ditullio *et al*., 2003; Gervais *et al*., 2002). In both of these situations the variability of the natural light environment is largely ignored, and results may therefore not accurately capture what is actually occurring in natural populations. Such measurements made under stable light conditions have been used to parameterise models of ocean productivity, or to validate satellite estimates of primary production (Behrenfeld *et al*., 2002; Tilstone *et al*., 2009). The validity of such models or validation approaches as representative of the marine environment is therefore questionable, unless the responses of phytoplankton to light variability can be taken into account.

Studying the effects of short-term random fluctuations in light is difficult in the laboratory, because of the inherent difficulty in accurately recreating these fluctuations in an experimental setup. Random variations in irradiance caused by light focussing, or turbulent mixing tend to be imposed on individual cells, whereas experimental light regimes are applied to whole

cultures (Wagner *et al*., 2006). Growing entire phytoplankton cultures under random light regimes, or light regimes which feature short flashes of high intensity light (such as those cause by wave focussing) is therefore a poor method of simulating natural random light fluctuations which are typically experienced by single cells only (Janssen *et al*., 1999; Nedbal *et al*., 1996). A more promising approach to reproduce this type of random light fluctuations is to use large scale mixed cultures grown under a non-random light regime. In such a setup turbulent mixing and surface waves cause random light fluctuations on the cell level, and the light regime applied to the culture is under the control of the experimenter. This method was used by Stramski *et al*. (1993) to study the responses of an optically thin culture of a marine chlorophyte to light fluctuations caused by wave focussing. Otherwise, this approach tends to be employed primarily in studies of photobioreactors which invariably involve high cell densities such that culture self-shading and possible nutrient depletion confounds results (Kliphuis *et al*., 2010; Ogbonna *et al*., 1995). The major problem with this approach is that the actual light fluctuations experienced by cells are difficult to determine, and equally difficult to control and reliably reproduce (although see Stramski and Legendre, 1992).

A common approach in experimental studies is to simplify random light fluctuations into a predictable light regime. Turbulent mixing is typically simulated by a cyclical increase and decrease in light intensity according to a

sinusoidal or exponential curve (van Leeuwe *et al*., 2005; Wagner *et al*., 2006) or using step changes in light level (Litchman, 2000). This approach has several advantages over attempting to accurately reproduce a stochastic light environment, notably:

- Light regimes are easily reproducible from their summary statistics.
- Comparing light regimes is significantly easier – it is possible to interrogate data to determine which responses are related to which properties of light regimes.
- The experimental setup can be relatively simple.

Although this approach can be criticised because the resultant light regimes lack realism, they nevertheless can provide insight into how phytoplankton respond to dynamic light environments. For example, comparing phytoplankton grown under a rapidly fluctuating light regime to a less rapidly fluctuating one can be used to identify differences in photophysiology between phytoplankton growing in a rapidly mixed environment, compared to one in which mixing is slower. Equally, using simplified light regimes to understand what parameters of the light regime (e.g. mean, median, etc.) phytoplankton acclimate to can give insight into how natural phytoplankton populations will respond to changes in the light environment (Lavaud *et al*., 2007; Litchman, 2000).

Diel periodicity in the light environment is comparatively easy to replicate in the laboratory. Reproducing the diel increase and decrease in irradiance is typically achieved by way of a sine wave (Kromkamp and Limbeek, 1993; Wagner *et al*., 2006) and this has been found to be reasonably consistent with natural light regimes (Mejdoul and Taqi, 2012).

It warrants mentioning that mathematical models can provide an alternative to the experimental approaches outlined above. Individual-based models are of particular use when studying phytoplankton responses to short term random light fluctuations. In such models hundreds or thousands of cells are individually tracked and combined to determine population responses (Ross *et al*., 2011; Ross and Sharples, 2004). This is particularly useful when studying light because the light history of cells is known, a factor which can significantly impact how cells respond to environmental changes (O'Brien *et al*., 2009). However, even using this approach, the complexity of natural random light fluctuations precludes realistic mathematical simulation (Talmy *et al*., 2013). Additionally, these models are difficult to validate, since the random nature of the light environment precludes accurate replication in an experimental environment, and still require parameterisation based on experimental data.

1.4. Phytoplankton growth under fluctuating light

The responses of phytoplankton growth rate to light variability are species specific, and are dependent on frequency and irradiance statistics of fluctuations (Flöder *et al*., 2002; Litchman, 2000; Wagner *et al*., 2006).

Nicklisch (1998) reported reductions in growth rates in cyanobacteria, diatoms and chlorophyta in response to fluctuations of an hour or less in duration, when compared with cultures grown under square-wave illumination. This reduction was greater in cyanobacteria than in diatoms and was also found to be lower in more rapidly fluctuating light. These results should be treated with caution however, since the integrated daily light dose was not comparable between fluctuating and square-wave light regimes, and also differed significantly between species within a light treatment.

Decreases in specific growth rate in response to fluctuating light were also reported by Wagner *et al*. (2006). However, in this study the daily light dose was significantly lower in the fluctuating light regime than in the non-fluctuating regime. Since lower irradiance reduces phytoplankton growth rate (Falkowski *et al*., 1985), the growth rate reduction observed by Wagner *et al*. (2006) is unlikely to be caused by light fluctuations alone. Consistently reduced growth rates in fluctuating light versus non-fluctuating have also been reported by Nicklisch and Fietz (2001) and Shatwell *et al*. (2012), the latter of which reported that the reduction in growth rate was more extreme

at higher light doses. This effect is corroborated by other authors in different species of diatoms (Lavaud *et al*., 2007; Mitrovic *et al*., 2003).

In contrast to the results reported above, some authors have reported an increase in growth rate when cultures are grown under fluctuating light regimes. van Leeuwe *et al*. (2005) found that growth rates of *Chaetoceros brevis* (a diatom) and *Pyramimonas* sp. (a flagellate) increased with more rapid fluctuations in the light regime (3-hour vs. 1-hour period) and were higher than or equal to those in comparable sinusoidal regimes. Faster growth under fluctuating light regimes were also reported by Litchman (1998) and Litchman (2000) for some species, however in these studies growth rate was generally higher under longer period fluctuations. It should be noted that Litchman (2000) reported only minor changes in growth rate for the majority of light regimes and in fact reported a slight decrease in growth rate for the green alga *Sphaerocystis schroeteri* grown under a fluctuating light regime versus a square wave regime. In each of these studies the amplitude of light fluctuations was relatively low, and the highest reported maximum irradiance was 400 µmol m^{-2} s^{-1} (van Leeuwe *et al*., 2005). Studies reporting reduced growth rates in fluctuating light tend to utilise much higher amplitude fluctuations, with maximum irradiance exceeding 900 µmol m^{-2} s^{-1} (Lavaud *et al*., 2007; Nicklisch, 1998; Nicklisch and Fietz, 2001; Shatwell *et al*., 2012; Wagner *et al*., 2006). This may have contributed to the inconsistency in the reported impact of light fluctuations on growth rate.

Despite the uncertainty in how light fluctuations on the timescale of minutes to hours affect growth rates the response is clearly species specific. Diatoms have consistently been found to cope better in fluctuating light than any other group with which they have been compared. That is to say that the difference in growth rate between cultures grown under fluctuating and those grown under non-fluctuating light is always more positive than in any other phytoplankton group studied (Litchman, 2000; van Leeuwe *et al*., 2005). Conversely cyanobacteria are consistently reported to cope poorly with light fluctuations (Nicklisch, 1998; Shatwell *et al*., 2012).

1.5. Photosynthesis and photoacclimation to intradiel light fluctuations

As photoautotrophic organisms, phytoplankton rely on the light dependant reactions of photosynthesis to produce two energy carrying molecules, ATP (adenosine triphosphate), and NADPH (nicotinamide adenine dinucleotide phosphate hydrogen). These then provide energy for carbohydrate synthesis, and ultimately other metabolic processes within the cells. A summary of photosynthesis is shown in Figure 1.5.1.

Light is a fundamental requirement of photosynthesis, however the effect of fluctuating light regimes on the rate of photosynthesis and the photosynthesis-irradiance response curve has received little attention in the literature. The limited data available suggest that a species-specific response

also occurs in photosynthesis rates. Carbon assimilation rates have been reported to increase with more rapid light fluctuations in the green alga *Dunaliella tertiolecta*, but decrease in the diatom *Thalassiosira weissflogii* (van de Poll *et al*., 2010).

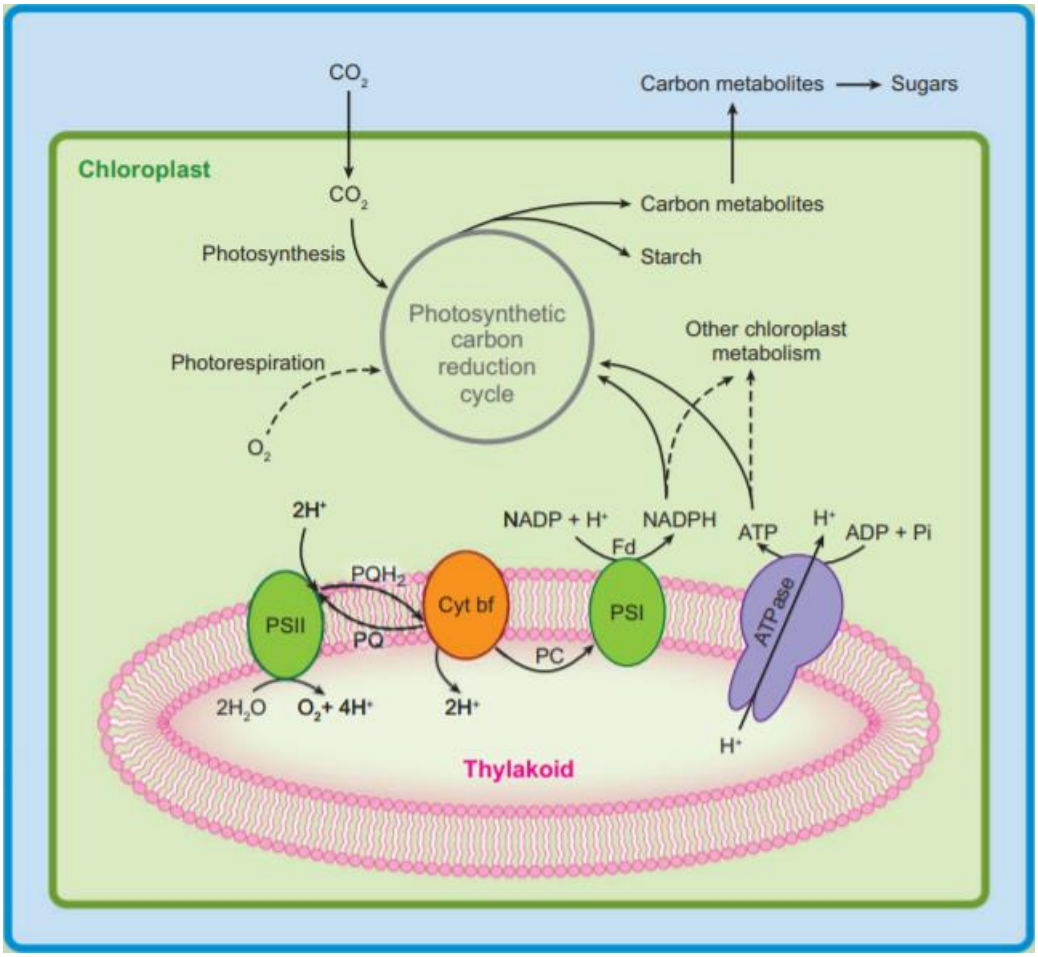

Figure 1.5.1. Overview of photosynthesis. Adapted from Baker, 2008

Ibelings *et al*. (1994) reported that higher amplitude fluctuations in light increased photosynthesis rates in both a cyanobacterium and a green alga, and that photosynthesis rates tended to be higher for cultures grown in fluctuating versus sinusoidal light regimes. However, in this study the daily

light dose was not equal between light regimes. Higher amplitude fluctuating light regimes also had a reduced daily light dose, which may have led to reduced photodamage, contributing to the higher photosynthesis rates.

In field studies there has been some research on the impact of intradiel light fluctuations on photosynthesis rates (Mallin and Paerl, 1992; Marra, 1978). A particular topic of interest is whether or not photosynthesis rates measured in bottles incubated at a fixed depth (i.e. under relatively static light environment) can accurately be used to describe photosynthesis in vertically mixed phytoplankton populations which experience a fluctuating light environment. This has been examined in several studies by comparing estimates of photosynthesis extrapolated from a number of incubations at fixed depths to estimates from bottles which are continuously moved up and down in the water column, and therefore experience a fluctuating light environment. (Köhler, 1997; Mallin and Paerl, 1992; Marra, 1978). Generally photosynthesis rates from samples experiencing a fluctuating environment are considerably higher than those extrapolated from incubations at fixed depths (Köhler, 1997; Marra, 1978). This discrepancy is mostly a result of light induced damage to the photosynthetic apparatus (see section 1.6 and chapter 5) in bottles fixed near the surface of the water (Köhler *et al*., 2001; Ross *et al*., 2011). The substantially different light dose between fixed depth and vertically moved incubations make both direct comparison between photosynthesis rates, and a clear understanding of how light fluctuations

impact photosynthesis, difficult. The use of natural phytoplankton communities, and limited knowledge of the fluctuating light regime that samples actually experience (Köhler, 1997; Marra, 1978) also make it difficult to apply the results of these experiments to understand how different fluctuating light environments might impact photosynthesis rates in different phytoplankton species.

It is also important to consider photoacclimation in phytoplankton in response to light fluctuations. Here photoacclimation is used to refer to the regulation of the process and components which determine light absorption and photosynthesis rates. In phytoplankton this typically involves changes in the complement and arrangement of light harvesting pigments, although changes related to the Calvin-Benson cycle activity (usually via the concentration of RUBISCO) may also be important (Dubinsky and Stambler, 2009; Falkowski and LaRoche, 1991; Moore *et al*., 2006).

Interestingly several authors have reported no significant changes in the concentration of light harvesting pigments in response to light fluctuations. Diatoms in particular have not been reported to change their quota of light harvesting pigments (most notably chlorophyll-*a*, but also others) when grown under a reasonable range of fluctuation amplitudes and when compared with non-fluctuating light regimes (Nicklisch, 1998; van de Poll *et al*., 2010; van Leeuwe *et al*., 2005). This lack of response appears to be conserved even when fluctuating light regimes have a slightly reduced daily

light dose versus non-fluctuating regimes (e.g. in van Leeuwe *et al*., 2005, average irradiance in fluctuating light regimes was 70% that of the sinusoidal regime). Wagner *et al*. (2006) in contrast, showed a reduction in light harvesting pigment content in fluctuating light. It is thought that the significantly lower daily light dose in fluctuating regimes (~75% reduction) is the cause of this. A similar lack of response to fluctuating light has been reported for green algae by some authors (Ibelings *et al*., 1994; Nicklisch, 1998), whilst others have reported an increase in light harvesting pigments (van de Poll *et al*., 2010). Each of these studies compared intra-diel light fluctuations to sinusoidal fluctuations with the same maximum irradiance. For the green alga *Dunaliella tertiolecta*, Havelkova-Dousova *et al*. (2004) found the light harvesting pigment quota of cells grown under fluctuating light was lower than that in cells grown under constant illumination of the same daily light dose. It has been suggested that these trends indicate that in fluctuating light regimes diatoms acclimate to the average light intensity, whilst acclimation in green algae is driven by both the maximum and average irradiance (Havelkova-Dousova *et al*., 2004; van Leeuwe *et al*., 2005).

1.6. Photoprotection in fluctuating light regimes

Light induced damage to the photosynthetic architecture (here referred to as photodamage) is an inevitable consequence of photosynthesis

and is enhanced under increased irradiance (Long *et al*., 1994; Tyystjärvi, 2008; Vass and Aro, 2007). In fluctuating light environments phytoplankton may experience rapid increases in irradiance that substantially increase the potential for photodamage on short timescales and may reduce photosynthetic efficiency (Alderkamp *et al*., 2010). A number of photoprotective mechanisms have been identified which act to dissipate excess photosystem II (PSII) excitation energy. These have been found to play an important role in preventing photodamage under fluctuating light regimes (Lavaud *et al*., 2007)

Non-photochemical quenching (NPQ) of PSII excitation energy is an important photoprotective mechanism in many species. In most species the xanthophyll cycle is the major pathway of NPQ (Muller *et al*., 2001), which utilises either the de-epoxidation of diadinoxanthin to diatoxanthin, or the de-epoxidation of violoaxanthin to zeaxanthin via antheraxanthin. Examination of the ratios of the various xanthophylls to one another has confirmed that xanthophyll cycling is an important photoprotective process in response to fluctuations in light (Havelkova-Dousova *et al*., 2004; van de Poll *et al*., 2010; van Leeuwe *et al*., 2005) and the activity of the xanthophyll cycle is directly related to the incident irradiance. The degree of non-photochemical quenching can also be determined from PSII fluorescence. Whilst there is some dispute as to how this is best achieved from fluorescence measurements (McKew *et al*., 2013) fluorescence-derived NPQ consistently

demonstrates a direct relationship with incident irradiance in fluctuating light regimes (Lavaud *et al*., 2007; van de Poll *et al*., 2010; Wagner *et al*., 2006).

In addition to xanthophyll cycling, green algae utilise state transitions to prevent absorption of excess, potentially damaging, light energy (Macintyre *et al*., 2000). State transitions have been implicated as an important response to fluctuations in irradiance and have been presented as an explanation for lower xanthophyll cycle activity relative to fluorescence-determined NPQ in green algae than in diatoms (Havelkova-Dousova *et al*., 2004; van de Poll *et al*., 2010; van Leeuwe *et al*., 2005; Wagner *et al*., 2006). State transitions may also be more important than xanthophyll cycling in green algae in preventing photodamage when cells are grown under high frequency (1-hour period) fluctuations (van Leeuwe *et al*., 2005).

Cyanobacteria lack a xanthophyll cycle and instead use state transitions and the Mehler reaction to dissipate excess light energy (Kana, 1992; van Thor *et al*., 1998). The apparent importance of xanthophyll cycling in response to fluctuations in irradiance suggests that this may be among the reasons why growth rates of cyanobacteria are more negatively affected than growth rates of phytoplankton species capable of xanthophyll cycling (Nicklisch and Fietz, 2001).

The quantum efficiency of photosynthesis, or PSII electron transport (measured from fluorescence) can be used to determine how effectively cells

are able to repair, and also prevent photodamage. Photosynthetic efficiency tends to decrease as incident light increases. However, in fluctuating light regimes this reduction is often less extreme in diatoms than in other species (van Leeuwe *et al*., 2005; Wagner *et al*., 2006). This, when taken together with high xanthophyll activity (i.e. rapid de-epoxidation) and a relatively large xanthophyll pool, has led several authors to conclude that diatoms are better adapted to fluctuating light regimes than other phytoplankton (Shatwell *et al*., 2012; van de Poll *et al*., 2011, 2010).

A study by Lavaud *et al*. (2007) suggests some diatoms may be better adapted to intra-diel light fluctuations than others. They reported that *Phaeodactylum tricornutum*, a diatom typically found in estuaries, was capable of much higher NPQ than *Skeletonema costatum*, a typically oceanic species. They also theorised that *P. tricornutum* is able to more rapidly activate and deactivate xanthophyll cycle enzymes, preventing unnecessary dissipation of energy by NPQ that could otherwise be used in photosynthesis, and maintaining a high quantum photosynthetic efficiency.

1.7. Conclusions and project scope

An important issue with the current research into phytoplankton under intradiel light variability is the lack of consistency in how the light environment is simulated. For example, whilst some studies conserve mean

irradiance between fluctuating light regimes, others conserve maximum irradiance (Havelkova-Dousova *et al*., 2004; Nicklisch, 1998). Substantial differences in how fluctuating light environments are altered between treatments has led some authors to report that fluctuating light enhances growth rates (Litchman, 2000), whilst others report the opposite (Lavaud *et al*., 2007). Much of the current research has focused on comparing fluctuating light regimes to sinusoidal ones, however it remains largely unclear how differences in the parameters of fluctuating light regimes (e.g. maximum intensity, frequency of fluctuations, amplitude of fluctuations, etc.) affect phytoplankton growth and photosynthesis, and to which parameters of fluctuating light regimes phytoplankton acclimate.

This study attempted to address these issues in several ways. Growth and photophysiology of two species of diatoms were studied in several fluctuating light regimes. In order to capture the impact of a range of aspects of the light environment on phytoplankton growth and photophysiology, light regimes were characterised by a range of mean and maximum irradiance and mixing amplitudes. The distribution of the light environment was also considered.

In mathematical models of marine phytoplankton populations, including those used to estimate global photosynthesis from satellite observations of ocean colour, photoacclimation may be described as a function of a single parameter of the light environments (Behrenfeld *et al*.,

2016; Graff *et al*., 2016). This carries an implied hypothesis that photoacclimation can be correctly predicted from a single aspect of the light regime which, if incorrect, could be a substantial source of error in current estimates of global marine photosynthesis. Using a range of light regimes, the first aim of this study was to examine whether or not this is the case. With the objective of determining which aspect of the light environment is most important in driving photoacclimation.

Secondly, photodamage and the mechanisms which are employed to mitigate it were investigated. Photodamage has been implicated as an important factor in controlling growth rates in dynamic light environments (Alderkamp *et al*., 2010). This study aimed to investigate how phytoplankton acclimated to fluctuating light regimes in order to prevent photodamage during peaks in irradiance, and how successful they were in accomplishing this.

Finally, this study aimed to investigate how differences in light fluctuations might impact photophysiology and photosynthesis throughout the day by measuring photophysiology across the photoperiod in two different light regimes. In the field, daily photosynthesis rates may be extrapolated from single measurements made at one time of day (Alderkamp *et al*., 2015; Brush *et al*., 2002; Carmack *et al*., 2004). One objective was to determine how acclimation across the photoperiod might affect the error in daily photosynthesis and primary productivity rates estimated in this way, and

how light fluctuations might impact this error. These data were also used to investigate several hypotheses on what limits growth in fluctuating light environments. Several factors have been implicated as a cause for the common observation that light fluctuations reduce growth rate (Lavaud *et al*., 2007; Nicklisch, 1998; Nicklisch and Fietz, 2001; Shatwell *et al*., 2012; Wagner *et al*., 2006). This study also aimed to examine the hypotheses that daily photosynthesis, photodamage, differences in resource allocation, or a combination of these could be responsible.

Throughout this thesis interspecific differences in growth and photophysiology are also discussed. Specifically, in the context of the hypothesis that variability in light is an important driving force in determining the habitat and ecological niche of phytoplankton (Lavaud *et al*., 2007).

2. Methods development - The light environment

2.1. Approximating the natural light environment

One of the most important considerations for this study was how to practically and accurately investigate natural light regimes in an experimental setting. Perhaps the most obvious method is to attempt to replicate the processes responsible for the marine light environment. Although this may be possible to some degree (Stramski and Legendre, 1992), the high level of disorder and randomness associated with many of these processes would lead to chaotic light environments which are difficult to control or replicate. Whilst such light environments may be realistic, interpreting and reproducing results would be very difficult, as would disentangling which aspects of the light environment phytoplankton respond to.

An alternative approach, which was taken here, is to 'dissect' the light environment, define it by several summary statistics and then reconstruct a simplified dynamic light regime based on these. This is a typical approach in laboratory studies, the advantages and disadvantages of this method were discussed in section 1.3.

2.2. The light regimes model

Light regimes were defined using a simple two-component model of irradiance experienced by a particle in a mixed water column. The model consisted of:

1. A solar irradiance component which simulates irradiance at the surface of the water column.
2. A simple model of mixing depth, defining the depth of the particle relative to the euphotic depth (defined here as the depth of 1% light penetration) at any given time.

The Beer-Lambert law of light attenuation was then used to calculate the irradiance as the simulated particle was mixed through the water column.

Studies of solar irradiance (in the absence of cloud cover) have demonstrated that the incident solar radiation is well predicted by relatively uncomplicated sinusoidal models (Mejdoul and Taqi, 2012). Here a simplified two-parameter sinusoidal model is used. This Equation is consistent with those used in many previous studies (see section 1.3), and is defined as:

$$I(t) = I_M \cdot sin\left(\frac{\pi t}{LP}\right) \qquad \textbf{2.2.1}$$

Where I_M is the maximum irradiance (i.e. at midday) LP is the length of the photoperiod and t denotes the time from the onset of the photoperiod.

To incorporate the mixing component the diel sinusoid defined above was transformed multiplicatively by a model of exponential decay, consistent with the Lambert-Beer law:

$$I(t) = I_M \cdot sin\left(\frac{\pi t}{LP}\right) e^{-(k_d \cdot Z_{rel})} \qquad \textbf{2.2.2}$$

In which k_d is the attenuation coefficient. Here this is a factor which defines the euphotic depth as the depth of 1% light penetration and is equal to $ln(100)$. Z_{rel} is the mixing depth relative to the euphotic depth and is defined according to Equation 2.2.3.

$$Z_{rel} = 0.5 \frac{z_{mix}}{z_{eu}} \left(1 - cos\left(\frac{2\pi t}{MP}\right)\right) \qquad \textbf{2.2.3}$$

Where $\frac{z_{mix}}{z_{eu}}$ is the maximum mixing depth relative to the euphotic depth, and MP is the mixing period (i.e. time taken for one full mixing cycle).

Equation 2.2.3 simulates mixing in a circular motion, similar to that experienced by cells entrained in Langmuir cells as shown in Figure 2.2.1. It may provide a poor simulation of deeper, convective mixing processes. The lack of realism in the light regimes used here has been discussed previously, and must be kept in mind when interpreting results.

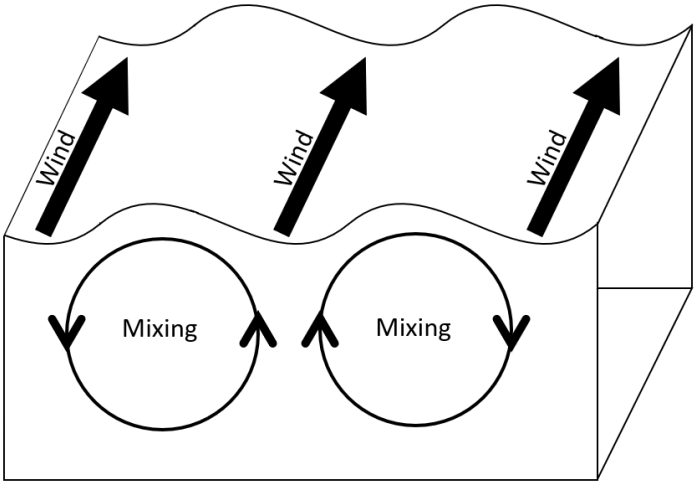

Figure 2.2.1. Langmuir circulation, responsible for changes in the light environment of mixed particles similar to those used in light regimes in this study.

2.3. Selection of light regimes

Light regimes used in this study, and the parameters used to define them are detailed in Table 2.3.1. Light regimes characterised by three different values of $\frac{z_{mix}}{z_{eu}}$ were used, simulating no mixing (sinusoidal, SI), mixing to 50% of the euphotic depth (low fluctuations, LF) and mixing to the euphotic depth (high fluctuations, HF). Two different values of mean irradiance were used, denoted by HL (high light, 273 µmol m^{-2} s^{-1}) and LL (low light, 185 µmol m^{-2} s^{-1}). These were selected such that the maximum irradiance in the HLSI (high light sinusoidal) regime was equal to the maximum irradiance in the LLLF (low light low fluctuating) regime. Based on preliminary data from stock cultures HL and LL mean irradiances were also selected to be saturating and sub-saturating to photosynthesis respectively. Square wave light regimes (SQ)

at the mean irradiance were used in order to explore the relationship between static and dynamic light regimes, something often neglected in studies involving fluctuating light. Parameters used to calculate the light regimes in Equations 2.2.1 to 2.2.3 are shown in Table 2.3.1. HL light regimes are illustrated in Figure 2.3.1. LL light regimes were identical in shape but are transformed vertically. All light regimes used a mixing period of 1 hour (*MP* in equation 2.2.3).

The phrases “fluctuating regimes” or “fluctuating light regimes” are here used to describe all regimes that are not square-wave. That is, SI, LF and HF regimes.

Table 2.3.1. Summary statistics of the light regimes used, Values of PAR have units µmol m^{-2} s^{-1}. An n/a value of $\frac{z_{mix}}{z_{eu}}$ indicates a square-wave light regime. *MP* = 1 hour in all light regimes. See Table II for details of symbols used. I_{Med} and I_{Med}^{D} are two different measures of the median irradiance and are described in section 2.4.

Regime	I_M	$\frac{z_{mix}}{z_{eu}}$	$\bar{I}$	I_{Med}	I_{Med}^{D}
HLSQ	273	n/a	273	273	273
HLSI	430	0	273.7	304.1	372.4
HLLF	1000	0.5	273.3	168.1	504.5
HLHF	1520	1	273.5	68.6	836.9
LLSQ	118	n/a	118	118	118
LLSI	185	0	117.8	130.8	160.2
LLLF	430	0.5	117.8	72.3	216.9
LLHF	660	1	118.8	29.8	356.3

Light intensities reported for light regimes reflect the mean irradiance within the culture vessels, measured at a resolution of approximately 1 cm using a spherical detector (see section 2.5).

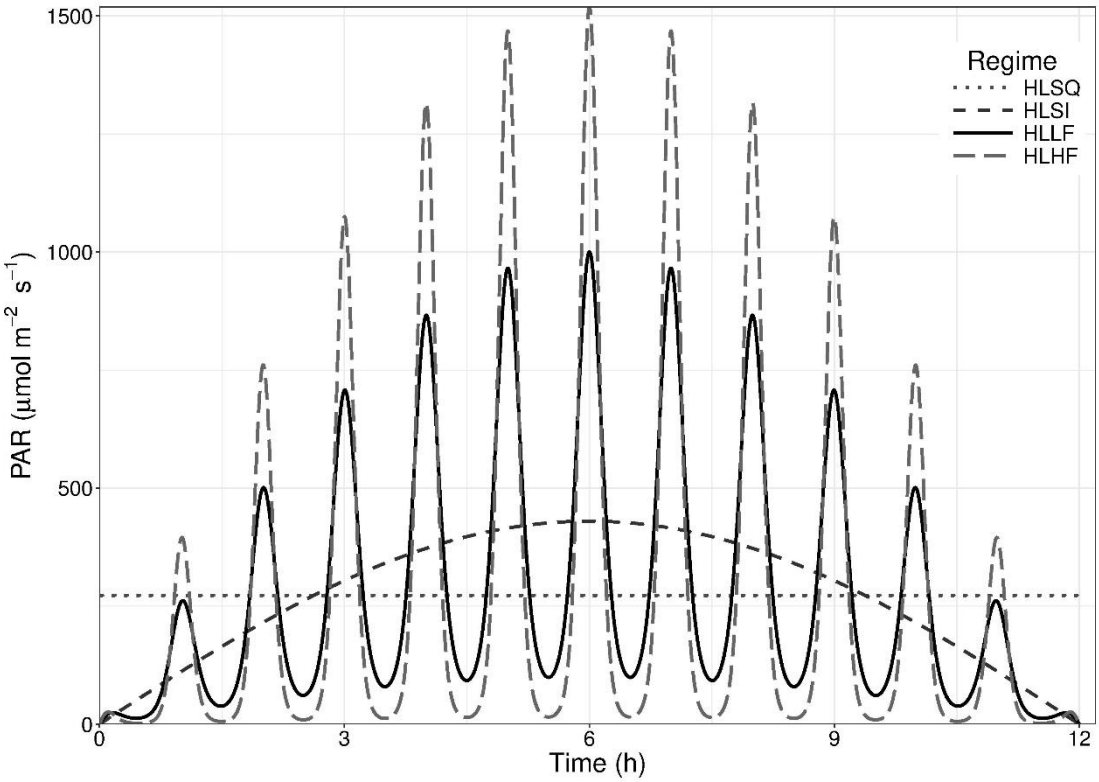

Figure 2.3.1. HL fluctuating and square-wave light regimes. See text and table 2.3.1 for description of the light regimes.

2.4. Physiologically relevant parameters in quantification of light regimes

Fluctuating light regimes in the literature are typically expressed in terms of the parameters used to calculate them (e.g. Alderkamp *et al*., 2012; Hoppe *et al*., 2015; Lavaud *et al*., 2007; Nicklisch, 1998). These parameters are not necessarily physiologically relevant over the course of the photoperiod and may not be useful in characterising phytoplankton acclimation to the light regime. For example, a high maximum irradiance may suggest that for a

period of the light regime the plastoquinone pool (PQ) is reduced, photosynthesis rates are saturated and the potential for photodamage is high. However, if the maximum irradiance is only sustained for a very small fraction of the photoperiod its overall effect on acclimation may be minimal. Some research indicates that changes in the maximum irradiance in rapidly fluctuating light environments have very little effect on phytoplankton acclimation, presumably because the maximum irradiance is sustained for such a short duration (Mouget *et al*., 1995; Veal *et al*., 2010). In order to address the question of which aspects of the light environment phytoplankton acclimate to, it is vital to define physiologically relevant parameters that can be used to characterise any light environment.

In laboratory studies the light dose (D) or mean irradiance ($\bar{I}$), which is simply D divided by the length of the photoperiod (LP, Equation 2.4.1) are very commonly used to characterise fluctuating light regimes and have consistently been found to be a poor indicator of photoacclimation (e.g. Dimier *et al*., 2009; Garcia-Mendoza *et al*., 2002; Hoppe *et al*., 2015; Litchman, 2003, 2000; Litchman *et al*., 2004)

$$\bar{I} = \frac{D}{LP} \qquad \textbf{2.4.1}$$

Several recent studies using satellite and field data have suggested using the median (I_{Med}), rather than the mean, as an indicator of photoacclimation (Behrenfeld *et al*., 2016; Graff *et al*., 2016) based on the

understanding that the redox state of the plastoquinone pool (PQ) is an important regulator of photoacclimation (Durnford and Falkowski, 1997; Escoubas *et al*., 1995; Falkowski and Chen, 2003; Foyer *et al*., 2012). As irradiance increases, PQ becomes increasingly reduced. Once the PQ is entirely reduced, and photosynthesis is saturated, subsequent increases in irradiance do not cause a change in redox state, and therefore carry no new information for photoacclimation (this is discussed in more detail in chapter 4). They do, however, affect the mean irradiance ($\bar{I}$). Median irradiance is less affected by supersaturating light levels and provides an intuitive parameter, representing the irradiance midpoint such that 50% of the photoperiod is spent above it, while 50% is spent below. In this study, the calculation of I_{Med} is trivial. Software and hardware limitations mean that the irradiance of the LEDs (light emitting diode) used to illuminate cultures changes at most once per second. Light regimes are composed of a finite number of irradiances from which I_{Med} is easily calculated. Mathematically I_{Med} can be defined according to Equation 2.4.2 from the probability density function (PDF), $p(I)$, which defines the relative probability that the irradiance will equal I within the photoperiod and has the associated cumulative distribution function (CDF) $P(I)$.

$$\int_0^{I_{Med}} p(I)\, dI = P(I_{Med}) = 0.5 \qquad \textbf{2.4.2}$$

Both $p(I)$ and $P(I)$ can be estimated from light regimes by kernel density estimation. Those calculated from HL light regimes are illustrated in Figure 2.4.1. These demonstrate that for these light regimes, as the mixing coefficient increases, a greater proportion of the photoperiod is spent at lower irradiances. This is clearly reflected by a reduction in I_{Med}, while $\bar{I}$ remains constant (Table 2.3.1).

I_{Med} as an indicator of photoacclimation attempts to account for the lack of change in PQ redox signalling at supersaturating irradiances. However, it does not account for variability in the photosynthetic efficiency with which light is utilised. Consider for example the HLHF, and HLSI regimes which have equal daily light dose. In the HLHF regime a greater proportion of that light dose is delivered at higher irradiances. Assuming a similar photosynthesis-irradiance response for both HLSI and HLLF regimes that saturates below I_M for HLHF, the efficiency with which light is used in photosynthesis (and therefore daily integrated photosynthesis), will be lower under the HLHF regime. A resultant reduction in the quantum efficiency of biomass accumulation may restrict energy availability for photoacclimation, or lead to differences in resource allocation between photoacclimation and growth (Wagner *et al*., 2006). Here a new parameter is proposed as a potential indicator for acclimation to dynamic light regimes, I_{Med}^{D}. This represents the irradiance level above and below which 50% of the light dose is delivered and can be defined mathematically in terms of the PDF $p(I)$, the light dose, and

the photoperiod length. Since the photoperiod (LP) is finite, for any given irradiance there is a maximum light dose that can be delivered at that irradiance, equal to the light dose from a square wave light regime (D_{sq} Equation 2.4.3).

$$D_{sq} = I \cdot LP \qquad \textbf{2.4.3}$$

For any given light dose (D) there is therefore a maximum fraction of that dose that could be delivered at a specific irradiance (Equation 2.4.4). Note that this fraction could be larger than 1.

$$\frac{D_{sq}}{D} = \frac{I \cdot LP}{D} \qquad \textbf{2.4.4}$$

The definite integral $\int_{I_1}^{I_2} p(I)\, dI$ gives the probability of the irradiance within the photoperiod being between I_1 and I_2, or the fraction of the photoperiod where irradiance is between these two values. Multiplying this by a variation of Equation 2.4.4 gives the fraction of the light dose delivered between I_1 and I_2 (Equation 2.4.5). This is defined as the integral of a PDF function, $d(I)$, which describes the relative proportion of the light dose delivered at irradiance I, and has associated CDF $D(I)$.

$$\left(\frac{I_2 \cdot LP}{D} - \frac{I_1 \cdot LP}{D}\right) \int_{I_1}^{I_2} p(I)\, dI = \int_{I_1}^{I_2} d(I)\, dI \qquad \textbf{2.4.5}$$

Based on Equation 2.4.5 I_{Med}^{D} can be calculated according to Equation 2.4.6.

$$\int_0^{I_{Med}^D} d(I)\ dI = D(I_{Med}^D) = \frac{I_{Med}^D}{D \cdot LP} \int_0^{I_{Med}^D} p(I)\ dI = 0.5 \quad \textbf{2.4.6}$$

As with $p(I)$ and $P(I)$, $d(I)$ and $D(I)$ can be estimated from light regimes by kernel density estimation and are shown for HL regimes in Figure 2.4.1. These clearly illustrate that for these light regimes as the mixing coefficient increases, a greater proportion of the light dose is delivered at higher irradiances. This is reflected in an increase in I_{Med}^D (Table 2.3.1).

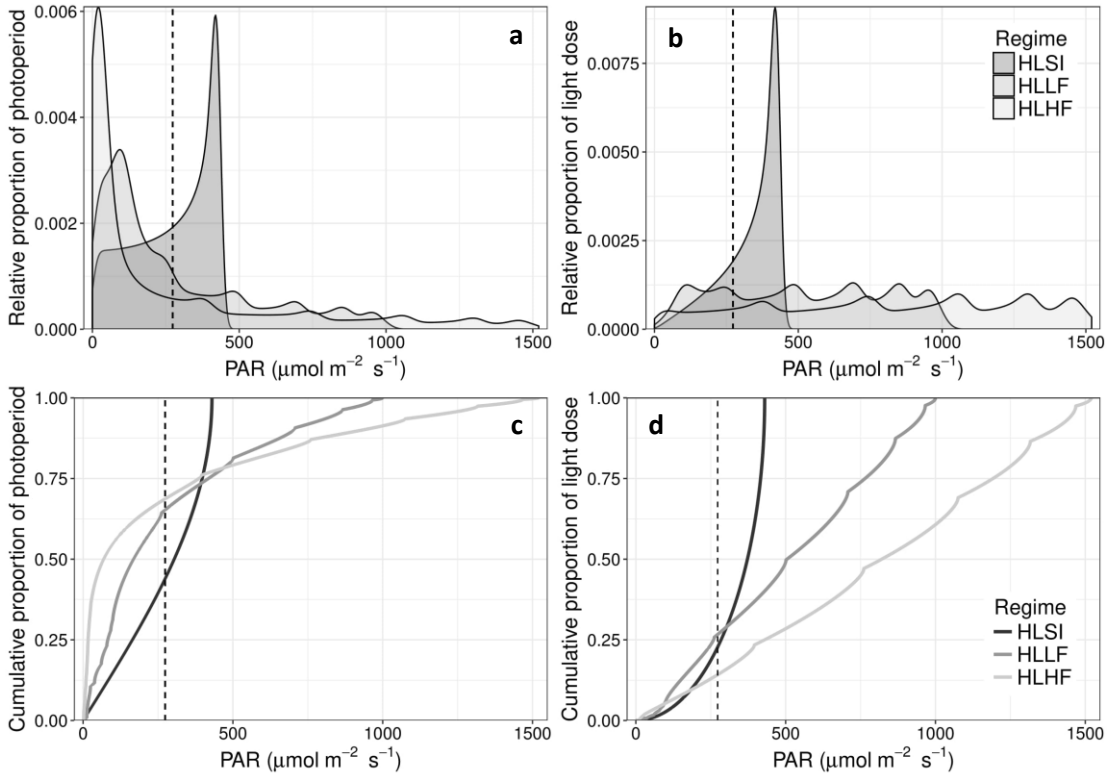

Figure 2.4.1. Relative (top) and cumulative (bottom) probability distributions for photosynthetically active radiation (PAR) in HL fluctuating regimes relative to light dose (right) and photoperiod (left). These are defined in the text as a = $p(I)$, b = $d(I)$, c = $P(I)$ and d = $D(I)$.

I_{Med} and I_{Med}^D are relevant to different physiological aspects of phytoplankton and describe the distribution of the light environment. An increase in I_{Med} suggests a greater degree of PQ reduction in the

photoperiod. In contrast, an increase in I_{Med}^{D} suggests a reduction in integrated daily photosynthetic efficiency. Importantly, because these two parameters are related to the distribution of the light environment, they can be calculated for any light regime, regardless of how the light regime is derived. This may be particularly useful in comparing both predictable light regimes derived from different formulae, or stochastic light regimes simulating random changes in irradiance. This study aims to investigate whether these parameters, or other more commonly used ones (see Table 2.3.1), can be used as reliable indicators of phytoplankton acclimation to fluctuating light regimes. Statistical methods used to test this are detailed in section 4.2.

2.5. Design and construction of LED setup

The physical construction of the apparatus used to deliver light regimes was also an important consideration for this project. The aim was to minimise variability in irradiance within the culture vessel itself to ensure that the measured responses of cultures could be predominantly attributed to the light regime itself and were minimally affected by other sources of light variability. To this end a number of setups were tested, three of which are presented here. Two of these are common laboratory setups, and the third was found to comparatively reduce irradiance variability within culture

vessels. These are illustrated in Figure 2.5.1. Setups 1 and 2 used 4 and 3 panels of LEDs respectively, positioned equally around the culture vessel. Setup 3 used 3 panels of LEDs, two of which were parallel and directed obliquely at the culture vessel, while the third was opposite and pointed directly at the centre of the vessel. In setup 1 and 2 the vertical positions of the LEDs were varied between LED panels in an attempt to reduce vertical heterogeneity of irradiance within the culture vessel.

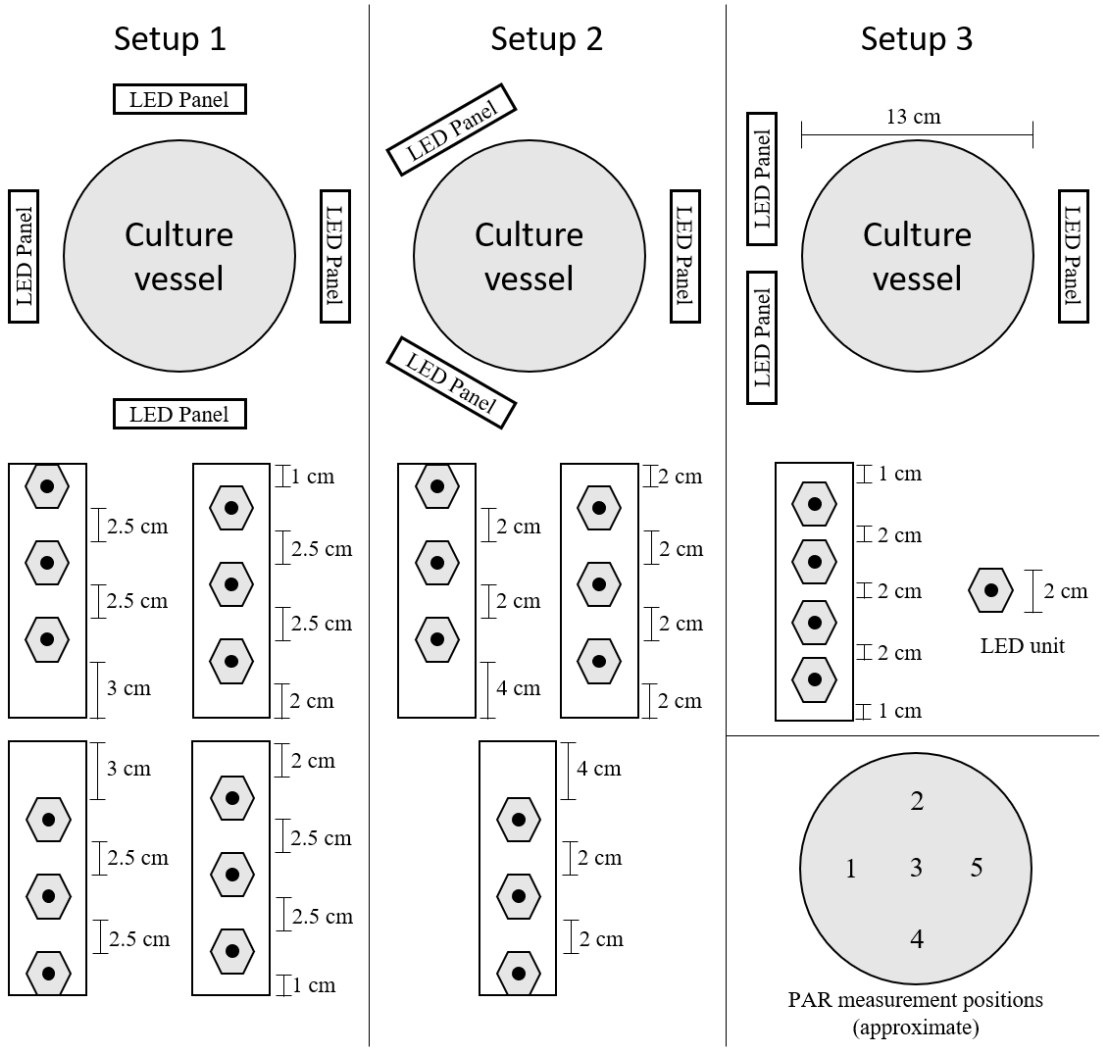

Figure 2.5.1. Three of the LEDs setups tested while attempting to reduce variability in irradiance within culture vessels. Upper section gives a top-down view, lower section indicates the positioning of LEDs on the panels shown. For setup 3 all three panels of LEDs were the same. All panels were approximately 2 cm from the culture vessel. The schematic in the bottom right indicates the approximate positions of measurements reported in Figure 2.5.2.

To assess the different setups, the culture vessels were filled with culture medium (see chapter 3) and PAR (photosynthetically active radiation) was measured using a spherical sensor at a range of depths at 5 positions within the vessel. These positions are indicated in Figure 2.5.1. Measured PAR values for the three light setups presented here are shown in Figure 2.5.2. Note that values of PAR reported here were not the maximum possible values in the final LED setup, but were measured using a consistent voltage supply (4.5 v) to LEDs on a test system.

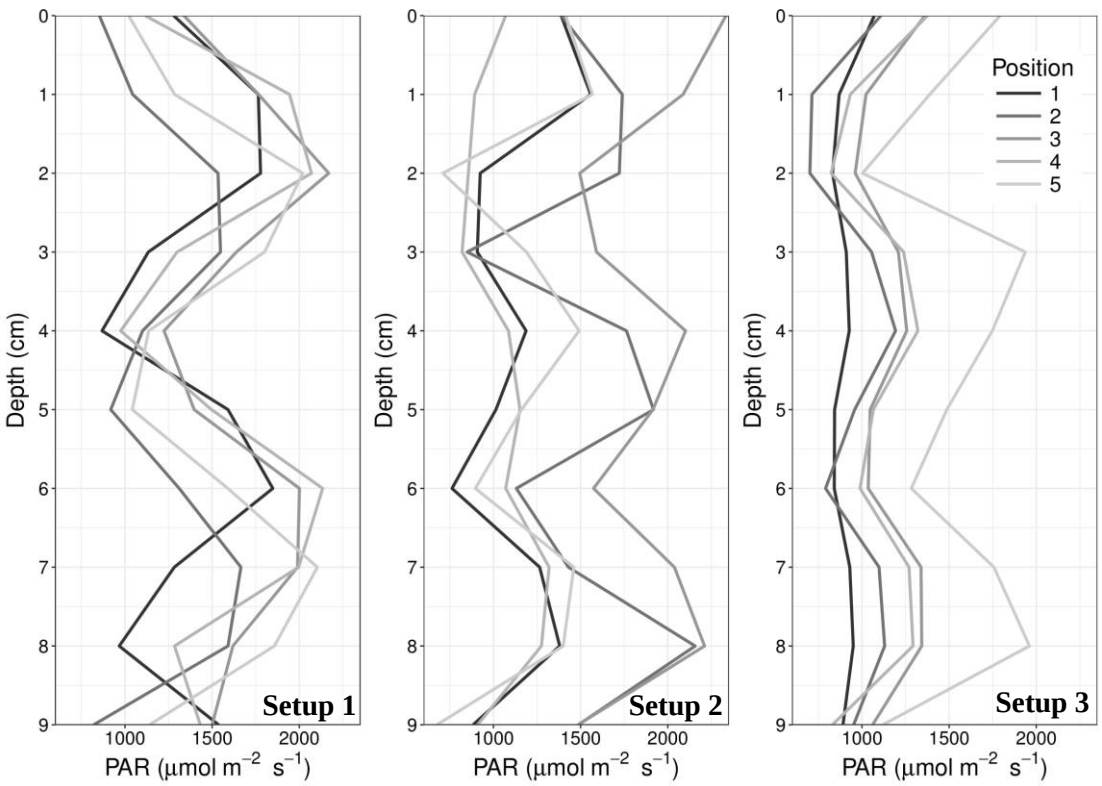

Figure 2.5.2. PAR values measured in culture vessel in 3 different LED setups. Setups and measurement positions are shown in Figure 2.5.1.

As would be expected, arranging the LEDs so they directly faced the culture vessel led to bright spots in front of the LEDs. This resulted in large

variability in PAR both vertically and horizontally, as can be seen in both setup 1 and 2. Offsetting the LEDs vertically so they were not all at the same height (as in Figure 2.5.1) had little effect on this. Positioning LEDs so they did not directly face the culture vessel (as two of the panels are in setup 3, Figure 2.5.1) was found to substantially reduce PAR variability. However, if all the LEDs were positioned in this way PAR was reduced to below what was required for light regimes described in Table 2.3.1. Setup 3 as shown in Figures 2.5.1 and 2.5.2 gave low variability in PAR compared with other approaches, but still delivered a mean irradiance sufficient for the light regimes used in this project. The standard deviation of measured PAR values was used as an objective measurement of variability. For setups 1, 2 and 3 the standard deviations of the data reported in Figure 2.5.2 are 385, 430 and 303 $\mu mol\ m^{-2}\ s^{-1}$ respectively. Demonstrating the reduced PAR variability in setup 3 compared with the other two setups. Setup 3 was therefore used in experiments.

2.6. A note on light quality

Light quality, or light spectra, is known to vary with depth because light attenuation is wavelength dependant (e.g. Morel and Maritorena, 2001). Phytoplankton are also known to respond differently to different wavelengths of light, and light absorption is wavelength dependant (Costa *et al*., 2013a;

Fujiki and Taguchi, 2002). Therefore, in order to accurately portray light variability caused by vertical mixing, the spectrum of the incident light should also be changed through the light regime. Current understanding of phytoplankton growth under dynamic light regimes is limited, variability in light quality introduces another layer of complexity into experiments. In addition, dynamically changing light spectra with changing light intensity is practically difficult. As a result, mixing-dependant changes in light quality were not addressed in this study.

3. General materials and methods

Note: Several analytical techniques are used in multiple data chapters and culture conditions remain similar between chapters. To avoid repetition, this chapter details methods which are used in multiple chapters. Methods specific to individual chapters are described at the beginning of those chapters.

3.1. Species and Culture conditions

The two diatoms *Thalassiosira pseudonana* (CCMP 1335) and *Phaeodactylum tricornutum* (CCMP 2561) were selected for this study. These species have been studied previously in fluctuating light conditions (Grouneva *et al*., 2016; Lavaud *et al*., 2016, 2007), and are often used as model laboratory species. The availability of previous research on these species against which to compare conclusions of this study was an important consideration in species selection.

Both species were grown in semi-continuous cultures under several dynamic light regimes (see chapter 2). Cultures (~500 ml) were continuously air bubbled and stirred and were maintained in exponential phase growth by frequent dilution in F/2 (Guillard, 1975; Guillard and Ryther, 1962) enriched artificial seawater (Berges *et al*., 2001). Temperature in cultures was

maintained at 20 ± 0.1 ^{o}C by incubation in water-jacketed vessels. Measurements were taken when cultures were in exponential phase, following an incubation period of approximately 2 weeks. Two replicates were achieved by growing two cultures simultaneously for each species. This process was then repeated using another two of cultures inoculated from stocks for a minimum of four replicates.

Light was provided by cool white LEDs. Emission spectra of LEDs used to illuminate cultures are illustrated in Figure 3.1.1 Light intensities reported for light regimes reflect the mean irradiance within the culture vessels, measured at a resolution of approximately 1 cm using a spherical detector.

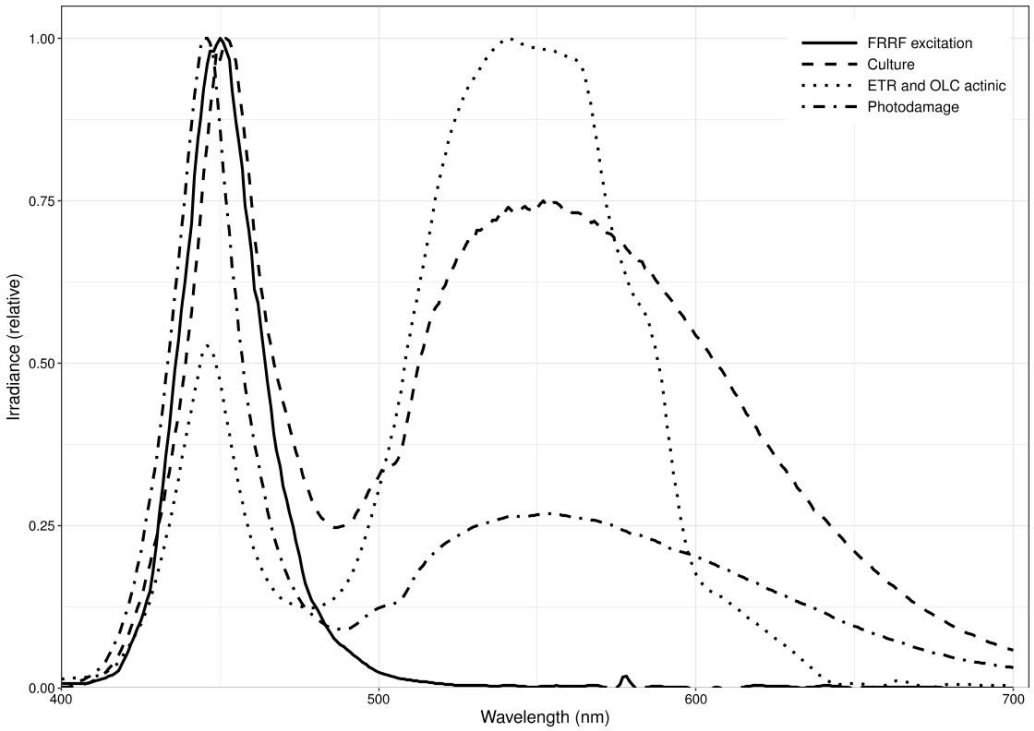

Figure 3.1.1. Emission spectra of LEDs used in excitation for single turnover FRRF measurements (section 3.4), LEDs used to illuminate cultures, actinic LEDs used in measurements of ETR and OLCs (sections 3.4 and 4.2) and LEDs used in measurement of photodamage (section 5.2). Values are normalised to a maximum of 1. Measured using a spectroradiometer (Macan).

Irradiance was controlled by a computer (software: Technologica Lab Control, U.K.).

The Equations used to describe the light environment over time and the different light regimes used in this project, are described in detail in chapter 2. Cultures were maintained optically thin to ensure the accuracy of the light regimes reported here.

Unless stated otherwise, all measurements were made at approximately midday in the light regimes, ± 2 hours, to maximise consistency in photophysiology between replicates.

3.2. Growth rate

Growth rates were calculated according to Equation 3.2.1 from extracted chlorophyll-*a* concentrations. See section 3.3 for details of the method used in chlorophyll-*a* extraction.

$$\mu = \frac{\ln([chl]_2) - \ln([chl]_1)}{t_2 - t_1} \qquad \textbf{3.2.1}$$

Where $[chl]_2$ and $[chl]_1$ are extracted chlorophyll-*a* concentrations measured at times t_1 and t_2 respectively.

3.3. *In vivo* absorption spectra and chlorophyll-*a* specific absorption coefficients

In vivo absorbance spectra of dark acclimated cultures were measured using an ICAM (integrating-cavity absorption meter) spectrophotometer (Olis CLARiTY). Absorbance spectra of live phytoplankton cannot be measured using a conventional spectrophotometer because the high turbidity of the samples causes substantial, wavelength dependant, scattering of incident light. As such, the resulting absorbance spectra can differ significantly from the actual absorbance spectra in terms of both shape and magnitude (Nelson and Prézelin, 1993; Stramski and Piskozub, 2003). This error can be avoided by use of an integrating cavity spectrophotometer, as was used here, in which the sample sits within a reflective sphere and the measuring light is applied perpendicular to the detector as a diffuse beam, rather than as a focussed beam, as in standard spectrophotometers (see Figure 3.3.1). This prevents scattering error by ensuring that scattered light is reflected around the sphere to be measured by the detector (Elterman, 1970; Fry *et al*., 1992). As well as measuring scattered light, measurement of the sample within a reflective sphere has the effect of substantially increasing the average pathlength relative to the actual size of the cuvette, since light is reflected through the sample multiple times. Although this is advantageous for measuring absorbance spectra in dilute or small volume samples, a correction must be applied in order to calculate the absorbance spectra across a 1 cm pathlength.

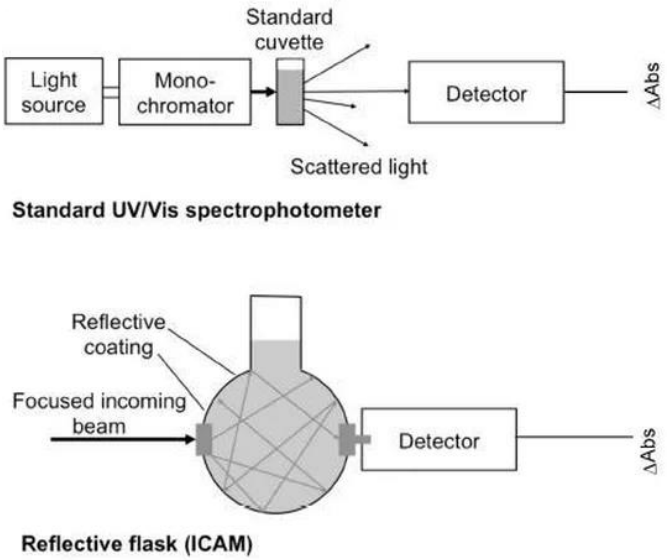

Figure 3.3.1. Comparison of a standard spectrophotometer with a fixed pathlength and an ICAM spectrophotometer.

Here a correction (Equation 3.3.1) was applied as described by Javorfi *et al.* (2006). This describes an empirical logarithmic relationship between absorbance measured using an ICAM spectrophotometer (A') and absorbance over a 1 cm pathlength (A). The coefficients of the correction (a_0 and a_1) were calculated based on absorbance values of the dye Coomassie blue (G-250) dissolved in methanol, measured using both the ICAM spectrophotometer, and a standard spectrophotometer with a 1 cm pathlength (Genesys spectrophotometer, Thermo Scientific). These coefficients were found to be variable on a day-to-day basis and were determined separately for each measurement. Three concentrations of Coomassie blue were used, the highest of which had a peak absorbance of 0.25 cm^{-1}. Care was taken to ensure that the peak absorbance of measured

culture samples was below the peak absorbance of the calibration samples. When fitting Equation 3.3.1 with Coomassie blue calibration samples the large number of very low absorbance values around the peak were found to considerably skew the fit. To avoid this only the upper 50% of absorbance data (i.e. values above the median) were used in the fit.

$$A' = a_0 \ln(1 + a_1 A) \qquad \textbf{3.3.1}$$

Both culture samples, and solutions of Coomassie blue were blank corrected. Culture samples were blank-corrected using F/2 growth medium, whilst solutions of Coomassie blue were blank corrected using methanol.

The parameters of Equation 3.3.1 varied throughout the experiment. The range of the calibration curves fitted to Equation 3.3.1 are illustrated in Figure 3.3.2. For practical reasons a number of diferent cuvettes were used throughout experiments. Optical differences between cuvettes used throughout the study are thought to be responsible for the variability in calibration curves shown in Figure 3.3.2.

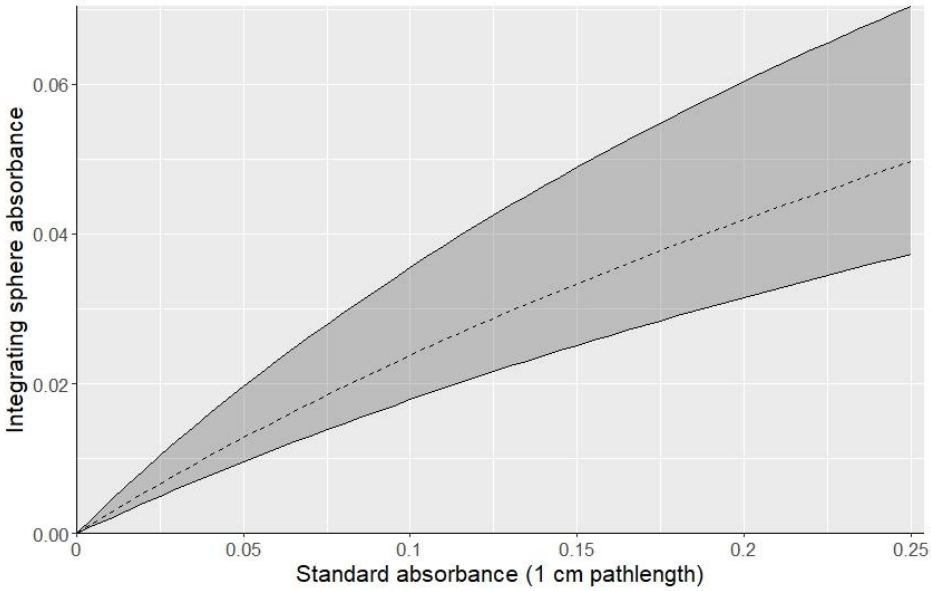

Figure 3.3.2. Range of calibration cuves resulting from fitting equation 3.3.1 to absorbance measures of Coomassie blue in an ICAM, and a standard linear spectrophotometer.

Following calculation of absorbance along a 1 cm pathlength, absorption coefficients were calculated according to Equation 3.3.2.

$$a(\lambda) = \frac{2.3A(\lambda)}{0.01} \qquad \textbf{3.3.2}$$

Where $a(\lambda)$ is the absorption coefficient (m^{-1}) at wavelength λ, $A(\lambda)$ is the corresponding absorbance in a 1 cm pathlength, the number 2.3 is a factor to convert log base 10 to base e. Chlorophyll-*a* specific absorption coefficients were then calculated according to Equation 3.3.3.

$$a^{chl} = \frac{\sum_{400}^{700} a(\lambda)}{(700 - 400)[chl]} \qquad \textbf{3.3.3}$$

Where a^{chl} is the chlorophyll-*a* specific absorption coefficient (m^2 [mg chl a]$^{-1}$), $a(\lambda)$ is the *in vivo* absorption coefficient at wavelength λ (m^{-1}), and $[chl]$ is the extracted chlorophyll-*a* concentration (mg m^{-3}).

In some cases, differences in light sources make it necessary to weight absorption coefficients to the emission spectra of the light sources in order to accurately compare measurements from different devices (e.g. see Suggett et al., 2004). Where required, this was done according to Equation 3.3.4 (Suggett et al., 2004).

$$\bar{a}^{chl} = \frac{\sum_{400}^{700}(a(\lambda) \cdot E(\lambda))}{\sum_{400}^{700} E(\lambda)\,[chl]} \qquad \textbf{3.3.4}$$

Where $\bar{a}^{chl}$ is the spectrally weighted chlorophyll-*a* specific absorption coefficient (m^2 [mg chl a]$^{-1}$) and $E(\lambda)$ is the irradiance at wavelength λ.

Chlorophyll-*a* concentrations of samples were determined fluorometrically following overnight extraction in cold 90% acetone. Before measurement samples, were centrifuged at 1000 rpm for 5 minutes to remove cell debris. Supernatant fluorescence was measured using a Trilogy Fluorometer (Turner Biosystems). Calibration of the fluorometer was performed using chlorophyll-*a* samples extracted from both species. To calibrate, the chlorophyll-*a* concentration of samples was determined

independently from absorption spectra (measured using Genesys spectrophotometer, Thermo Scientific) using the equations described by Ritchie (2006). As expected, fluorescence was linearly correlated with chlorophyll-*a* concentration within the range of values studied. The calibration is detailed in Figure 3.3.3.

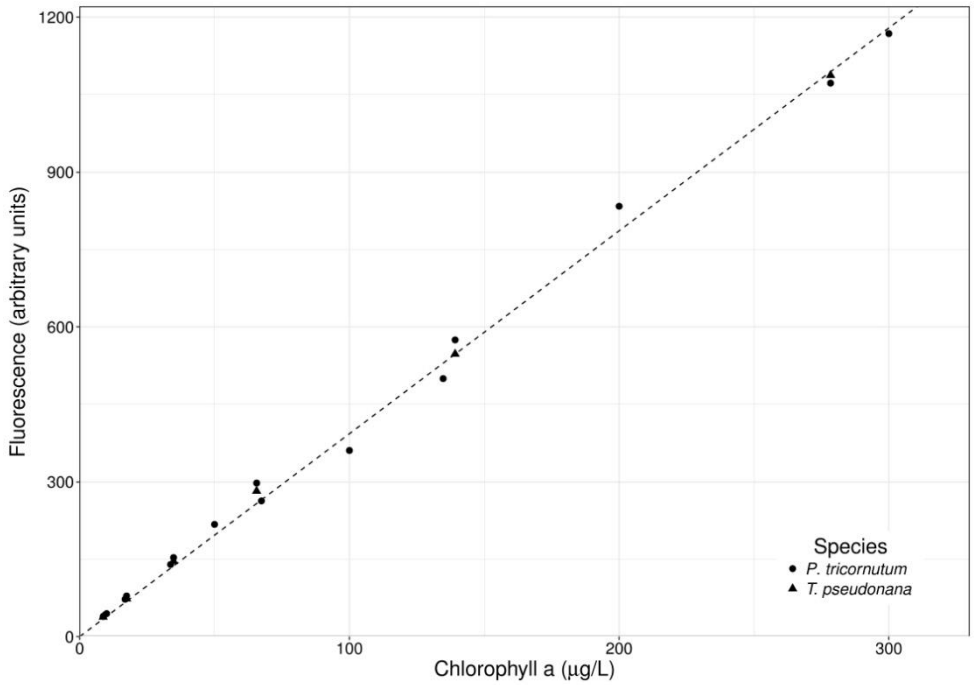

Figure 3.3.3. Calibration data for the Turner fluorometer used to measure chlorophyll-*a* concentration. Dashed line has slope 3.93 and R^2 0.99.

3.4. *In vivo* photosystem II fluorescence induction and electron transport

A fast repetition rate fluorometer (FRRF, Chelsea Technologies) was used to measure single turnover fluorescence characteristics of photosystem II (PSII) *in vivo*. This process delivers a series of rapid, subsaturating excitation pulses which progressively close PSII reaction centres by reducing the pool of Q_A (the primary electron acceptor of PSII). The short timescale over which the

excitation pulses are delivered (here 200 μs) does not permit reoxidation of Q_A by reduction of the plastoquinone pool (Kolber *et al*., 1998). Progressive closing of PSII reaction centres reduces the proportion of excitation energy that can be dissipated by PSII photochemistry (i.e. reduction of Q_A) and this instead is emitted as fluorescence, inducing a measurable increase in fluorescence over time. Measurement when all PSII reaction centres are open results in the minimum fluorescence (F_o), and the maximum proportion of energy dissipated by photochemistry, while measurement when all reaction centres are closed results in maximum fluorescence (F_m), and no deexcitation through photochemistry (Kolber *et al*., 1998). Thus, the maximum proportion of excitation energy used in photochemistry, typically referred to as the maximum photochemical efficiency of PSII designated as F_v/F_m can be calculated according to Equation 3.4.1.

$$\frac{F_v}{F_m} = \frac{F_m - F_o}{F_m} \qquad \textbf{3.4.1}$$

See Lavergne and Trissl (1995) and Trissl (2002) for a detailed explanation of the theory of fluorescence induction curves, and the derivation of this parameter. The rate at which reaction centres close, and fluorescence increases, during FRRF measurements is dependent on the effective cross section of PSII, designated σ_{PSII}, such that a more rapid increase in fluorescence is expected with a larger σ_{PSII}, and *vice versa*. Here σ_{PSII} was calculated as described in Kolber *et al*. (1998). A sample fluorescence

induction curve indicating values of F_o, F_m, F_v and σ_{PSII} is shown in Figure 3.4.1.

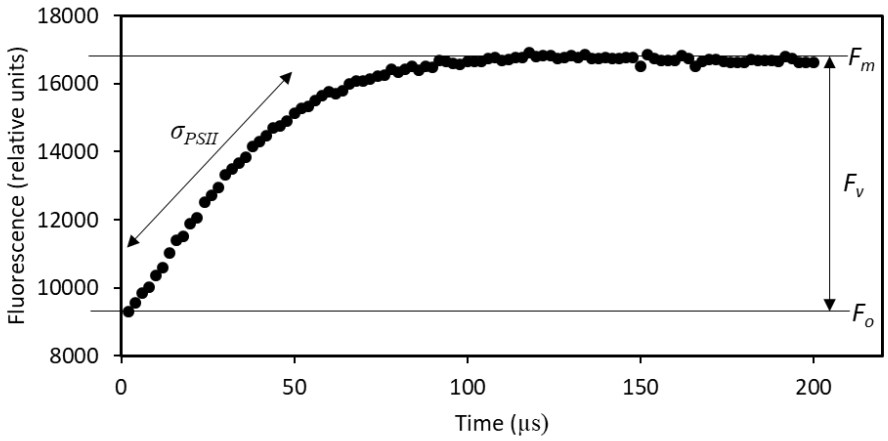

Figure 3.4.1. Sample fluorescence induction curve for *P. tricornutum.*

FRRF measurements were made following a 20 minute period of dark acclimation to allow maximum oxidation of Q_A. The FRRF protocol consisted of 100, 1 μs excitation pulses, separated by 1 μs. This was repeated 12 times at an interval of 100 ms. The resultant fluorescence induction curves were averaged to determine values of F_o, F_m and σ_{PSII}.

In addition to dark acclimated measurements, FRRF measurements were also made under actinic light. The initial fluorescence yield under actinic light differs from F_o in that PSII reaction centres are not all open, and is denoted by F' (Baker and Oxborough, 2004). FRRF measurements made under actinic light (F', F_m' and $\sigma_{PSII}{}'$ respectively) also differ from those made following dark acclimation as a result of variability in other deexcitation

pathways within PSII; in diatoms the most notable of which is non-photochemical quenching (Derks *et al*., 2015; Genty *et al*., 1989; Trissl, 2002). PSII photochemical efficiency under actinic light (F_q'/F_m') was calculated according to Equation 3.4.2. This provides an estimation of the quantum efficiency of PSII electron transport under the irradiance to which samples are acclimated (Genty *et al*., 1989), and is often referred to as PSII operating efficiency.

$$\frac{F_q'}{F_m'} = \frac{F_m' - F'}{F_m'} \qquad \textbf{3.4.2}$$

Measurements were taken under a range of actinic light intensities increased stepwise following an acclimation period of 5 minutes at each light step to allow establishment of equilibrium between processes within PSII and downstream reactions (e.g. electron transport chain and the Calvin cycle). The emission spectra of LEDs are shown in Figure 3.1.1. Light intensities used are detailed in Table 3.4.1. The temperature was maintained at 20°C throughout, using a water jacket surrounding the sample.

Table 3.4.1 PAR (µmol m^{-2} s^{-1}) values for light steps used in measurements of ETR.

Step	FRRF ETR
1	0
2	10
3	35
4	61
5	113
6	190
7	294
8	513
9	757
10	927
11	1256
12	1459

From these measurements, PSII electron transport rate (ETR, µmol e^- mg chl^{-1} s^{-1}) was calculated as the product of the PSII operating efficiency (F_q'/F_m'), the chlorophyll specific light absorption by PSII spectrally weighted to the spectra of the actinic LEDs ($\bar{a}_{act}^{chl}$,

Figure 3.1.1), and the irradiance (*I*) according to Equation 3.4.3 (Kromkamp and Forster, 2003).

$$ETR = I \cdot \frac{F_q'}{F_m'} \cdot 0.5\bar{a}_{act}^{chl} \qquad \textbf{3.4.3}$$

This calculation is based on the assumption that 50% of the light absorbed by chlorophyll is used in PSII (Gilbert *et al*., 2000). Amongst diatoms this assumption has been reported to be relatively accurate over a range of growth irradiances (Suggett *et al*., 2004).

It should be acknowledged that an alternative method of calculating ETR from FRRF measurements is possible based on the PSII functional antenna size. In this case the value of F_q'/F_m' in equation 3.4.3 can be substituted according to equation 3.4.4 (Gorbunov et al., 2001; Suggett et al., 2009)

$$\frac{F_q'}{F_m'} = \frac{\sigma_{PSII}'}{\sigma_{PSII}} \cdot \frac{F_q'}{F_v'} \cdot \frac{F_v}{F_m} \qquad \textbf{3.4.4}$$

As irradiance increases the difference between F' and F_m' within single turnover FRRF measurements decreases. As such the signal to noise ratio within the data also decreases (Figure 3.4.2). This has a greater impact on the precision of the right-hand side of equation 3.4.4 than on the left, as is evident when comparing the coefficient of variation (CV; the ratio of the standard deviation to the mean) between the two (Figure 3.4.3). Therefore, to minimise error in the calculation of ETR it was calculated as per equation 3.4.3. This method is also consistent with the method used in a number

articles cited throughout this thesis (e.g. Alderkamp et al., 2012; Dimier et al., 2009; Lefebvre et al., 2007; Shatwell et al., 2012; Wagner et al., 2006).

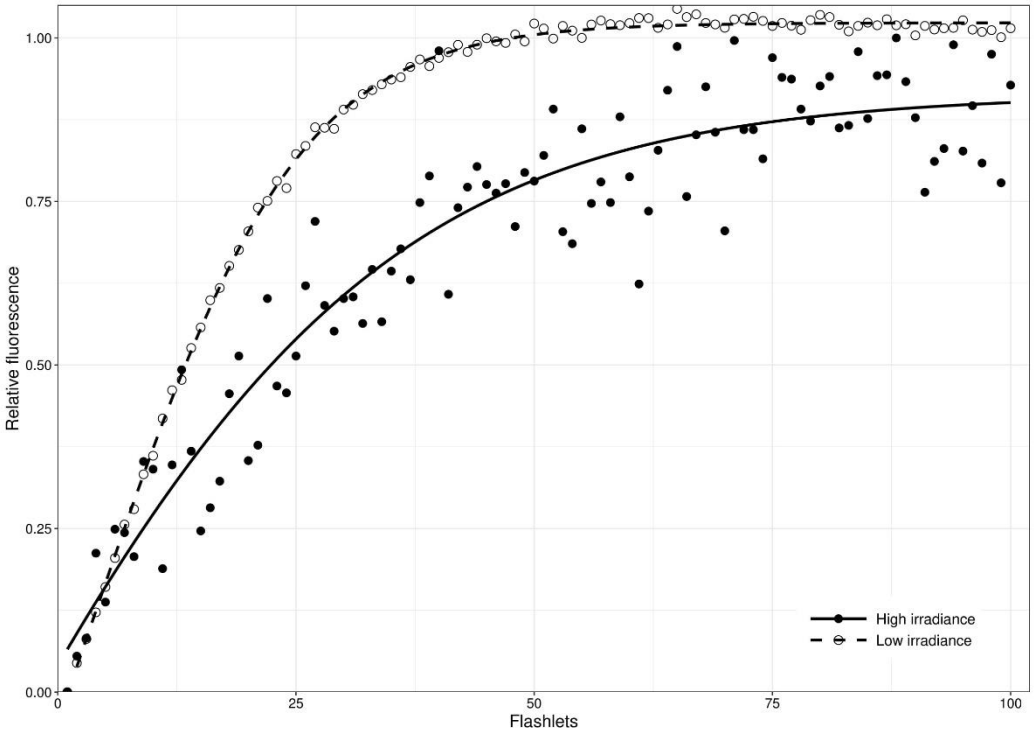

Figure 3.4.2. Two single turnover fluorescence induction curves curve for *P. tricornutum*, measured following acclimation to 10 µmol m^{-2} s^{-1} (low irradiance) and 1459 µmol m^{-2} s^{-1} (low irradiance). Fluorescence values were normalised to a range of 0-1. Lines are iterative fits based on equations presented in Kolber et al. (1998).

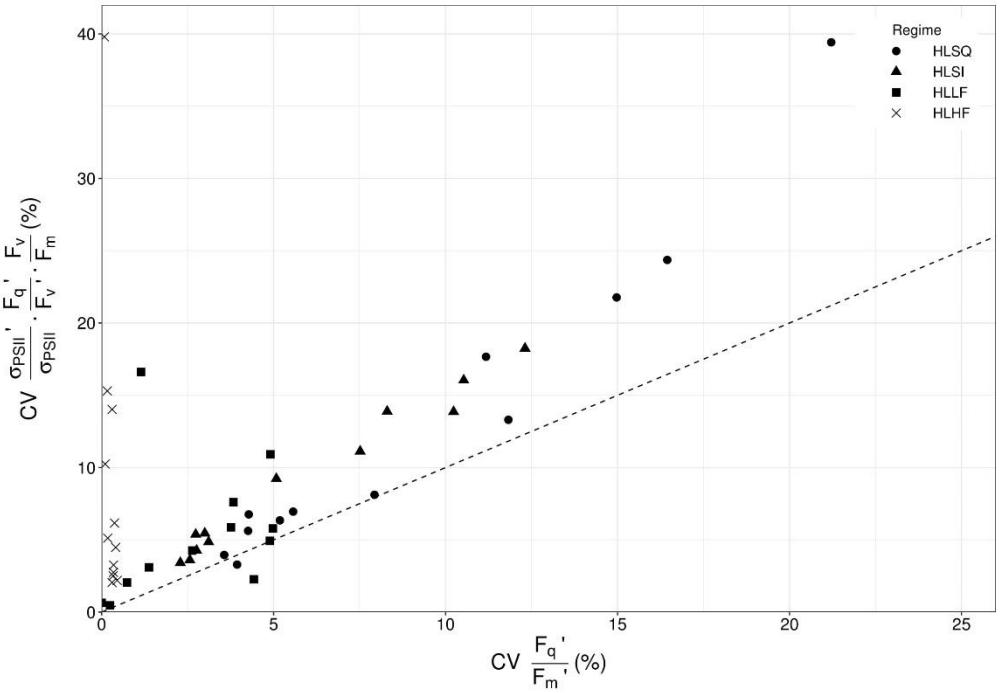

Figure 3.4.3. Coefficients of variation for the two sides of equation 3.4.4 for *P. tricornutum* grown under HL light regimes. See section 2.3 for details of light regimes. Dashed line is 1:1.

The relationship between ETR and irradiance was then fitted to Equation 3.4.5. This relationship was described by Bannister (1979) and includes a curvature parameter (b) not present in most other models of the photosynthesis irradiance response. It is used here following the recommendation of Jones *et al*. (2014), and the finding that b tended to differ between *T. pseudonana* and *P. tricornutum*.

$$ETR_{(I)} = ETR_{max} \frac{I}{\left({I_k}^b + I^b\right)^{\frac{1}{b}}} \qquad \textbf{3.4.5}$$

Where $ETR_{(I)}$ is the ETR at irradiance *I*, ETR_{max} is the maximum rate of ETR, I_k is the saturation irradiance for ETR, and b is a dimensionless curvature parameter for the model.

The initial slope of the ETR-irradiance response curve (α, µmol e^- [µmol phot]$^{-1}$ m^2 [mg chl]$^{-1}$) was calculated according to Equation 3.4.6.

$$\alpha = \frac{ETR_{max}}{I_k} \qquad \textbf{3.4.6}$$

3.5. Spectral correction of photosynthesis-irradiance curves

Cultures were grown under LEDs of different spectra than those used to measure P-I curves, either by ETR or O_2 evolution (see section 4.2 for details of O_2 evolution measurements). As such it was necessary to apply a spectral correction in order to estimate photosynthesis rates under the

growth irradiance. This is distinct from the spectral weighting of absorption coefficients described in section 3.4. Following Markager and Warwick (2001) the spectral matching parameter, absorption efficiency (A_e, dimensionless) was used. This is defined as the ratio of the spectrally weighted chlorophyll specific absorption coefficients. A_e between actinic LEDs used in both measurements of photosynthesis, and LEDs used to illuminate cultures, is described by Equation 3.5.1.

$$A_e(actinic:culture) = \frac{\bar{a}_{act}^{chl}}{\bar{a}_{cult}^{chl}} \qquad \textbf{3.5.1}$$

Where $\bar{a}_{act}^{chl}$ and $\bar{a}_{cult}^{chl}$ are the spectrally weighted chlorophyll specific absorption coefficients weighted to ETR/OLC actinic LEDs and culture LEDs respectively (Figure 3.1.1) calculated according to Equation 3.3.4. Photosynthesis-irradiance curves were then spectrally corrected by dividing α or α^{O_2} by A_e (Markager and Warwick, 2001). Note that the spectral correction has no impact on light saturated photosynthesis and therefore also effects the saturation irradiance (Equations 3.4.5 and 3.5.3). As a result the correction can also be applied by multiplying the irradiance in the P-I response by A_e with identical results. Unless specifically stated, reported P-I curves are not spectrally corrected. Spectral corrections were only performed when applying P-I curves to light regimes using culture LEDs. The values of A_e are not reported, but ranged between 0.92 and 0.95 as calculated by Equation 3.5.1.

3.6. Non-photochemical quenching

As with ETR, non-photochemical quenching (NPQ) was also calculated from steady-state fast repetition rate fluorometry data. Here the normalised Stern-Volmer coefficient (NSV) was used. This enables comparison in NPQ between samples with different values of $\frac{F_v}{F_m}$, and allows differences in the level of NPQ in dark acclimated samples to be investigated. Neither of these can be addressed using the Stern-Volmer coefficient (*SV*, Equation 3.6.1), which has historically been employed to investigate NPQ in microalgae (McKew et al., 2013).

$$SV = \frac{F_m - F'_m}{F'_m} \qquad \textbf{3.6.1}$$

The normalised Stern-Volmer coefficient was calculated according to Equation 3.6.2 (McKew et al., 2013).

$$NSV = \frac{F'_0}{F'_m - F'_0} \qquad \textbf{3.6.2}$$

Where F'_0 and F'_m are respectively the minimum and maximum PSII fluorescence under actinic light. *NSV* and *SV* are interrelated according to equation 3.6.3.

$$NSV = SV\left(\frac{F_m}{F_v} - 1\right) + \left(\frac{F_m}{F_v} - 1\right) \qquad \textbf{3.6.3}$$

The value of F_0' in equation 3.6.2 was calculated from measurements of PSII fluorescence (Equation 3.6.4) by the method described in Oxborough and Baker (1997).

$$F_0' = \frac{F_o}{F_v/F_m + F_o/F_m'} \qquad \textbf{3.6.4}$$

It is worth noting that this calculation assumes all reaction centres share a common antenna. In other words that PSII photosynthetic units are fully connected as per the lake model.

The NSV irradiance relationship was then fitted to a variation of the Hill Equation, as described in Equation 3.6.5.

$$NSV_{(I)} = \Delta NSV \frac{I^n}{{I_{50}}^n + I^n} + NSV_0 \qquad \textbf{3.6.5}$$

Where NSV_0 and ΔNSV describe the minimum NSV and the maximum increase in NSV (dimensionless), I_{50} is the half saturation irradiance for NSV, and *n* is a parameter describing the curvature of the model. Note that the maximum NSV (NSV_{max}) can be calculated by summing NSV_0 and ΔNSV according to Equation 3.6.6.

$$NSV_{max} = NSV_0 + \Delta NSV \qquad \textbf{3.6.6}$$

The NSV-irradiance relationship described here is functionally similar to the relationship described by Serôdio and Lavaud (2011), but includes a minimum NPQ parameter (NSV_0) to accommodate the use NSV as the

quantification of NPQ, rather than SV as was used by Serôdio and Lavaud (2011).

3.7. Statistical analysis

Statistical differences between variables measured under different light regimes were compared using a two-way ANOVA (analysis of variance) with light regime and species as independent variables. *Post hoc* Tukey tests were used to perform pairwise comparisons. Curve fitting was performed using the least squares method.

All statistical analyses were performed using the program R.

4. Photoacclimation: Light absorption and photosynthesis – How do cells acclimate to short term light variability?

4.1. Introduction

Whilst photoacclimation typically refers to a wide range of processes, including changes in the potential for photoprotection (Dubinsky and Stambler, 2009) this chapter deals specifically with those processes relating to light absorption, PSII electron transport, and photosynthetic CO_2 fixation.

Under static light conditions photoacclimation is well documented (Dubinsky and Stambler, 2009). As irradiance increases phytoplankton typically reduce light absorption, whilst increasing their maximum photosynthetic rate. Although phytoplankton must absorb light to photosynthesise, intracellular concentrations of molecules required for photosynthetic electron transfer and CO_2 fixation (such as plastoquinone and RUBISCO) limit the maximum amount of absorbed light that can be used photosynthetically. Excess light not used in photosynthesis can cause damage to the photosynthetic architecture (see chapter 5 for more details). As photosynthesis becomes increasingly light-saturated the potential for photodamage increases. For phytoplankton, light can therefore be likened to an essential nutrient that is harmful in high concentrations. When light is scarce phytoplankton acclimate to increase the fraction of available light that

is absorbed (Dubinsky and Stambler, 2009). Even so, the absolute amount of light energy absorbed may be relatively low and maintaining high concentrations of molecules involved in photosynthesis is energetically costly, and unnecessary if the rate of photosynthesis is light limited. Therefore, cellular concentrations of molecules such as RUBISCO tend to be relatively low (Losh *et al*., 2013), as is the maximum capacity for photosynthesis (Dubinsky and Stambler, 2009). As light intensity increases a smaller fraction of the available light is required to maintain the same rate of photosynthesis, and photosynthesis becomes increasingly light-saturated, increasing the potential for photodamage. Phytoplankton acclimate to increasing light intensity by reducing the fraction of available light which is absorbed by pigments, and by increasing the concentrations of molecules used in photosynthesis. This results in an increase in the capacity for photosynthesis and reduces the potential for photodamage (Dubinsky and Stambler, 2009).

Photoacclimation as discussed in this chapter has a comparatively long response time (Macintyre *et al*., 2000; Nymark *et al*., 2009). When the light environment is static (i.e. square wave) phytoplankton can fully photoacclimate to maximise photosynthesis and minimise photodamage throughout the photoperiod. If the light environment is dynamic, and rapidly fluctuates between photosynthetically limiting and saturating irradiance on timescales shorter than those required for photoacclimation, full acclimation is impossible. The rate constant for photoacclimation is considerably longer

than the period of light fluctuations used in this study (Macintyre *et al*., 2000; Nymark *et al*., 2009). As a result, phytoplankton are unable to fully acclimate to individual peaks and troughs in irradiance and must somehow integrate photoacclimation across a range of light intensities. It is currently unclear how this occurs.

Studies of photoacclimation to light fluctuations are highly inconsistent in how the light regime is simulated, and which parameters are controlled. This makes it difficult to determine which components of the light environment diatoms actually photoacclimate to. Several studies report no significant changes in both diatom light harvesting pigment quota, and absorption coefficients, in response to light fluctuations (Nicklisch, 1998; van de Poll *et al*., 2010; van Leeuwe *et al*., 2005). Meanwhile others report variability reflecting the differences in maximum (Yarnold *et al*., 2015) or average (Wagner *et al*., 2006) irradiance between fluctuating and non-fluctuating light regimes.

Rates of photosynthetic CO_2 fixation, and photosynthetic electron transport, place a fundamental restriction on phytoplankton growth, yet in the context of intra-diel light variability have received almost no attention. Several authors have suggested that reductions in growth rate under higher amplitudes of fluctuating light are caused by reduced overall photosynthetic efficiency (e.g. Litchman, 2000; Shatwell *et al*., 2012), however it remains unclear how the characteristics of the photosynthesis-irradiance (P-I)

response acclimate to predictable intradiel variability in irradiance. This chapter attempts to address this by investigating the relationship between a number of descriptors of the light environment and several parameters of photoacclimation. The aim of this chapter is to characterise photoacclimation to different amplitudes of light fluctuations, and to attempt to determine whether or not photoacclimation of the two diatoms studied can be predicted from parameters descriptive of the light regime (see sections 2.3 and 2.4 for details of the parameters in question).

4.2. Materials and methods

Culture conditions were as described in section 3.1. Growth rates, chlorophyll-*a* absorption coefficients, and FRRF measurements were all carried out at approximately midday within the photoperiod according to the methods described in sections 3.2 to 3.5.

Measurements of oxygen evolution were made using a Clarke electrode (Hansatech Oxygraph, Hansatech Instruments). The electrode was prepared using a 50% saturated solution of KCl as an electrolyte according to the following procedure:

1. A small drop of electrolyte was placed on the cathode.

2. This was covered with a square of thin paper spacer, care was taken to ensure this established a connection between the anode and cathode.
3. A square of PTFE membrane larger than the paper spacer was placed on top, and sealed with a rubber o-ring, making sure there were no air bubbles or tears in the membrane or paper.
4. The water-jacketed sample chamber was sealed around the electrode.

The electrode was calibrated following each preparation. Air saturated water which had been bubbled for ~10 minutes was used as the high end of the calibration, after which the strong reducing agent sodium dithionite was added to the water to reach 0% oxygen saturation. During calibration and measurement, the sample chamber was continuously mixed by a magnetic stirrer. The temperature in the sample chamber was maintained at 20^{o}C.

To increase the signal to noise ratio samples of cultures were concentrated to an approximate chlorophyll concentration of 1000 μg L^{-1} by centrifuging, using the procedure described in section 3.3. Oxygen light curves (OLCs) were then measured according to the following procedure: Samples were dark acclimated for 20 minutes, then 2 ml was added to the electrode sample chamber. Oxygen concentration was measured over a range of actinic light intensities increased stepwise following an initial dark step, each step was 5 minutes in duration. The temperature was maintained at 20^{o}C

throughout measurements using a water jacket surrounding the sample. Illumination was provided by Act 2 system LEDs (Chelsea Technologies Group). LED emission spectra were identical to those used in measurements of ETR as described in section 3.4, and can be seen in Figure 3.1.1 (page 38).

Due to instrumental limitations light steps could not be of the same intensities as those used to measure the ETR-irradiance response. These are detailed in Table 4.2.1, alongside those used in measurements of ETR for ease of comparison. At each light step the rate of oxygen evolution was calculated as the slope of a linear regression between oxygen concentration and time, using only the final 1-minute of each 5-minute step to allow establishment of an equilibrium between processes involved in oxygen evolution and uptake. Chlorophyll specific gross photosynthesis (P_{gross}, µmol O_2 mg chl^{-1} s^{-1}) at each light step was calculated by Equation 4.2.1.

Table 4.2.1. PAR values for light steps used in measurements of ETR and O_2 evolution.

	PAR (µmol m^{-2} s^{-1})	
Step	FRRF ETR	O_2
1	0	0
2	10	29
3	35	66
4	61	111
5	113	167
6	190	237
7	294	324
8	513	432
9	757	566
10	927	734
11	1256	941
12	1459	1200

$$P_{gross} = \frac{P_n - R}{[chl]} \qquad \textbf{4.2.1}$$

Where P_n is the net rate of photosynthesis measured within the sample chamber and R is the rate of respiration measured as the rate of change in oxygen concentration during the initial dark step. $[chl]$ is the

chlorophyll concentration of the sample measured as per section 3.3. This assumes there is no significant photorespiration or other light-dependant O_2 consumption, and that respiration is consistent throughout light steps.

Resultant values of P_{gross} were fitted to Equation 4.2.2. This is identical to Equation 3.4.5 with terms substituted.

$$P_{gross\ (I)} = P_{max} \frac{I}{\left(\left({I_k}^{O_2} \right)^{b^{O_2}} + I^{b^{O_2}} \right)^{\frac{1}{b^{O_2}}}} \qquad \textbf{4.2.2}$$

Where $P_{gross\ (I)}$ is the gross photosynthesis at irradiance I, P_{max} is the maximum rate of photosynthesis (µmol O_2 mg chl^{-1} s^{-1}), ${I_k}^{O_2}$ is the saturation irradiance for photosynthesis, and b^{O_2} is a curvature parameter for the model. The initial slope of the photosynthesis – irradiance response (P-I) curve was calculated according to Equation 4.2.3 and is denoted by α^{O_2}(µmol O_2 [µmol phot]$^{-1}$ m^2 [mg chl]$^{-1}$).

$$\alpha^{O_2} = \frac{P_{max}}{{I_k}^{O_2}} \qquad \textbf{4.2.3}$$

To avoid confusion the term photosynthesis is used exclusively when discussing the results of OLCs, while ETR is used in reference to data from fluorescence measurements.

Since measurements of ETR and O_2 evolution were made under light sources with the same emission spectra (Figure 3.1.1, page 38) they could be compared directly without any further spectral corrections. Unfortunately,

hardware restrictions prevented matching the irradiance of actinic LEDs between these two measurements (Table 4.2.1). To compare ETR and O_2 evolution ETR was calculated from the fitted ETR-irradiance response curves at the irradiance values used to measure O_2 evolution. The Act 2 system used for illumination in OLCs was provided on loan from Kevin Oxborough (Chelsea Technologies Group). Unfortunately, it was not available for the entirety of the project and a suitable replacement could not be found. As such measurements of O_2 evolution were only performed for cultures of *T. pseudonana* grown under a limited range of light regimes.

PSII photosynthetic unit size (n_{PSII}) was estimated based on measurements of σ_{PSII} and a^{chl}. Suggett *et al*. (2004) demonstrated that values of chlorophyll-*a* specific light absorption by PSII (a^{chl}_{PSII}) calculated from optical (as in this study) and biophysical measurement are highly correlated. Assuming equivalence of optical and biophysical measurements of $\bar{a}^{chl}_{PSII}$, n_{PSII} can be calculated according to Equation 4.2.4.

$$n_{PSII} = \frac{\bar{a}^{chl}_{PSII}}{0.675\sigma_{PSII}} \qquad \textbf{4.2.4}$$

Where n_{PSII} has units mol RCII [mol chl]$^{-1}$ and the factor 0.675 is used to convert nm^2 to m^2 and mg chl to mol chl, $\bar{a}^{chl}_{PSII}$ is calculated according to Equation 4.2.5, this is consistent with the calculation of ETR assuming 50% of the total light absorbed is transferred to PSII. In Equation 4.2.5 $\bar{a}^{chl}_{FRRF}$ is the

chlorophyll-*a* specific absorption coefficient weighted to the emission spectra of the FRRF excitation LEDs (see Figure 3.1.1), calculated according to Equation 3.3.4.

$$\bar{a}_{PSII}^{chl} = 0.5\bar{a}_{FRRF}^{chl} \qquad \textbf{4.2.5}$$

An alternative method to estimate n_{PSII} from FRRF measurements was described in Oxborough et al. (2012). However, this method requires knowledge of instrument-specific parameters that must be determined from independent calibrations between fluorescence measurements and flash-yield determinations of PSII reaction centre concentrations. Since these were not available for the instruments used in the present study the method described by Oxborough et al. (2012) could not be employed here.

To investigate what aspects of the light environment most influence the photoacclimation of phytoplankton exposed to variable light regimes, and whether photoacclimation can be predicted in terms of parameters descriptive of the light environment, a series of linear regressions were performed. An initial test for multicollinearity between descriptive parameters (parameters are summarised in Table 2.3.1) using the variance inflation factor (VIF) revealed substantial multicollinearity (VIF >> 10). This is to be expected since the number of light regimes is small, and some parameters may correlate since the light regimes vary predictably. As multicollinearity was high, rather than performing a single multiple linear

regression, linear regressions were performed separately for each parameter. This approach is also more in line with modelling approaches where photoacclimation may be described in terms of a single light regime parameter (e.g. Behrenfeld *et al*., 2016; Graff *et al*., 2016). To control for the potential for species-specific responses the species was included as an interaction term in the model. Since the intention was to exclusively examine photoacclimation in variable light regimes, data from square-wave regimes were excluded from this analysis.

4.3. Results

Chlorophyll-*a* specific light absorption coefficients, effective PSII antenna size (σ_{PSII}) and estimates of n_{PSII} derived from these are shown in Table 4.3.1 along with growth rates. Note that a decrease in n_{PSII} indicates an increase in the number of chlorophyll-*a* molecules per RCII. Both a^{chl} and n_{PSII} were significantly higher in *T. pseudonana* than in *P. tricornutum* ($F_{1,33}$=6.35 p=0.016, and $F_{1,34}$=19.96 p<0.01 respectively). In contrast σ_{PSII} was significantly larger in *P. tricornutum* than in *T. pseudonana* ($F_{1,43}$=16.1 p<0.01). Between HL and LL light regimes with similar fluctuation characteristics acclimation is consistent with that observed in square-wave light regimes to increased light. Namely, a reduction in a^{chl} and n_{PSII} and a concurrent increase in σ_{PSII} (Dubinsky and Stambler, 2009; Falkowski and Owens, 1980;

Moisan and Mitchell, 1999). Within fluctuating regimes an increase in fluctuation amplitude from SI to HF results in a consistent increase in a^{chl} and n_{PSII}, and little change in σ_{PSII} in both species, akin to acclimation to a reduction in irradiance under square-wave light regimes (Dubinsky and Stambler, 2009).

Table 4.3.1. Chlorophyll-*a* specific absorption coefficients (a^{chl}, m^2 mg chl^{-1}), effective PSII antenna size (σ_{PSII}, nm^2), PSII unit size (n_{PSII}, mol RCII mol chl^{-1}) and growth rate (μ, day^{-1}) for two species grown under a range of light regimes. Values in brackets are 1 standard deviation. Values that share a letter are not significantly different ($p>0.05$). Sets of letters are conserved between species. Grey fills graphically indicate the values on a scale from 0 to the maximum value for each parameter.

		HL Regimes				LL Regimes			
		HLSQ	HLSI	HLLF	HLHF	LLSQ	LLSI	LLLF	LLHF
T. pseudonana	a^{chl}	0. 0080^{a,b} (0.0008)	0.0063^{a,b,c,d} (0.0009)	0.0071^{a,b,c} (0.0016)	0.0087^{a} (0.0014)		0.0042$^{c.d}$ (0.0006)	0.0059^{a,b,c,d} (0.0010)	0.0082^{a} (0.00004)
	σ_{PSII}	1.77^{c,d,e} (0.15)	1.38^{f} (0.35)	1.32^{f} (0.16)	1.42^{e,f} (0.21)	2.19^{a,b,c} (0.19)	1.85^{c,d,e} (0.11)	1.86^{b,c,d,e} (0.16)	2.08^{a,b,c,d} (0.17)
	n_{PSII}	0.0066^{a,b} (0.0004)	0.0063^{a,b} (0.0017)	0.0070^{a,b} (0.0012)	0.0087^{a} (0.0020)		0.0033^{c} (0.0009)	0.0043^{b,c} (0.0009)	0.0053^{a,b,c} (0.00002)
	μ	0.76^{a} (0.12)	0.56^{b,c,d} (0.11)	0.51^{b,c,d,e} (0.03)	0.38^{c,d,e} (0.02)		0.36^{d,e} (0.07)	0.37^{c,d,e} (0.18)	0.32^{e} (0.12)
P. tricornutum	a^{chl}	0.0075^{a,b,c} (0.0011)	0.0053^{a,b,c,d} (0.0010)	0.0056^{a,b,c} (0.0002)	0.0081^{a,b} (0.0001)		0.0031^{d} (0.0008)	0.0044^{b,c,d} (0.0007)	
	σ_{PSII}	2.25^{a,b} (0.12)	1.54^{e,f} (0.02)	1.63^{d,e,f} (0.15)	1.62^{d,e,f} 0.04)	2.47^{a} (0.31)	1.92^{b,c,d,e} (0.15)	1.75^{c,d,e,f} (0.07)	
	n_{PSII}	0.0047^{b,c} (0.0009)	0.0050^{b,c} 0.0012)	0.0050^{b,c} (0.0001)	0.0071^{a,b} (0.0005)		0.0023^{c} (0.0008)	0.0032^{c} (0.0009)	
	μ	0.83^{a} (0.13)	0.77^{a} (0.06)	0.60^{a,b,c} (0.04)	0.51^{b,c,d,e} (0.02)		0.65^{a,b} (0.08)	0.48^{b,c,d,e} (0.02)	

Comparing square-wave and fluctuating light regimes shows a considerable reduction in σ_{PSII} when a sinusoidal or fluctuating component is included in light regimes, while a^{chl} tends to decrease, and n_{PSII} generally increases. Interestingly, a^{chl} in both species under a square-wave regime appears to be comparable to that of cells grown under a high amplitude fluctuating light regime of equivalent light dose. Assuming the increase in a^{chl} between LLSI and HLSI is conserved when light dose increases a^{chl} in a square-wave light regime may also be comparable to that under a sinusoidal light regime of higher light dose. In contrast n_{PSII} under a square-wave regime is statistically similar to that under a sinusoidal regime of the same dose in both species.

Growth rate was significantly lower in *T. pseudonana* than in *P. tricornutum* ($F_{1,43}$=40.1 $p<0.01$). Growth rates of both species were lower in LL light regimes compared with HL regimes with similar fluctuation characteristics and tended to decrease in fluctuating regimes as the fluctuation amplitude increased (i.e. from SI to HF). Compared with *P. tricornutum* growth rates of *T. pseudonana* show relatively little variability between SI and LF regimes. In both species growth under a square-wave regime was faster than under fluctuating regimes of the same dose, although this difference is only statistically significant when comparing HLSQ and HLHF regimes. *P. tricornutum* seems to be less negatively affected than *T. pseudonana* by the addition of variability to light regimes. Growth rates under

fluctuating light regimes are 93%, 72% and 62% of those under HLSQ for HLSI, HLLF, and HLHF regimes respectively for *P. tricornutum*. Meanwhile, for *T. pseudonana* growth rates under HLSI, HLLF and HLHF regimes are respectively 74%, 67% and 50% of the growth rate under HLSQ.

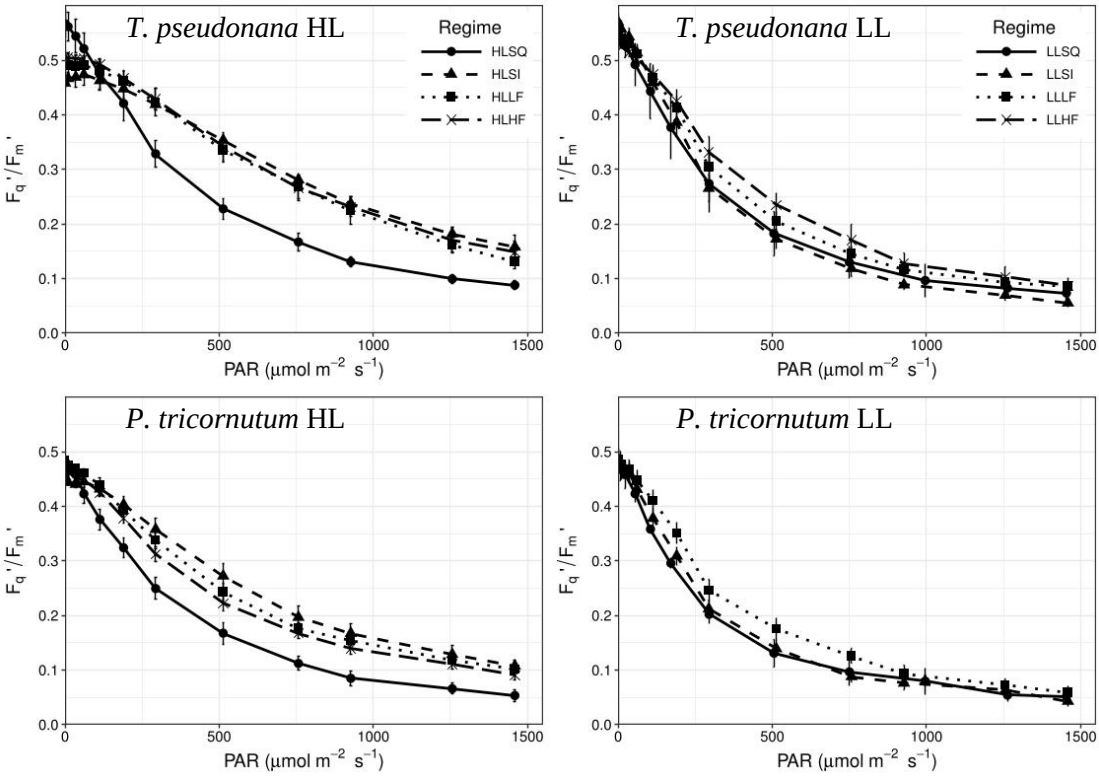

Figure 4.3.1. Relationship between PSII operating efficiency and light intensity in two diatoms grown under several fluctuating and square-wave light regimes. Error bars are 1 standard deviation.

PSII operating efficiency (F_q'/F_m') showed little response to changes in light fluctuations at LL (Figure 4.3.1), although it was considerably lower at any incident irradiance in HLSQ compared with HL fluctuating regimes. Under LL F_q'/F_m' generally decreased more rapidly with increased irradiance than under HL, regardless of light fluctuations, and generally decreased more

rapidly in *P. tricornutum* than in *T. pseudonana*. Dark acclimated, maximum photochemical quenching efficiency (F_v/F_m) also tended to be slightly higher in *T. pseudonana*.

Curve fits of the photosynthesis-irradiance response curves measured from ETR and O_2 evolution data are illustrated in Figures 4.3.2 and 4.3.3. Parameters of the fitted model are detailed in Table 4.3.2 and 4.3.3. For ETR measurements of the LLSQ regime α and ETR_{max} are missing because measurements of a^{chl} were not available, and these parameters could not be calculated from F_q'/F_m'. Data for I_k and b are shown because these parameters are independent of light absorption (Blache *et al*., 2011). Values of α, ETR_{max} and I_k were significantly higher in *T. pseudonana* than in *P. tricornutum* ($F_{1,37}$=34.5 p<0.01, $F_{1,37}$=51.0, p<0.01 and $F_{1,41}$=43.0, p<0.01 respectively), b was not significantly different between species ($F_{1,41}$=2.0, p=0.16).

Within fluctuating light regimes variability in ETR_{max} and α are consistent with the observed variability in a^{chl}. Both are consistently higher in HL regimes than in LL regimes with similar fluctuation characteristics and increase significantly between SI and HF fluctuating regimes. Compared with square-wave regimes, ETR_{max} is higher under fluctuating light regimes in both species. Conversely, α is lower under HLSI and HLHF regimes than under HLSQ. However, because α increases with fluctuation amplitude α under HLHF is equal to, or greater than, α under HLSQ. Among fluctuating regimes I_k

is significantly lower in LL regimes. Interestingly the trend in I_k with changing fluctuation amplitude is different between HL and LL. Under the former, I_k tends to decrease from SI to HF (although is slightly lower under HLLF than HLHF for *T. pseudonana*), while under the latter the reverse appears to be true. Compared with SQ regimes, I_k is typically higher under fluctuating

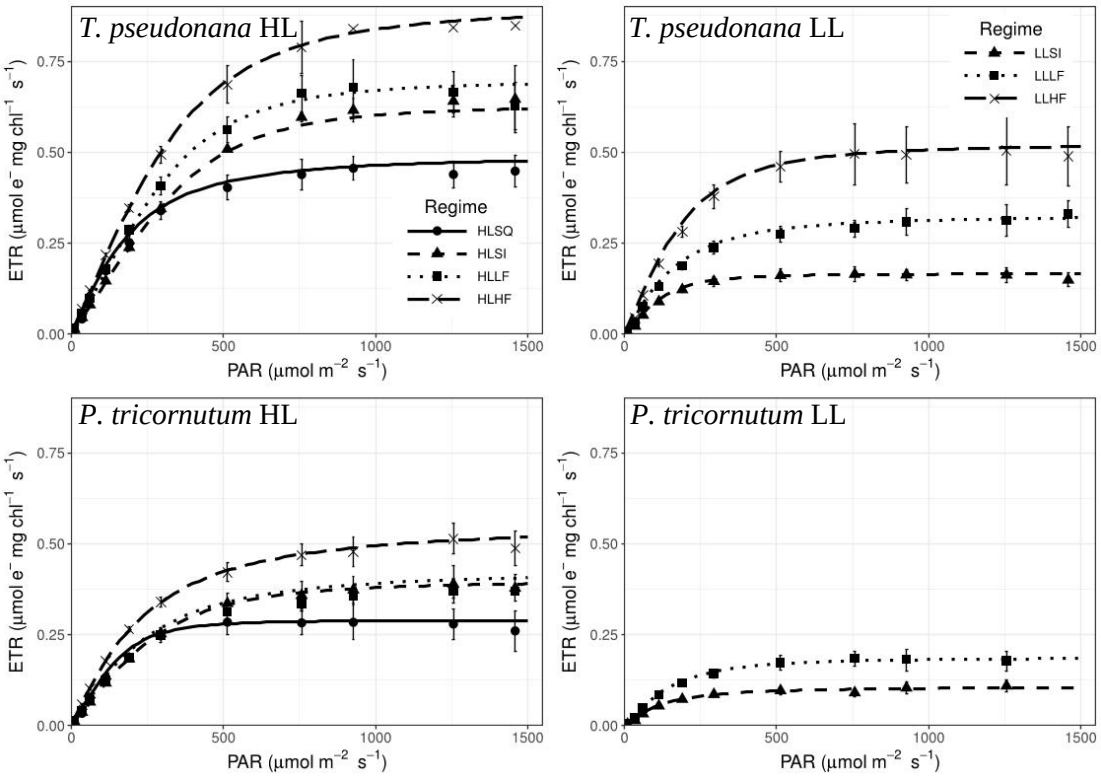

Figure 4.3.2. Relationship between PSII Electron transport rate and light intensity in two diatoms grown under several fluctuating and square-wave light regimes. Parameters of curves fits can be found in table 4.3.2. Error bars are 1 standard deviation.

regimes, although this difference is only significant at HL.

Notably, the parameters of the ETR-irradiance response for *T. pseudonana* are statistically similar between HLSQ and LLHF. The same is true for HLSQ and LLLF in *P tricornutum,* although the numerical difference is greater. Thus, the ETR-irradiance response measured under a square-wave

light regime is comparable to that a under a high amplitude fluctuating light regime with a lower light dose.

The curvature of the ETR-irradiance relationship, b, was variable between species and light regimes (Table 4.3.2). The physiological relevance of b is not well understood. It appears to be impacted by a number of factors, including intercellular and intracellular self-shading, PSII connectivity, and size of the plastoquinone pool (Jones *et al*., 2014). As such values of b are reported here for completeness but are not discussed.

Table 4.3.2. Parameters of the ETR-irradiance response curve for two species grown under a range of light regimes. Initial slope, α (µmol e^- [µmol phot]$^{-1}$ m^2 [mg chl]$^{-1}$), maximum ETR, ETR_{max} (µmol e^- [mg chl]$^{-1}$ s^{-1}), saturation irradiance, I_k (µmol m^{-2} s^{-1}) and curvature parameter, b (dimensionless). Values in brackets are 1 standard deviation. Values that share a letter are not significantly different (p>0.05). Sets of letters are conserved between species. Grey fills graphically indicate the values on a scale from 0 to the maximum value for each parameter.

		HL Regimes				LL Regimes			
		HLSQ	HLSI	HLLF	HLHF	LLSQ	LLSI	LLLF	LLHF
T. pseudonana	α	0.0019 ^{a} (1.4 x10^{-4})	0.0013 ^{c,d,e,f,g} (2.6 x10^{-4})	0.0015 ^{a,b,c,d,e} (7.7 x10^{-5})	0.0019 ^{a,b} (3.5 x10^{-4})		0.0010^{f,g} (6.8 x10^{-5})	0.0015^{b,c,d,e,f} (4.7 x10^{-4})	0.0020^{a,b,c} (1.5 x10^{-4})
	ETR_{max}	0.490^{c,d} (0.066)	0.628^{b,c} (0.177)	0.696^{a,b} 0.153)	0.896^{a} (0.141)		0.166^{f} (0.014)	0.327^{d,e,f} (0.116)	0.522^{b,c,d} (0.095)
	I_k	257.4^{d,e} (23.3)	493.7^{a} (63.5)	452^{a,b} (29.7)	463.7^{a} (30.3)	188.57^{e,f,g} (42.7)	167.3^{f,g} (18.2)	216.4^{e,f} (16.8)	263.7^{d,e} (37.6)
	b	1.71^{c} (0.23)	2.88^{a} (0.27)	2.77^{a,b} (0.03)	2.31^{a,b,c} (0.31)	1.61^{c} (0.33)	2.21^{a,b,c} (0.36)	1.67^{c} (0.50)	2.05^{a,b,c} (0.45)
P. tricornutum	α	0.0014 ^{b,c,d,e,f} (1.7 x10^{-4})	0.0011 ^{e,f,g} (1.4 x10^{-4})	0.0012 ^{d,e,f,g} (5.3 x10^{-5})	0.0018 ^{a,b,c,d} (1.1 x10^{-4})		0.0007 ^{g} (3.1 x10^{-5})	0.0009^{f,g} (4.9 x10^{-5})	
	ETR_{max}	0.290^{d,e,f} (0.051)	0.398^{c,d,e} (0.024)	0.424^{c,d,e} (0.054)	0.550^{b,c} (0.062)		0.107^{f} (0.021)	0.187^{e,f} (0.015)	
	I_k	211.5^{e,f,g} (21.3)	371^{b,c} (39.5)	320^{c,d} (12.7)	302^{c,d} (26.2)	141.8^{g} (15.7)	149.2^{f,g} (6.1)	203^{e,f,g} (10.9)	
	b	2.63^{a,c} (0.93)	2.20^{a,b,c} (0.18)	1.68^{c} (0.11)	1.47^{c} (0.08)	1.91^{a,b,c} (0.08)	1.42^{c} (0.09)	1.78^{b,c} (0.04)	

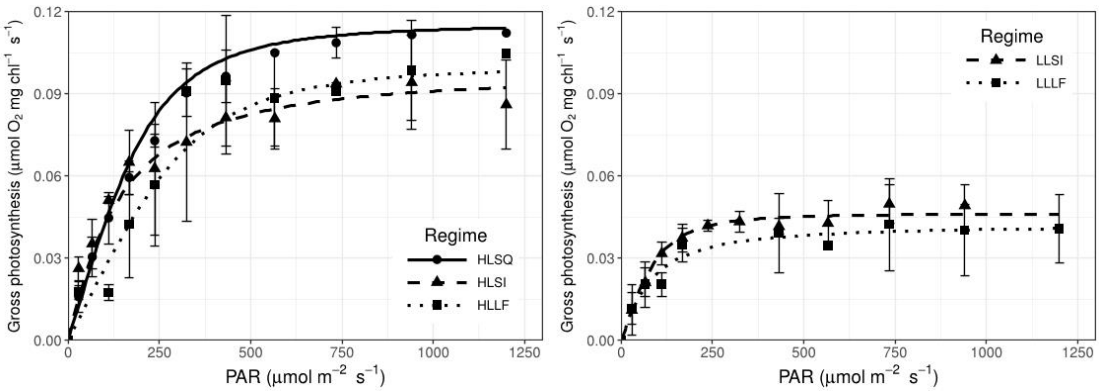

Figure 4.3.3. Relationship between O_2 evolution and light intensity in *T. pseudonana* grown under several fluctuating and square-wave light regimes. Parameters of curve fits can be found in table 4.3.3. Error bars are 1 standard deviation.

The P-I response for *T. pseudonana,* measured by O_2 evolution, is somewhat different to the ETR-irradiance response (Figure 4.3.3 and Table 4.3.3). Similar to measurements of ETR_{max}, P_{max} was significantly reduced by a decrease in mean irradiance, consistent with acclimation to square-wave light regimes (Dubinsky and Stambler, 2009). However, unlike in measurements of ETR, neither α^{O_2} or P_{max} were significantly affected by the inclusion of a fluctuating component in light regimes. Nor were they much affected by changes in the amplitude of fluctuations. In contrast with the trend in α, α^{O_2} somewhat decreased between SI and LF light regimes under both HL and LL. The saturation irradiance of O_2 production, ${I_k}^{O_2}$, did not significantly differ between HLSQ and HLSI regimes unlike I_k for ETR, and was only significantly higher under HLLF. Similar to ETR, ${I_k}^{O_2}$ was reduced under LL regimes compared with HL regimes. ETR under a square-wave regime was similar to that under a high amplitude fluctuation regime of lower dose. This does not appear to be the case for photosynthetic O_2 production. OLCs are

affected comparatively little by light fluctuations, and the light dose appears to dominate observed variability.

Table 4.3.3. Parameters of the photosynthesis-irradiance response curve measured by O_2 evolution for *T. pseudonana* grown under a range of light regimes. Initial slope, α^{O_2} (µmol O_2 [µmol phot]$^{-1}$ m^2 [mg chl]$^{-1}$), maximum gross photosynthesis, P_{max} (µmol O_2 [mg chl]$^{-1}$ s^{-1}), saturation irradiance, $I_k{}^{O_2}$ (µmol m^{-2} s^{-1}) and curvature parameter, b^{O_2} (dimensionless). Values in brackets are 1 standard deviation. Values that share a letter are not significantly different (p>0.05). Sets of letters are conserved between species.

		HL Regimes			LL Regimes	
		HLSQ	HLSI	HLLF	LLSI	LLLF
T. pseudonana	α^{O_2}	4.7 x10^{-4} ^{a} (1.4 x10^{-4})	5.7 x10^{-4} ^{a} (5.7 x10^{-5})	3.3 x10^{-4} ^{a} (1.8 x10^{-4})	4.3 x10^{-4} ^{a} (1.0 x10^{-4})	4.3 x10^{-4} ^{a} (1.4 x10^{-4})
	P_{max}	0.115^{a} (0.020)	0.089^{a} (0.024)	0.100^{a} (0.022)	0.046^{b} (0.004)	0.042^{b} (0.009)
	$I_k{}^{O_2}$	216.6^{a,b} (64.5)	169.4^{b} (24.9)	376.7^{a} (69.2)	119.5^{b} (43.7)	98.9^{b} (7.0)
	b^{O_2}	2.34^{a} (1.16)	1.29^{a} (0.47)	2.54^{a} (1.22)	2.1^{a} (1.0)	1.27^{a} (0.03)

Whether photoacclimation can be reliably described in terms of a single parameter of the light regime was investigated using several linear regressions. Correlation coefficients for these regressions, and the best predictive model for each measure of photoacclimation, are reported in Table 4.3.4. Overall I_{Med}^{D} was the parameter best able to predict photoacclimation as measured by the variables in Table 2.3.1. I_{Med}^{D} was the most strongly correlated parameter with 3 of the 6 variables, and only correlated poorly with σ_{PSII}. Since I_M and I_{Med}^{D} were highly collinear within LF and HF regimes, R^2 for models using I_M are also relatively high. Mean irradiance, $\bar{I}$ correlated relatively strongly with σ_{PSII} and ETR_{max}, and was highly correlated with I_k.

Table 4.3.4. R^2 values for a series of linear regressions between parameters descriptive of the light environment and several indicators of photoacclimation in *T. pseudonana* and *P. tricornutum* grown under fluctuating light. Highest R^2 values are in bold and the linear model these derive from are given. Values in brackets are p-values for the regression terms directly above them. Species (*Spp*) is included as an interaction term. For details of abbreviations and symbols see Table II.

		I_M	$\frac{z_{mix}}{z_{eu}}$	$\bar{I}$	I_{Med}	I_{Med}^D
a^{chl}	R^2	0.58	0.52	0.34	0.15	**0.59**
	Model (p-value)	$0.0025 + 6.70 \times 10^{-6} I_{Med}^D + 0.0019 Spp - 1.2 \times 10^{-6} \left(I_{Med}^D \cdot Spp\right)$				
		(0.001)	(<0.001)	(0.053)	(0.560)	
σ_{PSII}	R^2	0.19	0.02	**0.65**	0.30	0.28
	Model (p-value)	$2.02 - 0.0015\bar{I} + 0.29 Spp - 0.0019(\bar{I} \cdot Spp)$				
		(<0.001)	(0.012)	(0.078)	(0.014)	
n_{PSII}	R^2	0.64	0.35	0.58	0.13	**0.71**
	Model (p-value)	$0.0015 + 7.30 \times 10^{-6} I_{Med}^D + 0.0017 Spp - 4.45 \times 10^{-7} \left(I_{Med}^D \cdot Spp\right)$				
		(0.016)	(<0.001)	(0.054)	(0.850)	
α	R^2	0.63	**0.67**	0.31	0.24	0.60
	Model (p-value)	$0.0008 + 0.0008 \frac{z_{mix}}{z_{eu}} + 0.0003 Spp + 5.74 \times 10^{-5} \left(\frac{z_{mix}}{z_{eu}} \cdot Spp\right)$				
		(<0.001)	(<0.001)	(0.030)	(0.945)	
ETR_{max}	R^2	0.78	0.37	0.72	0.09	**0.81**
	Model (p-value)	$0.0740 + 0.0006 I_{Med}^D - 0.0034 Spp + 0.0005 \left(I_{Med}^D \cdot Spp\right)$				
		(0.183)	(<0.001)	(0.954)	(0.004)	
I_k	R^2	0.44	0.08	**0.90**	0.28	0.56
	Model (p-value)	$57.7 + 1.00\bar{I} - 52.2 Spp + 0.70(\bar{I} \cdot Spp)$				
		(0.071)	(<0.001)	(0.177)	(<0.001)	

In contrast, I_{Med} was found to be a consistently poor predictor of photoacclimation and although $\frac{z_{mix}}{z_{eu}}$ was well correlated with α it was very poorly correlated with several other variables. With the exception of α, species was not a significant predictor of measurements of photoacclimation. However, the species interaction term was a significant predictor of variability in σ_{PSII}, ETR_{max} and I_k. Table 4.3.4 indicates that σ_{PSII} and I_k in *P. tricornutum* increases far less than that for *T. pseudonana* as $\bar{I}$ decreases. Meanwhile, the regression model for ETR_{max} presented in in Table 4.3.4

indicates that ETR_{max} increased more rapidly with an increase in I_{Med}^{D} in *T. pseudonana* than in *P. tricornutum*.

4.4. Light harvesting and acclimation of the PSII antenna

Under static square-wave light regimes photoacclimation of light harvesting is described along a gradient from high light to low light. Under acclimation from high to low light cells are characterised by increased cellular chlorophyll, which results in greater pigment packaging and a corresponding decrease in chlorophyll specific light absorption. This coincides with an increase in either the number of PSII units (n-type acclimation), an increase in the size of the effective PSII antenna (σ-type acclimation), or a combination of the two (Brunet *et al*., 2011; Dubinsky and Stambler, 2009). The addition of a fluctuating component to the light environment clearly alters this response (Rascher and Nedbal, 2006). Within fluctuating light regimes of equal dose photoacclimation of a^{chl} and n_{PSII} to increasing fluctuation amplitude appears functionally similar to high light acclimation. From SI to HF regimes *T. pseudonana* and *P. tricornutum* increase a^{chl}, which can be consistent with a reduction in cellular chlorophyll concentration (Bricaud *et al*., 2010; Fujiki and Taguchi, 2002). This could also in part reflect an increase in light absorption by photoprotective and accessory pigments (Dimier *et al*., 2009; van de Poll *et al*., 2010; van Leeuwe *et al*., 2005). Such an increase in a^{chl} with the

amplitude of light fluctuations is consistent with a number of previous observations (Fietz and Nicklisch, 2002; Flameling and Kromkamp, 1997; Hoppe *et al*., 2015; Shatwell *et al*., 2012; Wagner *et al*., 2006), and may indicate maximum irradiance is an important driver in acclimation of light harvesting. Interestingly this appears to be the reverse of photoacclimation in cyanobacteria and green algae, in which increasing fluctuating amplitude drives acclimation comparable to that under decreasing square-wave irradiance (Fietz and Nicklisch, 2002; Havelkova-Dousova *et al*., 2004; Ibelings *et al*., 1994).

The concurrent increases in a^{chl} and n_{PSII}, combined with little variation in σ_{PSII}, is suggestive of an increase in number, but reduction in size of photosynthetic units (PSUs, Suggett *et al*., 2007). PSU n-type acclimation to light fluctuations in which the number of PSUs increase while their size decreases is consistent with observations of the picoeukaryote *Pelagomonas calceolate* (Dimier *et al*., 2009), and at least two other diatom species (Fietz and Nicklisch, 2002; Kromkamp and Limbeek, 1993). This is thought to enable exploitation of a wide range of irradiances, as are found in highly fluctuating light environments (Dimier *et al*., 2009; Wagner *et al*., 2006). Although acclimation of PSUs to light fluctuations appears to be primarily n-type, a decrease in σ_{PSII} between SQ and fluctuating regimes is indicative of σ-type acclimation. Dimier *et al*. (2009) have previously suggested that acclimation mode is dependent on the timescale of light variability. With σ-type

acclimation being of greater importance than n-type in acclimation to lower frequency fluctuations and vice versa. Here σ-type acclimation appears only relevant when an initial fluctuation component is added from SQ to SI and does not appear to occur between SI and LF or HF regimes.

The apparent importance in n-type acclimation to light fluctuations in regimes of equal light dose is interesting given the greater resource cost when compared with σ-type (Six *et al*., 2008). This suggests that photoacclimation to light fluctuations is energetically more costly than acclimation to square-wave light regimes.

Differences in a^{chl}, n_{PSII}, and σ_{PSII}, between HL and LL are consistent with acclimation to the lower mean irradiance (Dubinsky and Stambler, 2009). It appears that acclimation of light harvesting in fluctuating light follows the mean irradiance whilst being modulated by the amplitude of light variability, apparently as a result of changes in the maximum irradiance. Some previous studies have compared fluctuating light regimes to non-fluctuating regimes of different mean irradiance (e.g. Nicklisch, 1998; van Leeuwe *et al*., 2005). Present data indicate that photoacclimation under these circumstances should be interpreted with caution, as disentangling acclimation to the mean irradiance and the magnitude of light variability may be difficult.

4.5. Photosynthesis and alternative electron sinks

Within fluctuating light regimes of equal dose, differences in ETR are predominantly driven by changes in light absorption (Figure 4.3.2 and Table 4.3.1). Differences in F_q'/F_m' are minimal under fluctuating light regimes (Figure 4.3.1), indicating it does not contribute to variability in ETR. Differences in F_q'/F_m' between square-wave and fluctuating light regimes are discussed later in this section.

Increasing fluctuation amplitude from SI to HF enhanced the ETR-irradiance response by significantly increasing α and ETR_{max}. The impact on the saturation irradiance, I_k, appears dependant on mean irradiance. I_k does not change significantly between fluctuating HL cultures and increases from SI to HF in LL cultures. An increase in ETR_{max}, and tendency to increase I_k, with increasing fluctuation amplitude has been observed in several species (Hoppe *et al*., 2015; Shatwell *et al*., 2012). This could be interpreted as acclimation to increase photosynthetic utilisation of high irradiance peaks in fluctuating regimes (e.g. in Shatwell *et al*., 2012). Comparing measurements of ETR with those of O_2 evolution suggests otherwise (Figure 4.5.1).

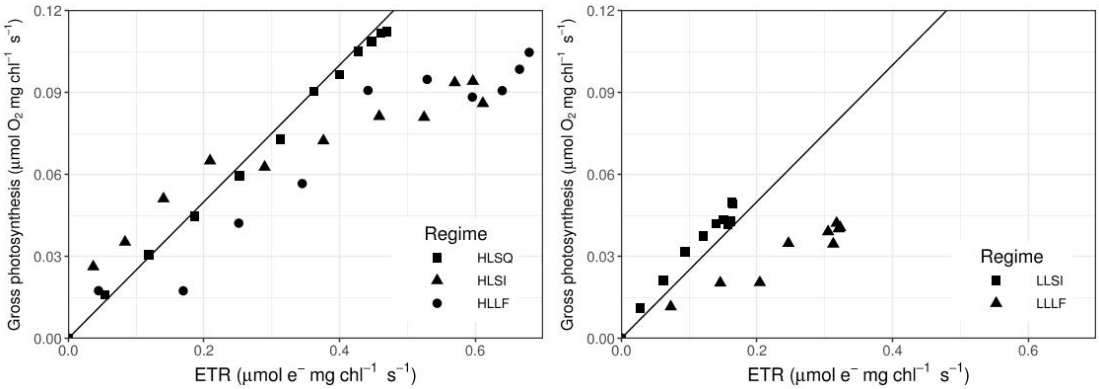

Figure 4.5.1. Comparison of ETR and O_2 evolution as measurements of photosynthesis in *T. pseudonana* growth under several fluctuating and square-wave light regimes. Trend line indicates a ratio of 4:1 electrons:O_2.

While ETR_{max} increases with fluctuation amplitude, P_{max} is not significantly affected at either HL or LL. Theoretically, evolution of 1 molecule of O_2 requires the transfer of 4 electrons. Under square-wave light regimes the relationship between measurements of ETR and O_2 evolution are consistently linear, and approximately conform to this ratio across a number of species (Lefebvre *et al*., 2007; Suggett *et al*., 2009). Under HLSQ and LLSI (LLSI being the least variable of the fluctuating regimes) the present measurements of *T. pseudonana* also conform to this ratio. However, under fluctuating light the ratio of ETR to O_2 evolution deviates from the expected linear relationship such that the electron efficiency of O_2 evolution decreases with increasing light. This observation may explain an apparent contradiction in research on phytoplankton photosynthesis under fluctuating light. Namely that studies using ETR as a measure of photosynthesis report strong acclimation of maximum photosynthesis (Hoppe *et al*., 2015; Shatwell *et al*., 2012), but studies using O_2 evolution generally do not (Fietz and Nicklisch, 2002; Flameling and Kromkamp, 1997). Wagner *et al*. (2006) previously

identified this and attributed the reduction in the electron efficiency of oxygen evolution to an increase in alternative electron sinks. In linear electron transport electrons are removed from water and delivered to NADP+ (nicotinamide adenine dinucleotide phosphate). Several processes provide alternative sinks to NADP+ for these electrons including the Mehler reaction (Claquin *et al*., 2004), plastoquinone terminal oxidase (PTOX), and cyclic electron transport around PSII (Onno Feikema *et al*., 2006; Wagner *et al*., 2016).

When using ETR as a measure of photosynthesis, comparison between different species or different growth environments carries the assumption that the fraction of electrons used in linear electron transport is consistent. Under square-wave light this appears to be the case (Lefebvre *et al*., 2007; Suggett *et al*., 2009). However, present data and others indicate acclimation to fluctuating light involves a relative increase in the fraction of electrons contributing to alternative electron sinks under conditions of high irradiance (Su *et al*., 2012; Wagner *et al*., 2016, 2006). Rather than concluding that the change in ETR_{max} under fluctuating regimes is a response to maximise photosynthesis in high irradiance peaks, it is instead hypothesised to be a photoprotective mechanism to dissipate excess excitation energy (Lavaud *et al*., 2002b; Onno Feikema *et al*., 2006). This highlights that the interpretation of ETR as a measure of photosynthesis under fluctuating light must be approached with caution, and alternative electron sinks need to be

considered. It was recently demonstrated in *P. tricornutum* that an increase in alternative electron sinks was an important process in acclimation to fluctuating light (Wagner *et al*., 2006). Present data indicates the same is true of *T. pseudonana*. Changes in cyclic electron transport around PSII have been shown to be a significant contributor to differences in alternative electron sinks arising from acclimation to fluctuating light in *P. tricornutum* (Wagner *et al*., 2016). It is currently unclear whether or not PSII cyclic electron transport plays a role as an alternative electron sink in *T. pseudonana.*

In comparison to fluctuating light regimes the ETR-irradiance response under the square-wave regime is considerably diminished. Differences in alternative electron sinks mean this is not the same for O_2 evolution, which is comparatively enhanced under square-wave light. Intriguingly the apparent enhancement of the ETR irradiance response with increased fluctuation amplitude (here attributed to alternative electron sinks) results in statistically similar ETR-irradiance curves between HLSQ and LLHF in *T. pseudonana*.

Changes in the relative importance of alternative election sinks do not satisfactorily explain variability in I_k and ${I_k}^{O_2}$ in fluctuating light regimes. A substantial increase in ${I_k}^{O_2}$ between HLSI and HLHF suggests acclimation to more efficiently utilise high irradiance peaks. This is consistent with the increase in I_k from LLSI to LLHF in *T. pseudonana*, and from LLSI to LLLF in *P. tricornutum* but not with the apparent lack of a significant change in I_k under HL fluctuating regimes. It is suggested here that the high values of I_k reported

under HL fluctuating regimes represent a physiological limit to the saturation irradiance, and hence do not significantly differ between light regimes. This is supported by other studies of these species, which report saturation irradiances for photosynthesis below those found here (Bates and Platt, 1984; Costa *et al*., 2013a; Geider *et al*., 1985; Nymark *et al*., 2009; Sobrino *et al*., 2008).

Differences between HL and LL of either measurement of the P-I response are consistent with acclimation to the light dose. That is, a reduction in saturation irradiance and maximum photosynthetic rate, as well as a tendency for the initial slope to be reduced (Dubinsky and Stambler, 2009; Falkowski and Owens, 1980; Macintyre *et al*., 2002). The more rapid decrease in F_q'/F_m' with increasing irradiance under LL also suggests acclimation to the light dose.

4.6. Characterising photoacclimation from parameters of fluctuating light environments

In order to accurately predict phytoplankton responses to changes in light variability it is necessary to understand which aspects of the light environment drive photoacclimation processes. This is particularly relevant in the modelling and interpretation of productivity during changes in ocean stratification, as well as for estimating global primary production and

photosynthesis from satellite measurements of ocean colour (Behrenfeld *et al*., 2016; Bellacicco *et al*., 2016; Nicklisch *et al*., 2008). Here a simplistic approach was used to test if a single aspect of the light regime can be used to predict a range of photoacclimative processes. Since only two mean irradiances were investigated, correlation between $\bar{I}$ and photoacclimation must be interpreted cautiously. As noted previously, several previous studies have found $\bar{I}$ to be a poor predictor of photoacclimation to fluctuating light (e.g. Dimier *et al*., 2009; Garcia-Mendoza *et al*., 2002; Hoppe *et al*., 2015; Litchman, 2003, 2000; Litchman *et al*., 2004). However, most of these studies compared fluctuating light regimes of equivalent $\bar{I}$, but different fluctuation characteristics. It should not be concluded that $\bar{I}$ does not impact photoacclimation without comparing light regimes of different $\bar{I}$. Shatwell *et al*. (2012) conducted a comprehensive study of growth and ETR of several phytoplankton under square-wave and fluctuating light regimes with a range of $\bar{I}$. They found that changes in $\bar{I}$ resulted in similar trends of photoacclimation between fluctuating and square-wave regimes, but these trends were shifted by the inclusion of a fluctuating component. Present data suggest a similar conclusion; that photoacclimation in fluctuating light follows $\bar{I}$ whilst being modulated by light variability.

The mechanisms of photoacclimation in diatoms remain relatively unknown. In phytoplankton the oxidation state of PQ appears to act as a signal for photoacclimation (Durnford and Falkowski, 1997; Escoubas *et al*.,

1995; Foyer *et al*., 2012; Oelze *et al*., 2008). The redox state of PQ represents a ratio between PSII light harvesting and the ability of a cell to utilise photochemically quenched energy. A highly reduced PQ pool indicates that light is being absorbed faster than it can be used, and *vice versa*. If light absorption is greater than utilisation, and PQ is highly reduced, cells photoacclimate to reduce their content of light harvesting pigment (Escoubas *et al*., 1995; Oelze *et al*., 2008). For a given cell in a dynamic light regime the degree of reduction within PQ increases with irradiance from light-limited to light-saturated photosynthesis (Melis, 1999). Once photosynthesis is light-saturated subsequent increases in irradiance have little effect on the redox state of PQ, and therefore have no effect on photoacclimation driven by PQ redox signalling. Based on this a number of authors have used I_{Med} rather than $\bar{I}$ as an indicator of photoacclimation in modelling studies (Behrenfeld *et al*., 2016; Graff *et al*., 2016; Siegel *et al*., 2013; Westberry *et al*., 2008). The median is less affected by extreme values than the mean and so is hypothesised to more closely relate to PQ redox state in a dynamic light environment in which irradiance is saturating for part of the photoperiod. Present data do not appear to support this hypothesis. In fact, I_{Med} overall appears to be worst predictor of photoacclimation among the parameters studied here. However, this does not mean that redox signalling is unimportant in photoacclimation. The FRRF method used to measure ETR only reports on the redox state of Q_A and has minimal effect on the redox

state of PQ (Falkowski and Raven, 2007; Suggett *et al*., 2003). However, during measurements of ETR under actinic light the redox potential of Q_A is assumed to be in equilibrium with that of PQ. Processes involving alternative electrons sinks discussed in the previous section occur downstream of PQ oxidation/reduction and need not be considered here (Lavaud *et al*., 2002b). Assuming the saturation irradiance for ETR is equivalent to the irradiance at which PQ becomes fully reduced, the fraction of the photoperiod during which PQ is partially oxidised can be estimated as the portion of time irradiance is below I_k. This represents the fraction of the photoperiod for which PQ redox signalling provides information on the incident irradiance. For the remainder of the photoperiod it is assumed that PQ is entirely reduced, and further increases in irradiance have minimal effect on PQ redox state. Note that this assumes the ETR-irradiance response does not change significantly over the course of the photoperiod which is unlikely to be correct (see chapter 6). The fraction of the photoperiod for which irradiance is below I_k is shown in Figure 4.6.1. Values of I_k were spectrally corrected as described in section 3.5 before making this estimation. These values are quite consistent

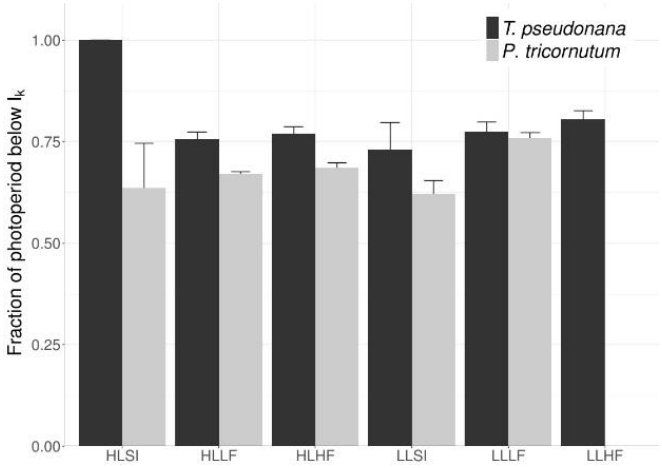

Figure 4.6.1. Fraction of the photoperiod for which irradiance is subsaturating to ETR in two diatoms grown under several fluctuating and square-wave light regimes. Error bars are 1 standard deviation.

between light regimes ranging from 0.73 to 0.80 in *T. pseudonana* (excluding HLSI at which I_k is above I_M) and from 0.62 to 0.75 in *P. tricornutum*. Within species, the fraction of the photoperiod for which irradiance is subsaturating to ETR is only significantly different from the other light regimes under HLSI for *T. pseudonana* and LLLF for *P. tricornutum* ($p<0.05$, 2-way ANOVA with post-hoc Tukey HSD). Otherwise the fraction of the photoperiod that is not saturating to ETR is statistically similar across fluctuating light regimes. Under square-wave light regimes phytoplankton tend to acclimate such that I_k follows the light intensity (e.g. Arrigo *et al*., 2010; Lefebvre *et al*., 2007; Mouget *et al*., 1995). This data suggests that under fluctuating light regimes phytoplankton may photoacclimate such that I_k follows the distribution of light intensity throughout the photoperiod, consistent with acclimation controlled by the redox state of PQ. This begs the question: If the fraction of the photoperiod below I_k is so consistent, why then is it so poorly correlated with I_{Med}? The answer is apparent when the overall distribution of irradiance throughout the photoperiod is considered and is a direct result of the light regimes used in this study. Figure 2.4.1c in chapter 2 (page 31) shows the cumulative distribution function (CDF) of light throughout the photoperiod, on which I_{Med} is the irradiance at the 50th percentile. Figure 2.4.1d (page 31) shows that the CDFs for the fluctuating light regimes intersect at approximately the 75th percentile, such that above this value I_{Med} no longer accurately describes the irradiance distribution. This is also approximately the

value of I_k. The linear regressions reported in Table 4.2.4 were repeated using the irradiance values at the 80th percentile (P_{80}^I, not shown), above this intersection. P_{80}^I was more strongly correlated with all measurements of photoacclimation than I_{Med}, and strongly correlated with some variables (Table 4.6.1). This suggests that although distribution of irradiance within the photoperiod may be a useful indicator of photoacclimation (consistent with control by PQ redox signalling), the measurement of the irradiance distribution requires careful consideration. The use of I_{Med} as an indicator of photoacclimation may not be appropriate, and the saturation irradiance for ETR (or the irradiance at which PQ becomes reduced) should be considered when using a measure of the irradiance distribution as an indicator of photoacclimation.

Table 4.6.1. R^2 values for a series of linear regressions between PAR at the 50th (I_{Med}) and 80th (P_{80}^I) percentile and several indicators of photoacclimation in *T. pseudonana* and *P. tricornutum* grown under fluctuating light.

	I_{Med}	P_{80}^I
a^{chl}	0.15	0.42
σ_{PSII}	0.30	0.57
n_{PSII}	0.13	0.69
α	0.24	0.43
ETR_{max}	0.09	0.82
I_k	0.28	0.83

Thus far only PQ redox signalling has been considered as a mechanism of photoacclimation. Several recent studies have identified photoreceptors in phytoplankton that act as controls on photoacclimation distinct from PQ redox signalling (Depauw *et al*., 2012; Jaubert *et al*., 2017; Nymark *et al*., 2009). These have been identified in both *T. pseudonana* and *P. tricornutum*

(Costa *et al*., 2013b; Takahashi *et al*., 2007). Although they are predominantly discussed in reference to the acclimation of non-photochemical quenching (e.g. Costa *et al*., 2013a) they are also important in photoacclimation of the P-I response, and appear to be related to acclimation to high light (Costa *et al*., 2013b). Control of photoacclimation by photoreceptors may reduce the usefulness of any measure of the distribution of irradiance across the photoperiod that seeks to predict photoacclimation in terms of redox signalling. Present data supports this, suggesting that in fluctuating light regimes the maximum irradiance and I_{Med}^{D} (which is closely correlated with the maximum irradiance) are good indicators of some parameters of photoacclimation. This is not consistent with PQ redox signalling but may reflect the involvement of photoreceptors in the control of photoacclimation.

Overall the present data is not sufficient to conclude which aspects of fluctuating light environment control photoacclimation, but it highlights that the use of the median as an indicator of photoacclimation may be inappropriate. Generally, it appears that no single parameter of the light environment is sufficient to describe photoacclimation as a whole in dynamic light environments. Recently, Graff and Behrenfeld (2018) reached a similar conclusion in a field study of phytoplankton during a mixing event. They noted that a single relationship may be insufficient to describe the photoacclimation response.

4.7. Summary and conclusions

Photoacclimation of *T. pseudonana* and *P. tricornutum* to fluctuating light is fundamentally different to that under square-wave regimes. In response to increasing fluctuation amplitude photoacclimation appears to be dominated by photoprotective responses to high irradiance peaks. It is characterised by an increase in alternative sinks for PSII electrons under high irradiance, an increase in the chlorophyll specific absorption coefficient and an apparent increase in the number, but reduction in size, of PSU (Fietz and Nicklisch, 2002; Wagner *et al*., 2006). Although photoacclimation is still driven by the changes in the mean irradiance (or light dose) as it is under static light regimes, it is also modulated by the amplitude of light variability in fluctuating regimes. In natural populations this drives significant variability in photophysiology between stratified and well-mixed water columns (Lewis *et al*., 2018; Moore *et al*., 2006) and is an important consideration for interpretation of satellite estimates of marine productivity (Behrenfeld *et al*., 2016; Graff and Behrenfeld, 2018). The mechanisms of photoacclimation are still being uncovered. Currently it is not entirely clear which aspects of the light environment control photoacclimation, but it appears than no single parameter is a sufficient indicator on its own. Rather, the overall distribution of the light environment needs to be taken into account.

Among laboratory studies a reduction in growth rate as intradiel light fluctuations increase in amplitude is commonly reported in most

phytoplankton species (Lavaud *et al*., 2007; Nicklisch, 1998; Nicklisch and Fietz, 2001; Shatwell *et al*., 2012; Wagner *et al*., 2006). Such a reduction was also found here for *T. pseudonana* and *P. tricornutum.* Although changes in the maximum rate of PSII electron transport appear to indicate acclimation to better utilize high irradiance peaks in fluctuating light regimes, these were actually a result of changes in alternative election sinks, and did not reflect changes in photosynthesis rates (Su *et al*., 2012; Wagner *et al*., 2006). As dynamic light regimes increase in fluctuation amplitude a greater fraction of the light dose is delivered at light levels saturating to photosynthesis (see Figure 2.4.1d in chapter 2, page 31). As a consequence of the limited acclimation of photosynthesis and the changing distribution of the light dose, the efficiency with which cells can use the available light declines (Litchman, 2000; Wagner *et al*., 2006). In addition, photoacclimation of the light harvesting apparatus to fluctuating light regimes appears to be energetically costly, perhaps more so than to static light regimes (Dimier *et al*., 2009; Six *et al*., 2008). The combination of these two factors may be the cause for the reduction in growth rates of phytoplankton under fluctuating light environments.

5. Photoprotection by non-photochemical quenching – Responses to short-term light variability and consequences for photodamage

5.1. Introduction

An inevitable consequence of photosynthesis is photodamage to PSII. The rate of PSII photodamage is correlated with the incident irradiance, and under high irradiance photodamage may exceed repair processes, resulting in a reduction of the efficiency with which PSII operates (Baroli and Melis, 1996; McKew *et al*., 2013; Ting and Owens, 1994). To minimise photodamage and the associated reduction in photosynthetic efficiency diatoms employ several mechanisms to safely dissipate or prevent the absorption of excess irradiance. In order to maximise growth rates diatoms must balance energy investment in mechanisms to reduce photodamage whilst also compensating for the potential reduction in photosynthesis rates caused by photodamage itself (Raven, 2011; Wagner *et al*., 2006).

Diatom responses to minimise photodamage operate over a wide range of timescales (see summary in Macintyre *et al*., 2000), and therefore different processes may be relevant dependant on the rate of change of irradiance. For the timescales of irradiance variability used here, previous research has identified non-photochemical quenching (NPQ) as one of the most important processes in minimising photodamage (Lavaud *et al*., 2007; Wagner *et al*., 2006). In diatoms, NPQ principally occurs through the

depoxidation of diadinoxanthin to diatoxanthin, which is controlled by the build-up of a transthylakoid proton gradient, and allows excess absorbed photons to be dissipated as heat (Lavaud and Goss, 2014; Lavaud and Kroth, 2006). Notably, NPQ can be rapidly activated and deactivated when cells experience light fluctuations thus enabling diatoms to minimise photodamage during periods of high light, whilst maintaining high rates of photosynthesis during periods of low light (van de Poll *et al*., 2011, 2010). The capacity and kinetics of NPQ are known to vary between different species, potentially reflecting their ecological niche (Lavaud *et al*., 2007; Lavaud and Lepetit, 2013; Petrou *et al*., 2011).

In addition to NPQ and other processes which reduce photodamage, D1 repair is important in maintaining a high photosynthetic efficiency under periodic high light intensities (Lavaud *et al*., 2016). Recent studies have highlighted interspecific differences in the repair capacity of diatoms (Lavaud *et al*., 2016; Wu *et al*., 2012). Similarly to NPQ, these may relate to the ecological niche of the study species.

Both NPQ and D1 repair are rapid regulatory processes, the interaction between which is important in maintaining a high photosynthetic efficiency in diatoms (Lavaud *et al*., 2016). The relatively high rate constants of these processes make them particularly important in acclimation to intradiel light fluctuations (Macintyre *et al*., 2000). Although interspecific differences in both NPQ and repair have been noted (Lavaud *et al*., 2016, 2007), little

research has examined variability in these processes between and within species in response to dynamic light environments. Changes in energy investment in NPQ and repair may have consequences on photosynthesis rates (e.g. by reducing photodamage or increasing photosynthetic efficiency) and may directly or indirectly affect growth rates by detracting from energy investment in growth or reducing energy available from photosynthesis. This chapter aims to examine variability in NPQ and repair of photodamage in response to dynamic light regimes, to investigate how the study species acclimate to minimise photodamage and how successful they are in achieving this in dynamic light environments.

5.2. Materials and methods

Culture conditions were as described in section 3.1. FRRF measurements of NPQ were carried out at approximately midday within the photoperiod according to the methods described in section 3.6.

PSII photodamage and repair can be studied immunochemically through measurement of the D1 protein or PsbA (Bouchard *et al*., 2005) or through fluorescence measurements of photochemical efficiency (Ragni *et al*., 2010). Here the latter approach was used.

Experimental methodology largely followed Ragni *et al*. (2010), using lincomycin (Sigma) at a concentration of 0.9 mM as an inhibitor of PSII repair.

Samples extracted at approximately midday in the light regimes were incubated in a range of light levels. These were sampled periodically and then moved to darkness for a recovery period of 30 minutes. Following recovery samples were measured in an FRRF. Two different treatments of lincomycin were used as follows:

1. Lincomycin added at start of incubation
2. Lincomycin added at start of recovery period

Of these, the results from treatment 1 represents gross photodamage, while treatment 2 represents net photodamage in the light.

As in Ragni *et al*. (2010), cells were incubated at 100, 250, 550 and 1100 µmol phot. m^{-2} s^{-1} (±5%) and sampled for measurement at 5, 15, 30 and 60 minutes. Measurements of F_v/F_m were used to determine photodamage and repair rates. LED excitation spectrum is shown in Figure 3.3.1 (page 38).

Rate constants of PSII reaction centre photodamage are generally calculated as in Ragni *et al*. (2008) assuming first order reaction kinetics in the inactivation of PSII. These can be calculated from F_v/F_m by fitting F_v/F_m measured under gross photoinhibition (treatment 1 above) to a model of exponential decay, as described in Equation 5.2.1.

$$F_v/F_{m_{(t)}} = F_v/F_{m_{(0)}}\, e^{-k_i t} \qquad \textbf{5.2.1}$$

Where k_i is the rate constant for photodamage and $F_v/F_{m_{(t)}}$ and $F_v/F_{m_{(0)}}$ represent values of F_v/F_m at time *t* and time 0 respectively.

In order to determine the rate of PSII reaction centre repair some previous studies have calculated a rate constant for net photoinhibition based on an exponential decay model of F_v/F_m in the absence of lincomycin during illumination (treatment 2) (McKew *et al*., 2013; Ragni *et al*., 2010, 2008). Repair rate is then calculated by subtracting the rate constant for net photoinhibition from that for gross photoinhibition. This approach is described by Equations 5.2.2 to 5.2.4 using notation from Ragni *et al*. (2008).

$$GPiR = -\frac{\Delta ln\left(F_v/F_{m_{LIN}}\right)}{\Delta t} \qquad \textbf{5.2.2}$$

$$NPiR = -\frac{\Delta ln(F_v/F_m)}{\Delta t} \qquad \textbf{5.2.3}$$

$$RR = NPiR - GPiR \qquad \textbf{5.2.4}$$

In Equations 5.2.2 to 5.2.4 $GPiR$ is the rate constant for gross photodamage using measurements of F_v/F_m made in the presence of lincomycin and $NPiR$ is the rate constant for net photodamage using measurements of F_v/F_m made in the absence of lincomycin during illumination. RR is not actually a rate constant for repair, rather it gives a number which relates the rate of repair to the rate of gross photodamage that cannot easily be converted to a rate constant (Campbell and Tyystjärvi, 2012). In this study an alternative approach is proposed to determine rate constants of PSII reaction centre repair (k_r) by fitting data to a two compartment model based on that proposed by Kok (1956). A variation of the model was described in Campbell and Tyystjarvi (2012).

This model assumes an equilibrium between photodamage acting on undamaged PSII reaction centres and repair acting on damaged PSII reaction centres is reached after some time at a certain level of photoinhibition. Although the mechanism of PSII reaction centre repair is highly complex it appears to be rate limited by a single process, namely the degradation of damaged D1 proteins (Campbell and Tyystjärvi, 2012; Melis, 1999; Nixon *et al*., 2010). This process follows first order reaction kinetics with respect to the concentration of damaged reaction centres (Tyystjärvi *et al*., 1994). Based on this, the rate at which damaged PSII reaction centres (RCIIs) are repaired (rep) can be calculated according to Equation 5.2.5.

$$rep = -k_r \cdot [RCII_i] \qquad \textbf{5.2.5}$$

Where $[RCII_i]$ is the concentration of damaged RCIIs and k_r is the rate of repair. Similarly, from Equation 5.2.1, the rate of photodamage of functional RCIIs (dam) is given by Equation 5.2.6.

$$dam = -k_i \cdot \left[RCII_f\right] \qquad \textbf{5.2.6}$$

Where $\left[RCII_f\right]$ is the concentration of functional RCIIs and k_i is the rate of photodamage. Equations 5.2.5 and 5.2.6 describe a simple 2 compartment equilibrium model which is illustrated in Figure 5.2.1. These two Equations can be combined to calculate the rate of change in $\left[RCII_f\right]$ according to Equation 5.2.7.

$$\frac{\delta[RCII_f]}{\delta t} = k_r \cdot [RCII_i] - k_i \cdot \left[RCII_f\right] \qquad \textbf{5.2.7}$$

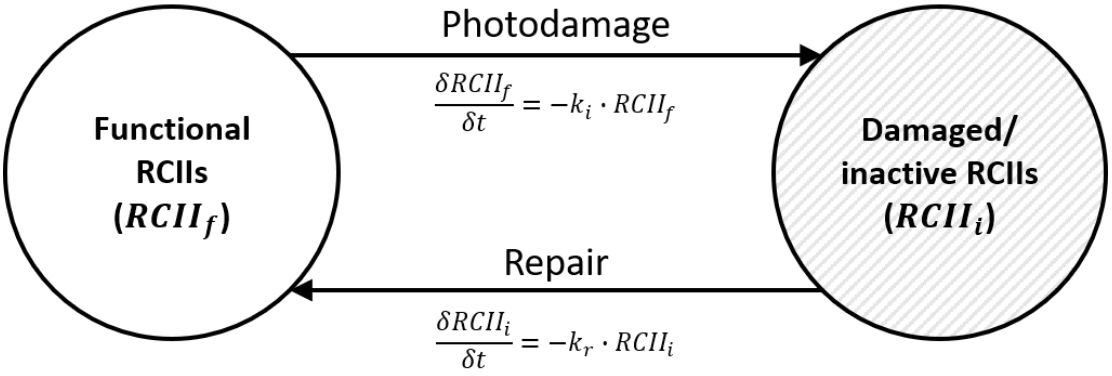

Figure 5.2.1. Equilibrium model of PSII reaction centre damage and repair. See text for description.

To fit the model to measurements of F_v/F_m it was assumed that the fraction of total reaction centres which are functional is directly proportional to the value of F_v/F_m relative to its maximum, $F_v/F_{m_{max}}$. Such that if F_v/F_m = 0 no RCIIs are functional and if F_v/F_m = $F_v/F_{m_{max}}$ all RCIIs are functional. The fraction of functional RCIIs ($RCII_f$) is given by Equation 5.2.8.

$$RCII_f = \frac{F_v/F_m}{F_v/F_{m_{max}}} \qquad \textbf{5.2.8}$$

Since $RCII_f$ represents the fraction of functional RCIIs from 0 to 1 it follows that $RCII_i$, the fraction of damaged RCIIs, can be calculated by Equation 5.2.9. This assumes that the concentration of RCIIs is static over the course of the measurement.

$$RCII_i = 1 - RCII_f \qquad \textbf{5.2.9}$$

Equation 5.2.7 can therefore be rewritten as Equation 5.2.10.

$$\frac{\delta RCII_f}{\delta t} = k_r\left(1 - RCII_f\right) - k_i \cdot RCII_f \qquad \textbf{5.2.10}$$

The value of k_i in Equation 5.2.10 can be determined directly from cultures in which RCII repair has been inhibited by lincomycin (as in treatment 1) by fitting F_v/F_m to Equation 5.2.11, a variation of Equation 5.2.1. Note that value of k_i determined from Equation 5.2.11 is equal to k_i determined from Equation 5.2.1 and $GPiR$ in Equation 5.2.2.

$$RCII_{f\,(t)} = RCII_{f\,(0)} e^{-k_i t} \qquad \textbf{5.2.11}$$

Where $RCII_{f\,(t)}$ and $RCII_{f\,(0)}$ are the fraction of functional RCIIs at time t and time 0 respectively. The repair rate constant can then be found by solving Equation 5.2.10 for k_r, using measurements of F_v/F_m from cultures in which RCII repair during illumination has not been inhibited by lincomycin, and k_i determined from 5.2.11. This can either be solved numerically, or by fitting measurements of F_v/F_m to the analytical solution to Equation 5.2.10 which is given by Equations 5.2.12 and 5.2.13. Here the latter approach was used.

$$RCII_{f\,(t)} = C \cdot e^{-t(k_r+k_i)} + \frac{k_r}{k_r+k_i} \qquad \textbf{5.2.12}$$

In Equation 5.2.12 *C* is a constant that relates the value of $RCII_f$ at time *t* to its initial value. Solving for *t*=0 gives *C* (Equation 5.2.13).

$$C = RCII_{f\,(0)} - \frac{k_r}{k_r+k_i} \qquad \textbf{5.2.13}$$

When fitting the model, $RCII_{f\,(0)}$ was initially fit in Equation 5.2.11 and the same value was used in fitting Equation 5.2.13.

The use of $RCII_f$ rather than raw values of F_v/F_m removes the assumption of the model formulation in Campbell and Tyystjärvi (2012) that the initial value of F_v/F_m is the maximum. This was important because F_v/F_m of samples which were not repair inhibited was found to increase over time under the lowest light treatment. Indicating that samples had suffered some photodamage at the start of the measurement. Using $RCII_f$ makes no assumptions of the physiological state of photodamage of cells at the beginning of the measurement. The calculation of $RCII_f$ as per Equation 5.2.8 was performed using the maximum recorded value of $F_v/F_{m_{max}}$ in the culture to which the data pertains. To the author's knowledge, this study is the first presentation and implementation of the model presented by Kok (1956) using $RCII_f$.

As mentioned above the rate of PSII repair (k_r) may be limited by a single process, the degradation/removal of the damaged D1 protein from PSII (Campbell and Tyystjärvi, 2012; Melis, 1999; Nixon *et al*., 2010). If this is the case, and the rate of this process is only proportional to the concentration of damaged PSIIs, then k_r may be expected to show Michaelis-Menten kinetics with respect to k_i, the rate of photodamage (Wu *et al*., 2012). The relationship between k_i and k_r can therefore be hypothesised to be described by Equation 5.2.14.

$$k_r = \frac{k_r^{max} k_i}{k_i^M + k_i} \qquad \textbf{5.2.14}$$

Where k_r^{max} is the saturated (maximum) value of k_r and k_i^M is the value of k_i when k_r is half of k_r^{max}. Where possible k_i and k_r were fitted to Equation 5.2.14 to test whether these show Michaelis-Menten kinetics.

5.3. Results

Both the initial NPQ (NSV_0) and the light dependant increase in NPQ (ΔNSV) were significantly greater in *P. tricornutum* ($F_{1,38}$=74.5, p <0.001 and $F_{1,38}$=32.0, p <0.001 respectively) than in *T. pseudonana* (Figure 5.3.1 and Table 5.3.1). The maximum capacity for NPQ, NSV_{max}, was also significantly higher in *P. tricornutum* ($F_{1,38}$=68.7, p<0.001), reaching up to 1.7 times greater levels under the HLHF regime. In contrast I_{50} was significantly greater in *T. pseudonana* ($F_{1,38}$=10.4, p = 0.003). The curvature parameter, n, did not differ significantly between species ($F_{1,38}$=1.2, p=0.23).

T. pseudonana showed little difference in NSV_0 and NSV_{max} between fluctuating light regimes at HL, and no significant change from LL to HL. However, NSV_{max} was significantly lower under LLSI than in other LL fluctuating regimes as a result of a reduction in ΔNSV. In contrast *P. tricornutum* significantly increased NSV_{max} as the amplitude of light fluctuations increased from HLSI to HLHF, but showed no significant variability in NPQ irradiance response under LL. Significantly higher ΔNSV values under

HL regimes means NSV_{max} in *P. tricornutum* was also significantly higher under HL than LL.

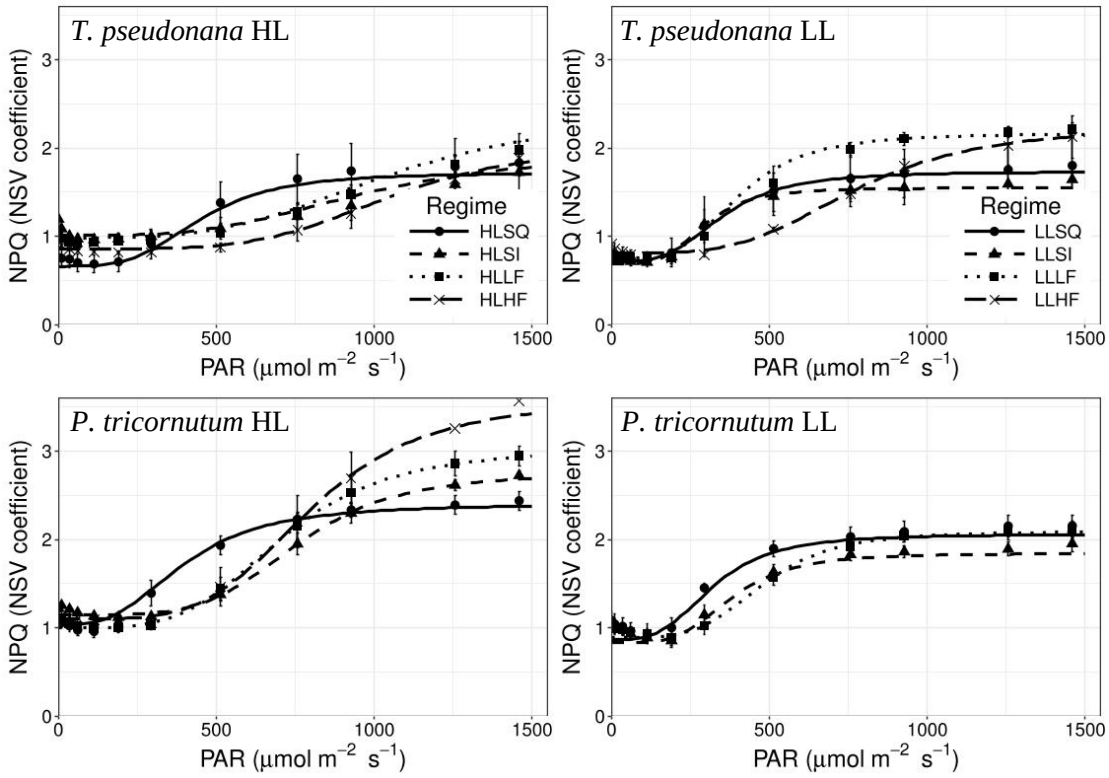

Figure 5.3.1. NPQ-irradiance response of two diatoms grown under a range of fluctuating and non-fluctuating light regimes. Parameters of curve fits are detailed in table 5.3.1. Error bars are 1 standard deviation.

Table 5.3.1. Parameters of the NPQ (NSV) irradiance response for two species grown under a range of light regimes. Initial value (NSV_0), maximum increase (ΔNSV) and maximum capacity for NPQ (NSV_{max}) have no units, as do values of the curvature parameter (n). Half-saturation irradiance (I_{50}) has units µmol m^{-2} s^{-1}. Values in brackets are 1 standard deviation. Values that share a letter are not significantly different (p>0.05). Sets of letters are conserved between species. Grey fills graphically indicate the values on a scale from 0 to the maximum value for each parameter.

		HL Regimes				LL Regimes			
		HLSQ	HLSI	HLLF	HLHF	LLSQ	LLSI	LLLF	LLHF
T. pseudonana	NSV_0	0.66^{f} (0.09)	$1.01^{a,b,c}$ (0.07)	$0.99^{a,b,c,d}$ (0.09)	$0.86^{b,c,d,e,f}$ (0.01)	$0.71^{a,b,c,d}$ (0.04)	$0.69^{e,f}$ (0.05)	$0.73^{d,e,f}$ (0.02)	$0.81^{c,d,e,f}$ (0.05)
	I_{50}	488.2^{d} (21.2)	$963.7^{a,b}$ (209.5)	$1053.0^{a.b}$ (152.7)	1058.7^{a} (96.1)	350.3^{d} (66.6)	290.5^{d} (45.9)	$438.9^{c,d}$ (30.8)	777.1^{b} (118.3)
	ΔNSV	$1.06^{d,e}$ (0.18)	$0.94^{d,e}$ (0.15)	$1.43^{b,c,d,e}$ (0.05)	$1.20^{c,d,e}$ (0.14)	$1.02^{d,e}$ (0.27)	0.86^{e} (0.15)	$1.52^{b,c}$ (0.09)	$1.43^{b,c,d}$ (0.32)
	n	$3.69^{b,c}$ (0.42)	$3.48^{c,b}$ (0.76)	$3.53^{b,c}$ (0.49)	$4.61^{a,b}$ (0.31)	$3.46^{b,c}$ (0.67)	$3.98^{a,b,c}$ (0.30)	$3.79^{b,c}$ (0.12)	$3.82^{a,b,c}$ (0.27)
	NSV_{max}	$1.72^{e,f}$ (0.24)	$1.95^{d,e,f}$ (0.15)	$2.31^{b,c,d}$ (0.12)	$2.06^{c,d,e,f}$ (0.13)	$1.73^{d,e,f}$ (0.31)	1.55^{f} (0.17)	$2.25^{b,c,d}$ (0.07)	$2.24^{c,b,e}$ (0.36)
P. tricornutum	NSV_0	$1.03^{a,b,c}$ (0.21)	1.15^{a} (0.02)	$1.00^{a,b,c}$ (0.001)	$1.1^{a,b}$ (0.06)	$0.87^{a,b,c,d}$ (0.12)	$0.83^{c,d,e,f}$ (0.01)	$0.90^{b,c,d,e}$ (0.003)	
	I_{50}	397.0^{d} (33.3)	758.0^{b} (52.9)	$707.0^{b,c}$ (26.9)	797.3^{b} (77.8)	320.7^{d} (23.3)	378.9^{d} (4.3)	$476.4^{c,d}$ (25.2)	
	ΔNSV	$1.37^{b,c,d,e}$ (0.28)	$1.60^{b,c}$ (0.03)	$2.03^{a,b}$ (0.17)	2.47^{a} (0.49)	$1.19^{c.d.e}$ (0.04)	$1.05^{d,e}$ (0.15)	$1.21^{c,d,e}$ (0.10)	
	n	3.00^{c} (0.26)	4.77^{a} (0.33)	$4.10^{a,b,c}$ (0.29)	$4.35^{a,b}$ (0.54)	$3.33^{b,c}$ (0.66)	$3.97^{a,b,c}$ (0.11)	$4.33^{b,c}$ (0.25)	
	NSV_{max}	$2.40^{b,c,d}$ (0.05)	$2.75^{b,c}$ (0.03)	$3.03^{a,b}$ (0.17)	3.57^{a} (0.54)	$2.05^{c,d,e,f}$ (0.14)	$1.88^{d,e,f}$ 0.14)	$2.10^{c,d,e,f}$ (0.09)	

In both species NSV_{max} was somewhat lower under square-wave irradiance than under fluctuating regimes at HL, but this was only found for *T. pseudonana* at LL. The 50% saturation irradiance (I_{50}) increases from LL to HL in both species and tended to be higher in fluctuating light than under square-wave regime. Fluctuation amplitude has little effect on I_{50} at HL, but correlated with I_{50} at LL such that I_{50} increased from LLSI to LLHF. Curvature of the NPQ irradiance response (n) was relatively unaffected by light regime, although it was significantly lower under HLSQ than under HL fluctuating regimes in *P. tricornutum*.

Unfortunately, photodamage and repair in LL regimes could not be reported for *P. tricornutum*. An error in the addition of lincomycin to some samples reduced the available replicates to below 3 in LL *P. tricornutum* cultures.

The rate of gross photodamage (k_i) increased approximately linearly with irradiance above a threshold (Figure 5.3.2). Below this threshold irradiance (given as intercept in Table 5.3.2) gross photodamage was negligible. At both HL and LL, k_i increased more rapidly in the square-wave regimes than in fluctuating regimes. Within HL fluctuating regimes k_i in *P. tricornutum* was lowest under the highest amplitude fluctuating regime (HLHF) whereas in *T. pseudonana* k_i was lowest under the least fluctuating regime HLSI.

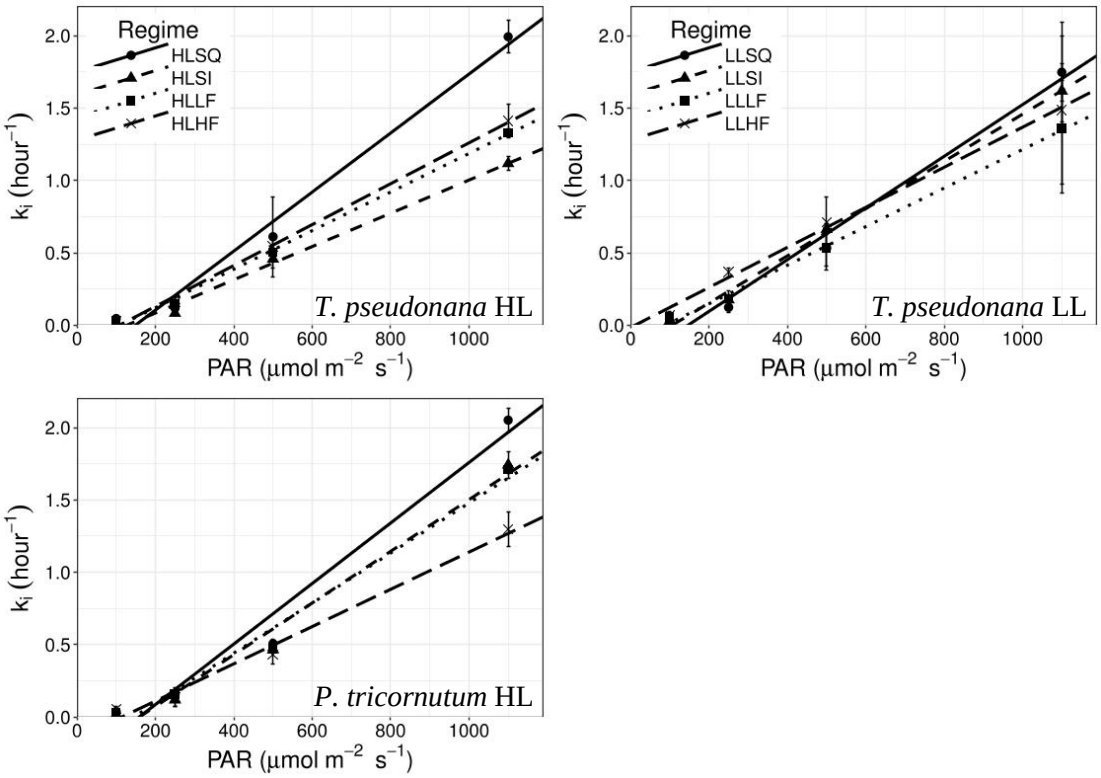

Figure 5.3.2. Gross photodamage in two diatoms grown under a range of fluctuating and non-fluctuating light regimes. Parameters of trendlines are detailed in table 5.2.2. Error bars are 1 standard deviation.

Gross photodamage did not greatly differ between species but tended to be slightly higher in *P. tricornutum*. For *T. pseudonana* k_i was similar between LL and HL.

Table 5.3.2. Parameters of the linear trendlines fit to PSII gross photodamage (k_i) versus PAR in Figure 5.3.2.

	T. pseudonana		*P. tricornutum*	
Regime	Slope (µmol m^2 s $hour^{-1}$)	Intercept (µmol m^{-2} s^{-1})	Slope (µmol m^2 s $hour^{-1}$)	Intercept (µmol m^{-2} s^{-1})
HLSQ	0.00203	147.0	0.00208	157.3
HLSI	0.00115	127.8	0.00178	158.9
HLLF	0.00133	110.7	0.00173	144.4
HLHF	0.00142	109.2	0.00128	113.2
LLSQ	0.00180	146.8		
LLSI	0.00163	105.0		
LLLF	0.00133	87.7		
LLHF	0.00138	12.1		

Rate constants for repair of PSII photodamage, k_r, are shown with respect to PAR in Figure 5.3.3. It was hypothesised that PSII repair would show Michaelis-Menten kinetics with respect to k_i. The relationship between k_r and k_i is shown in Figure 5.3.4.

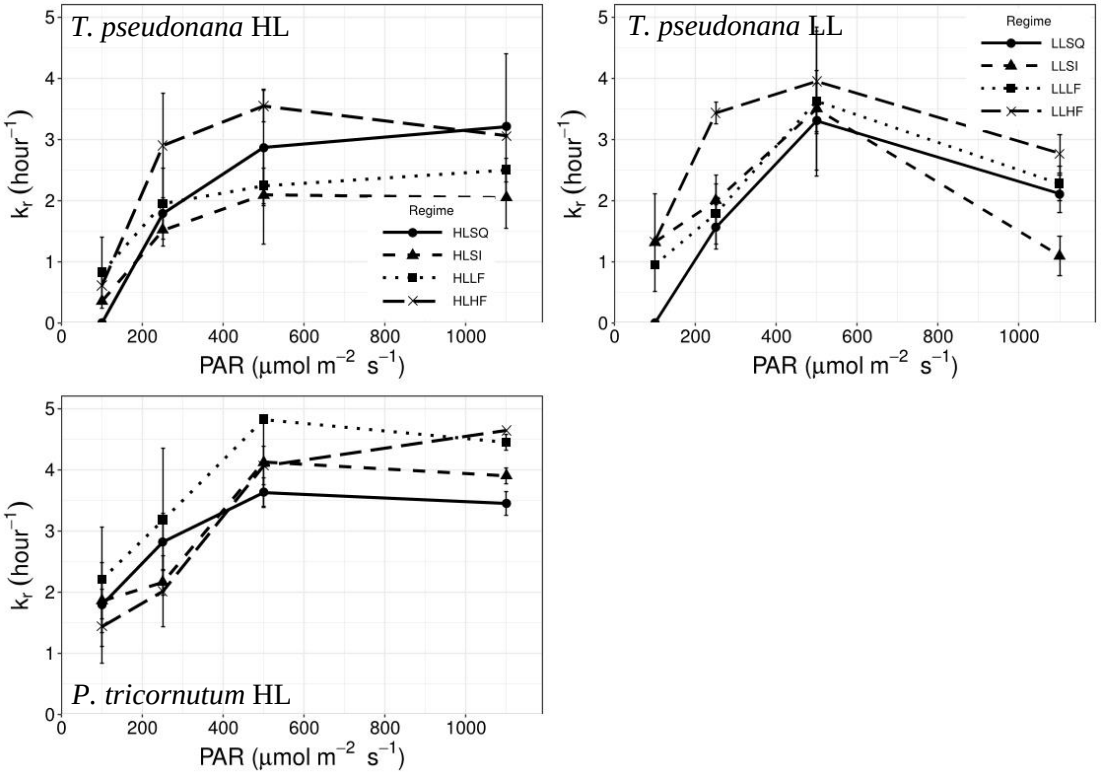

Figure 5.3.3. Rates of repair of PSII photodamage (k_r) with respect to PAR in two diatoms grown under a range of fluctuating and non-fluctuating light regimes. Error bars are 1 standard deviation.

At HL the rate of repair of PSII photodamage, k_r, approximately followed Michaelis-Menten kinetics with respect to the rate of photodamage (Figure 5.3.4). This was not the case under LL. Data reported for LL *T. pseudonana* and preliminary data for LL *P. tricornutum* (not shown due to a lack of replicates, see above in this section) show a consistent reduction in k_r at the highest recorded k_i, or highest irradiance. In fact, careful observation

of Figure 5.3.4 reveals that in some cases under HL regimes k_r is also reduced at the highest k_i, most notably in *T. pseudonana* at HLSQ. However, this occurs to a much lesser degree than at LL.

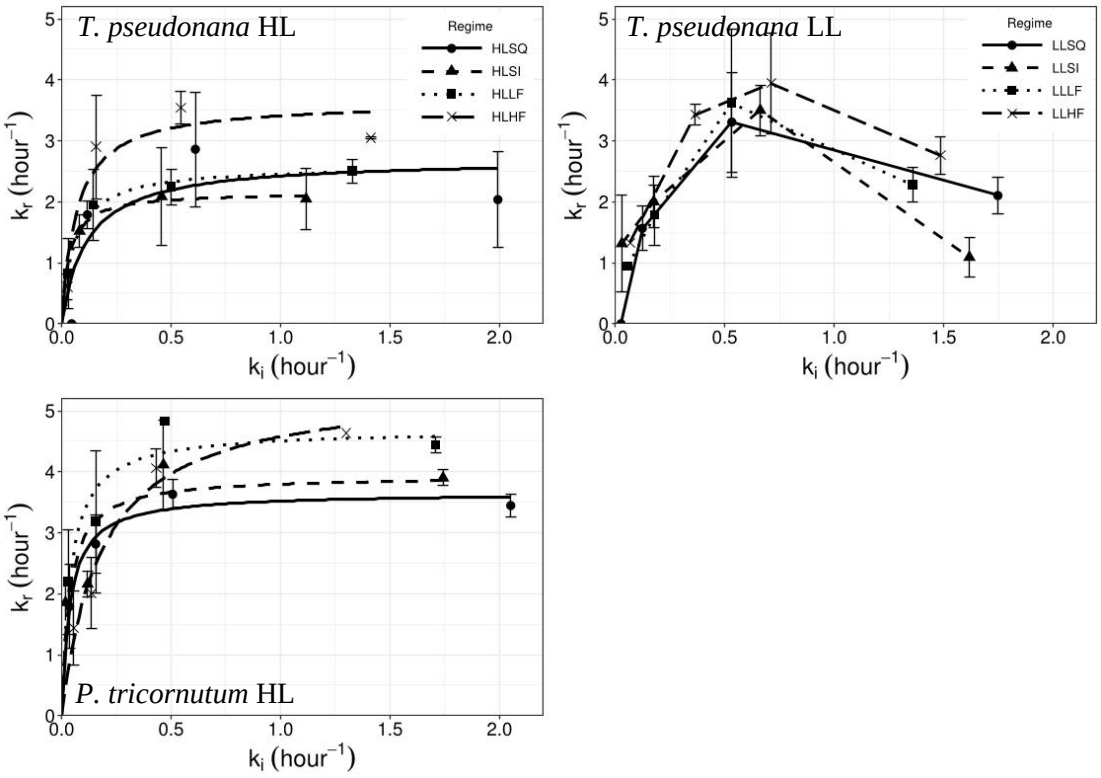

Figure 5.3.4. Rates of repair of PSII photodamage (k_r) with respect to photodamage (k_i) in two diatoms grown under a range of fluctuating and non-fluctuating light regimes. HL data are fit to the Michaelis-Menten equation, details of the curve fits are given in table 5.2.3. Error bars are 1 standard deviation.

From values of k_i^M in Table 5.3.3, and from Figure 5.3.4, it is apparent that k_r saturated at quite low values of k_i, and was consistently saturated below 550 μmol m^{-2} s^{-1}, the third highest of the four light intensities used to investigate PSII damage and repair.

Table 5.3.3. Parameters of the Michaelis-Menten fits to PSII repair (k_r) versus gross photodamage (k_i) in Figure 5.3.4.

	T. pseudonana		*P. tricornutum*	
Regime	k_r^{max} (hour^{-1})	k_i^M (hour^{-1})	k_r^{max} (hour^{-1})	k_i^M (hour^{-1})
HLSQ	2.70	0.12	3.66	0.04
HLSI	2.16	0.03	3.93	0.04
HLLF	2.59	0.06	4.69	0.04
HLHF	3.64	0.07	5.42	0.18

Unlike gross photodamage, k_r was markedly different between species, and much higher in *P. tricornutum*. At 1100 µmol m^{-2} s^{-1} k_r for *P. tricornutum* was 1.7, 1.9, 1.8 and 1.5 times higher than k_r for *T. pseudonana* under HLSQ, HLSI, HLLF and HLHF respectively. This is also apparent in the values of k_r^{max} (Table 5.3.3), the maximum rate of PSII repair, assuming a Michaelis-Menten fit is appropriate. *P. tricornutum* also exhibited much higher values of k_r than *T. pseudonana* at the lowest light intensity. For *P. tricornutum* repair was not only faster, but also more strongly activated at low irradiances.

In *P. tricornutum,* k_r differed between light regimes, particularly the maximum k_r. Using either k_r^{max} from the Michaelis-Menten fits (Table 5.3.3) or k_r at the highest light level k_r increased from HLSQ to HLHF. This indicates an apparent increase in the capacity for PSII repair as the amplitude of light fluctuations increased. This was corroborated by preliminarily data at LL but was not the case for *T. pseudonana*. At HL there was little difference in k_r in *T. pseudonana* under 3 of the 4 light regimes although the capacity for PSII repair was higher under HLHF than under other HL regimes. At LL k_r in *T.*

pseudonana is difficult to compare between light regimes, in general it appears consistent with k_r under HL in that it is similar between SQ, SI and LF regimes, but slightly higher under the HF regime.

5.4. Acclimation of NPQ to fluctuating light and interspecific differences

Non-photochemical quenching has previously been highlighted as an important photoprotective mechanism under conditions of fluctuating light (Havelkova-Dousova *et al*., 2004; Lepetit *et al*., 2017; van de Poll *et al*., 2010; van Leeuwe *et al*., 2005), principally because it can be rapidly activated and deactivated (Miloslavina *et al*., 2009; Roháček *et al*., 2014). That the mechanism of NPQ in diatoms is principally controlled via the pH gradient across the thylakoid membrane (Derks *et al*., 2015; Goss *et al*., 2006; Lavaud and Goss, 2014; Lavaud and Kroth, 2006) serves to explain several characteristics of the NPQ irradiance response observed here.

Firstly, the variability in I_{50} both between species and light regimes. During non-saturated electron transport, protonation of the thylakoid lumen by reduction of plastoquinone and other compounds is countered by formation of ATP and the Mehler reaction which causes the transport of protons back across the thylakoid membrane (Cardol *et al*., 2011; Curien *et al*., 2016; Järvi *et al*., 2013). This prevents the accumulation of a transthylakoid proton gradient. As photosynthesis becomes saturated these processes become increasingly decoupled and a transthylakoid proton

gradient is established (Schonknecht *et al*., 1995). Therefore NPQ can be expected to begin to saturate somewhat after the saturation of PSII electron transport (Giovagnetti *et al*., 2014; Serôdio and Lavaud, 2011). Directly comparing measurements of I_{50} with those of I_k reported in chapter 4 illustrates this (Figure 5.4.1). The relationship between I_k and I_{50} was the same for *T. pseudonana* and *P. tricornutum* and was unaffected by light regime. As indicated by the linear trendline in Figure 5.4.1 I_{50} is approximately 2.2 times higher than I_k in all cultures. This is consistent with the hypothesis put forward by Serôdio and Lavaud (2011) that the relationship between the saturation of NPQ and ETR is principally dependant on the mechanism of the xanthophyll cycle. NPQ via the xanthophyll cycle can occur either by conversion of diadinoxanthin to diatoxanthin (DD-DT), or the conversion of violaxanthin to zeaxanthin via the intermediary antheraxanthin (VAZ). *T. pseudonana* and *P. tricornutum,* being diatoms, utilise only DD-DT (Goss and Jakob, 2010) so the relationship between I_k and I_{50} is expected to be conserved between the two species. Notably, the slope of the relationship between I_k and I_{50} found here (2.2) is very similar to the mean value of 2.39

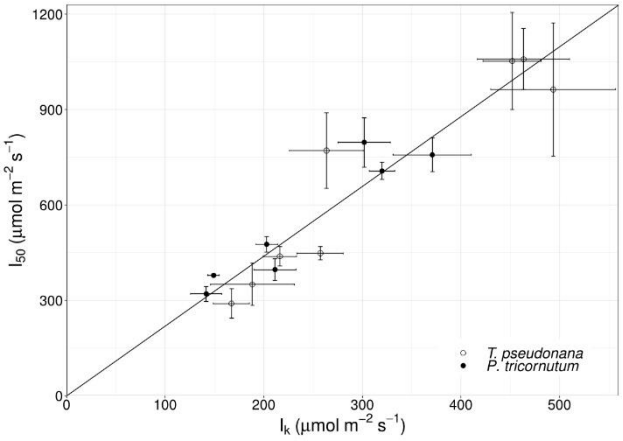

Figure 5.4.1. Relationship between ETR saturation irradiance (I_k) and NPQ saturation irradiance (I_{50}) in 2 diatoms. Line has slope 2.2 and R^2 0.89. Error bars are 1 standard deviation.

reported by Serôdio and Lavaud (2011) for species having DD-DT type xanthophyll cycle. The variability in the saturation I_{50} therefore does not represent acclimation of NPQ per se, rather it reflects the effects of photoacclimation on I_k.

The second characteristic of the NPQ-irradiance response that may be explained in terms of NPQ control by thylakoid lumen pH is the high reported values of n, the curvature parameter. In the Hill Equation from which the NPQ-irradiance curve fit used here is derived, the value of n indicates the degree of cooperativity of the reaction. Values of $n > 1$ indicate positive cooperativity in which an initial reaction increases the probability of subsequent reactions and values of $n < 1$ indicate negative cooperativity in which the opposite is true (e.g. Perutz, 1989). Data indicate activation of NPQ is highly positively cooperative (Table 5.3.1). It has been suggested for diatoms that the accumulation of a transthylakoid proton gradient causes a conformational change in the binding site of epoxidized xanthophylls (diadinoxanthin) within the light harvesting antenna complex (Lavaud and Kroth, 2006; Ruban *et al*., 2004). This allosteric control of xanthophyll de-epoxidation appears to switch xanthophylls to a so-called “activated state”, resulting in rapid, positively cooperative activation of NPQ with little change in transthylakoid pH gradient (Lavaud and Kroth, 2006; Lepetit *et al*., 2012; Ruban *et al*., 2004). Values of n greater than 1 for the NPQ-irradiance response reported here and elsewhere (Barnett *et al*., 2015; Serôdio and

Lavaud, 2011) similarly indicate cooperative allostery of NPQ. This appears to be largely independent of light environment.

Finally, NPQ control by transthylakoid pH gradient is important in understanding the slight initial decrease in NPQ with increased irradiance. This is most evident in cultures of *P. tricornutum* but also occurs in *T. pseudonana* (Figure 5.3.1). NPQ is principally understood in the context of photoprotection against high light intensities, this is inconsistent with elevated NPQ at low irradiances (Muller *et al*., 2001). Rather than being photoprotective, this observation can be attributed to chlororespiration. Chlororespiration causes reduction of plastoquinone in the dark, resulting in the establishment of a weak transthylakoid pH gradient (Bennoun, 2002). In diatoms this is sufficient to stimulate xanthophyll cycle activity, and therefore NPQ, in conditions of darkness (Cruz *et al*., 2011; Grouneva *et al*., 2009; Jakob *et al*., 2001). The impact of chlororespiration on NPQ is not described by the current model of the NPQ-irradiance response. To compensate for this model weakness, elevated values of NPQ at low light intensities were excluded when fitting the NPQ-irradiance response curves shown in Figure 5.3.1. Recently, chlororespiration has been found to be important in maintaining growth rate under rapidly fluctuating light by regulating the redox state of the plastoquinone pool. Nawrocki *et al*. (2018) found growth rates in cells incapable of chlororespiration is reduced under light fluctuations (60s period) compared with cells capable of chlororespiration. Although the current data is

insufficient to conclude this, the strong impact of chlororespiration on the plastoquinone pool in diatoms may contribute to the competitive advantage that this group appears to have in growth rate under fluctuating light (Dijkman and Kroom, 2002; Lavaud *et al*., 2002b; Litchman, 2000; Nicklisch, 1998).

Thus far this section has focussed on aspects of the NPQ-irradiance response which are related to the control of NPQ by thylakoid lumen pH. These are either relatively insensitive to light regime and species (n, and chlororespiration), or dependant on acclimation of other processes and do not strictly represent acclimation of the NPQ-irradiance response (I_{50}). In contrast, the capacity for NPQ (NSV_{max}) indicates significant species-specific acclimation of NPQ in response to the light regime. The 1.5-fold increase in NPQ from HLSQ to HLHF in *P. tricornutum* demonstrates high plasticity for NPQ in this species compared with *T. pseudonana* in which NPQ was comparatively inflexible and significantly lower than in *P. tricornutum* at HL. As well as modifying NSV_{max} in response to light fluctuations at HL *P. tricornutum* also increased its capacity for NPQ from LL to HL while *T. pseudonana* did not. *P. tricornutum* is known to exhibit particularly high plasticity in NPQ compared with other species (Lavaud *et al*., 2016, 2007; Lavaud and Lepetit, 2013; Lepetit *et al*., 2017). This is thought to confer a competitive advantage in conditions of fluctuating light by reducing photodamage during irradiance peaks (Lavaud *et al*., 2007). Indeed, growth

rates reported in chapter 4 (Table 4.3.1, page 65) support this, as growth of *P. tricornutum* was less negatively affected by light fluctuations than growth of *T. pseudonana* at HL.

5.5. Target for PSII photodamage

Gross PSII photodamage (k_i) is not simply dependant on light dose (Figure 5.3.2). Rather, the target of photodamage is variable between light regimes. Under HL, k_i appears to be somewhat reduced by light variability (particularly in *P. tricornutum*) indicating a reduction in the target of photodamage. Within fluctuating light regimes an increase in k_i for *T. pseudonana* from HL to LL similarly indicates an increase in the target of photodamage (McKew *et al*., 2013). To further investigate the target of photodamage, and how acclimation to light variability may affect it, two models of photodamage can be considered.

In the first PSII photodamage occurs following production of a singlet oxygen by the reduction of an already reduced primary quinone acceptor, Q_A (Krieger-Liszkay *et al*., 2008; Vass *et al*., 1992). In other words, excitation of a closed PSII reaction centre in which Q_A is reduced results in the production of a reactive oxygen species which causes damage to the D1 protein (Krieger-Liszkay, 2005; Vass and Aro, 2007). In this model gross photodamage should be proportional to the density of the incident photons, the fraction of closed PSII reaction centres, and the size of the PSII functional antenna (Baroli and

Melis, 1998; McKew *et al*., 2013; Melis, 1999). This can be quantified from FRRF measurements according to Equation 5.5.1.

$$k_i \propto E(1 - q_p)\sigma_{PSII}' \qquad \textbf{5.5.1}$$

Where E is irradiance and σ_{PSII}' is the functional cross section of the PSII antenna measured under actinic light as described in section 3.4. The parameter q_p in Equation 5.5.1 is the coefficient of photochemical quenching, which, under the assumption of zero connectivity between reaction centres is equivalent to the fraction of open reaction centres (Baker and Oxborough, 2004). Therefore $1 - q_p$ is equivalent to fraction of closed PSII reaction centres, this is often called the PSII excitation pressure and approximates the fraction of Q_A that is reduced (Huner *et al*., 1998; Hüner *et al*., 2013; NDong *et al*., 2003). Equation 5.5.2 describes the calculation of q_p from parameters measured by FRRF.

$$q_P = \frac{F_m' - F'}{F_m' - F_o'} \qquad \textbf{5.5.2}$$

Figure 5.5.1 shows that the model of gross photodamage described by Equation 5.5.1 does not accurately represent photodamage measured here. For the data to reflect this model, data in Figure 5.5.1 should be accurately described by a single trendline. While it somewhat resolves the differences in k_i between different light regimes this model fails to explain differences in k_i between HL and LL in *T. pseudonana*.

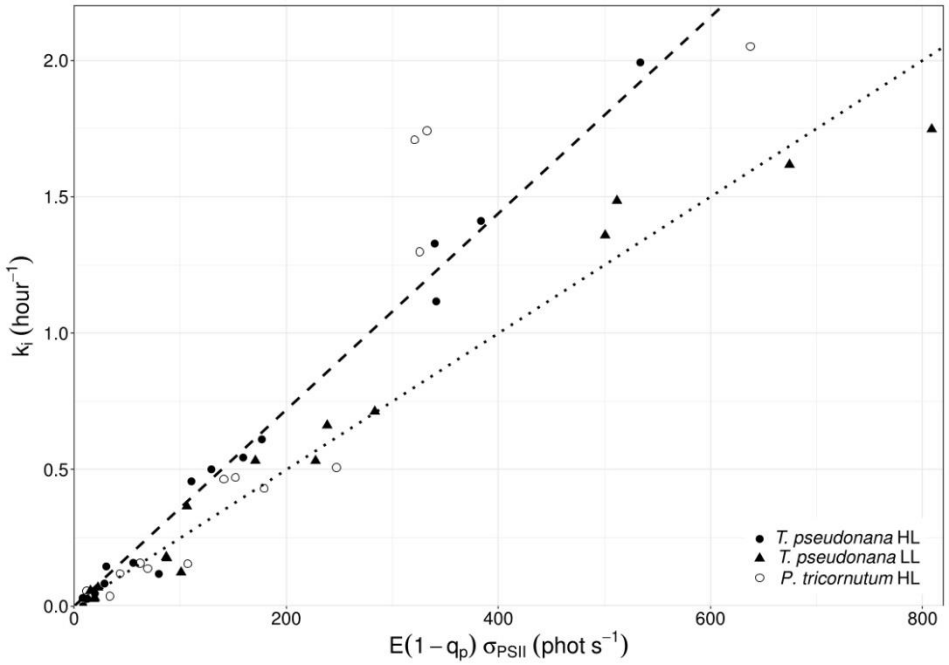

Figure 5.5.1. Relationship between gross photodamage and the product of irradiance, the PSII functional antenna and the fraction of reduced PSII reaction centres for two diatoms grown under a range of light regimes. Dashed trendline for *T. pseudonana* HL and *P. tricornutum* HL has slope 0.0037 and R^2 0.92. Dotted trendline for *T. pseudonana* LL has slope 0.0025 and R^2 0.97.

An alternative model ascribes PSII photodamage to direct excitation of a closed PSII reaction centre (McKew *et al*., 2013). In this model photodamage is independent of light absorption and can be described by Equation 5.5.3

$$k_i \propto E(1 - q_p) \qquad \textbf{5.5.3}$$

This model arises from the hypothesis that primary PSII photodamage results from direct excitation of the manganese cluster in the water splitting complex of PSII (Dau and Haumann, 2008; Tyystjärvi, 2008). This is supported by recent work demonstrating that the action spectrum of PSII photodamage in *P. tricornutum* and other phytoplankton closely match the absorption spectrum of manganese (Hakala *et al*., 2005; Havurinne and Tyystjärvi, 2017;

Soitamo *et al*., 2017). Current data was consistent with this model between all light regimes and across both species (Figure 5.5.2).

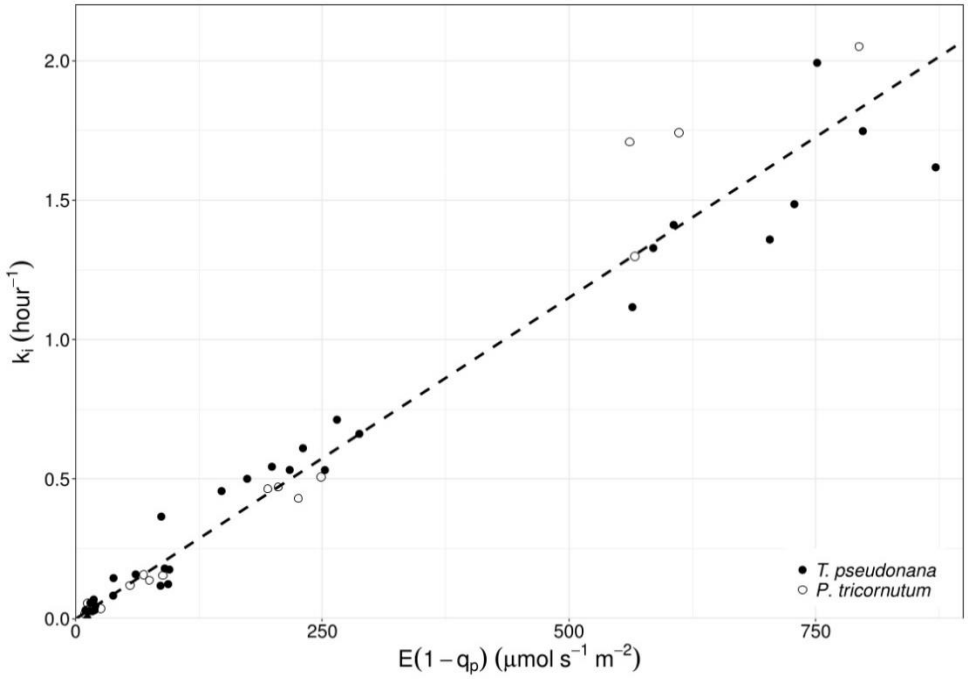

Figure 5.5.2. Relationship between gross photodamage and the product of irradiance and the fraction of reduced PSII reaction centres for two diatoms grown under a range of light regimes. Dashed trendline has slope 0.0023 and R^2 0.96.

Gross photodamage is therefore modulated by processes which affect the excitation pressure within PSII reaction centres (McKew *et al*., 2013). In this study acclimation of light absorption, photochemical quenching, and non-photochemical quenching all serve to alter PSII excitation pressure at any given irradiance, either by reducing excitation or increasing deexcitation of PSII reaction centres (Gray *et al*., 1996; Hüner *et al*., 2013; Maxwell *et al*., 1995). Examining q_p directly illustrates the effect of acclimation to fluctuating light on excitation pressure (Figure 5.5.3). At HL acclimation to fluctuating light substantially reduces PSII excitation pressure compared with acclimation

to a square-wave light regime, reinforcing the conclusion put forward in chapter 4 that acclimation to fluctuating light is driven by photoprotection. Conversely, Figure 5.5.3 shows little difference in q_p between fluctuating light regimes, particularly at high irradiances.

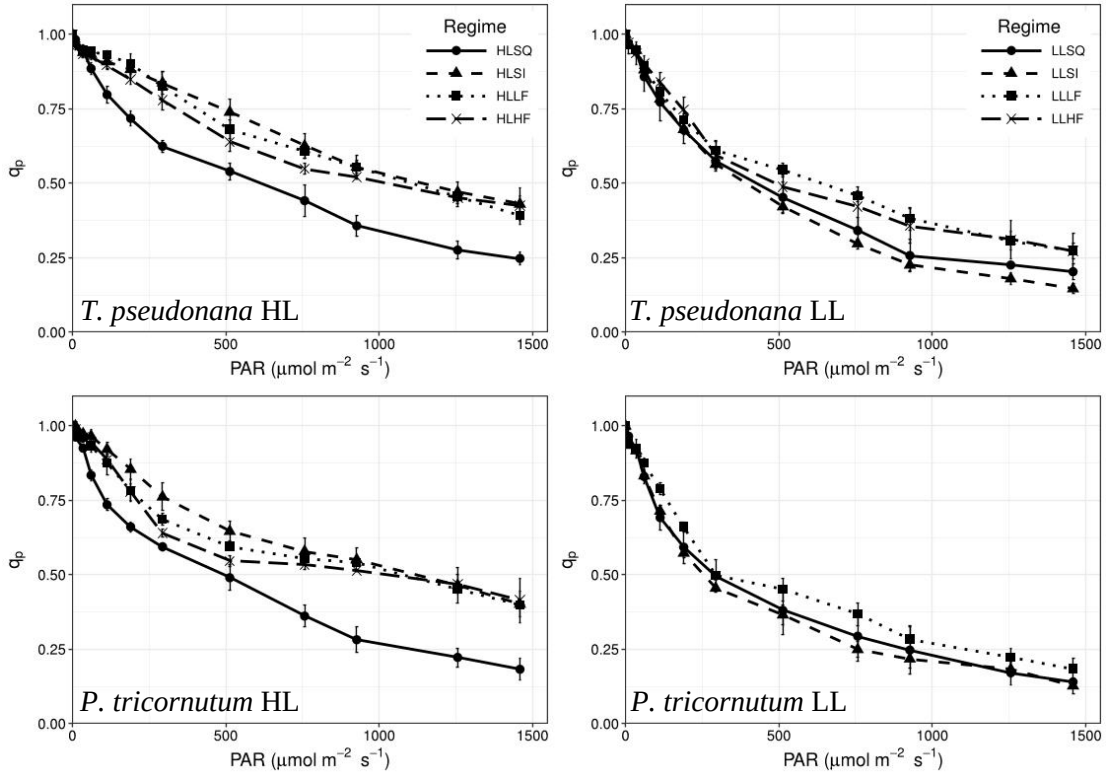

Figure 5.5.3. Photochemical quenching coefficient in response to irradiance in two diatoms grown under a range of fluctuating and non-fluctuating light regimes. Error bars are 1 standard deviation.

It is possible to quantify the effectiveness of several process which impact excitation pressure in mitigating gross photodamage by calculating the number of photochemical charge separations per photodamage incident at PSII. Based on the values of PAR and k_i presented in Figure 5.3.2 a target size for photodamage, σ_i, can be quantified according to Equation 5.5.4.

$$\sigma_i = \frac{k_i}{PAR} \qquad \textbf{5.5.4}$$

The number of PSII photochemical charge separations per photodamage incident can then be calculated from σ_i, q_p and the PSII functional antenna in the light, ${\sigma_{PSII}}'$ according to Equation 5.5.5 (Campbell and Tyystjärvi, 2012). This describes the ratio of the functional antenna size for photochemistry in the light to the antenna size for photodamage, and as such is here denoted as ${\sigma_{PQ}}'/\sigma_i$.

$$\frac{\sigma_{PQ}\prime}{\sigma_i} = \frac{(q_p \times \sigma_{PSII}\prime)}{\sigma_i} \qquad \textbf{5.5.5}$$

Since ${\sigma_{PSII}}'$ is the functional antenna size for light absorption by PSII photochemistry and is downregulated by NPQ in the light (Gorbunov *et al*., 2001) its inclusion in Equation 5.5.5 accounts for the impacts of these two aspects on excitation pressure. Meanwhile q_p accounts for the impact of photochemical quenching.

Values of σ_i are shown in Figure 5.5.4, while ${\sigma_{PQ}}'/\sigma_i$ is shown in Figure 5.5.5. Higher values of ${\sigma_{PQ}}'/\sigma_i$ in *T. pseudonana* than in *P. tricornutum* under low irradiance can probably be attributed to differences in PSII antenna size and q_p. *P. tricornutum* was found to have a larger PSII antenna (see chapter 4), and lower $q_p$under low irradiances (Figure 5.5.3) and therefore experiences more photodamage relative to the activity of photochemistry than *T. pseudonana* when irradiance is low. However, at high irradiance ${\sigma_{PQ}}'/\sigma_i$ is comparable between the two species. The larger PSII antenna, and

lower q_p can also be invoked to explain the lower values of σ_{PQ}'/σ_i in *T. pseudonana* at LL, compared with HL under low irradiances.

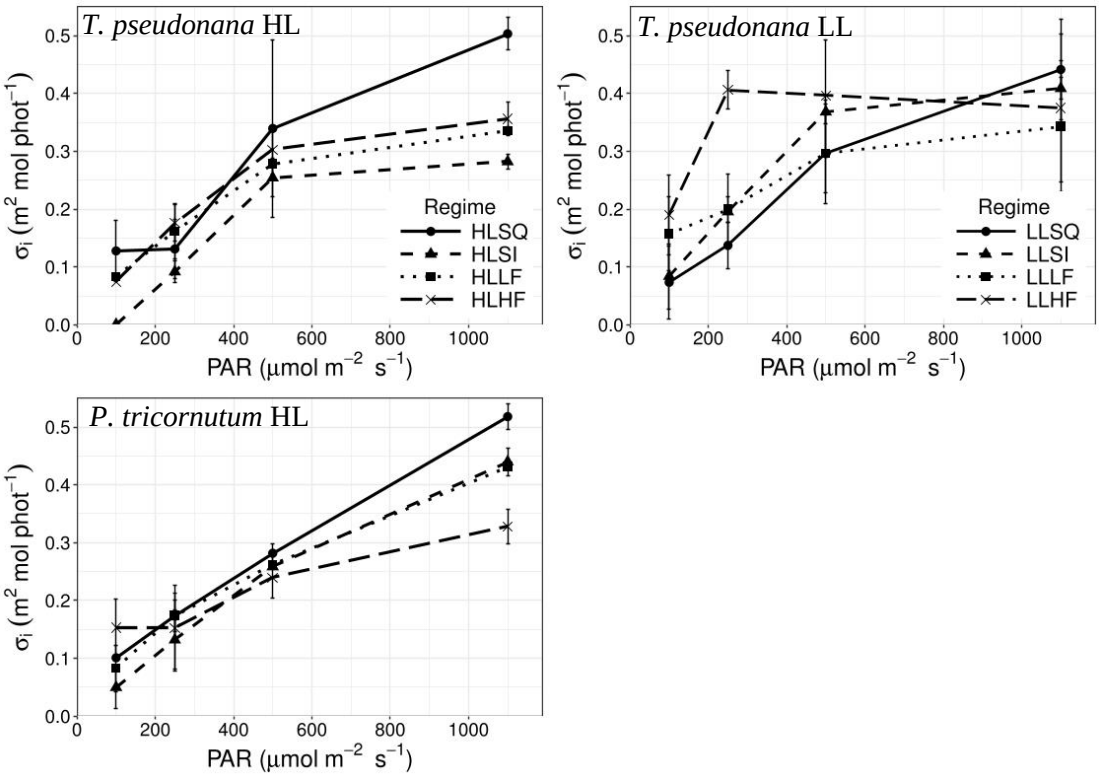

Figure 5.5.4. Target size for photodamage in two diatoms grown under a range of fluctuating and non-fluctuating light regimes. Error bars are 1 standard deviation.

With the exception of cultures grown under the HLSQ regime there is very little difference in σ_{PQ}'/σ_i between light regimes in *T. pseudonana*. Again, the lower σ_{PQ}'/σ_i in HLSQ cultures is likely to be caused by a combination of lower q_p and higher σ_{PSII}. Interestingly, there is a very small difference in σ_{PQ}'/σ_i between HLSQ and other light regimes in *P. tricornutum*, despite the much lower q_p under this light regime. The high level of NPQ in this species in all HL light regimes may be responsible for this. An increase in NPQ between HLSQ and HLLF may also be responsible for the differences in

$\sigma_{PQ}{}'/\sigma_i$ between light regimes at the highest irradiance, although this impact is relatively small overall.

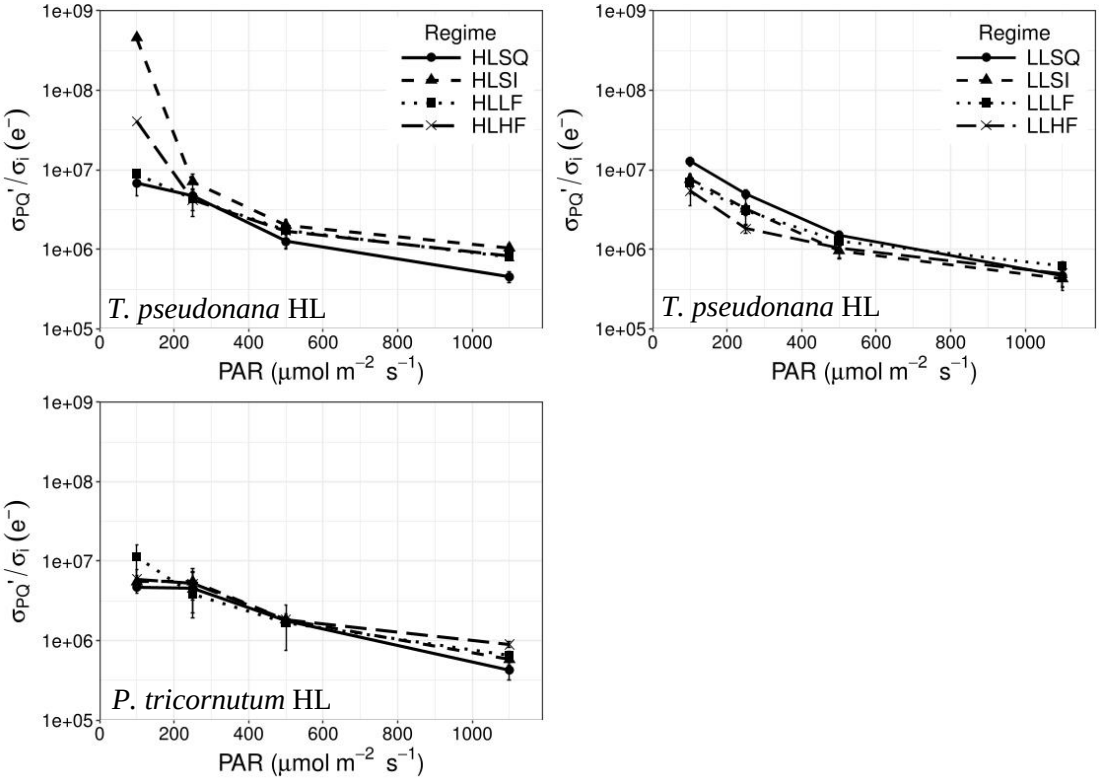

Figure 5.5.5. Number of photochemical charge separations per photodamage event in two diatoms grown under a range of fluctuating and non-fluctuating light regimes. Error bars are 1 standard deviation. Note the logarithmic scale of the y-axis.

In general, the PSII functional antenna size, NPQ and photochemical quenching have been found to mitigate photodamage at lower irradiance by reducing excitation pressure, but have a minimal impact on photodamage under higher light levels (Hurry *et al*., 1996; Li *et al*., 2002; Tyystjärvi, 2008). This is demonstrated here by the minimal differences in $\sigma_{PQ}{}'/\sigma_i$ between all cultures at the highest two light levels. An increase in high irradiance peaks from SI to HF, and minimal variability in $\sigma_{PQ}{}'/\sigma_i$ under high irradiances suggests that cells are more susceptible to gross photodamage under higher

amplitude light fluctuations. Such differences in photodamage have previously been proposed as one reason for the reduction in growth rate associated with fluctuating light (van Leeuwe *et al*., 2005). In natural populations, this may be instrumental in limiting growth in deeply mixed water columns (Alderkamp *et al*., 2010).

5.6. Comparing models of net photodamage and PSII repair

Figure 5.3.4 reports rates of repair of PSII photodamage calculated according the model proposed in section 5.2. This model of net PSII photodamage is somewhat novel in the use of $RCII_f$ rather than raw values of F_v/F_m and describes an equilibrium model of PSII damage and repair. An alternate model described in Ragni *et al*. (2008) involves simply modelling F_v/F_m under net photodamage as an exponential decay function, independent of gross photodamage (Key *et al*., 2010; McKew *et al*., 2013; Ragni *et al*., 2010, 2008). For simplicity this model is referred to as the Ragni model, while the model proposed in this study is referred to as the functional Kok model. The Ragni model was outlined in Equations 5.2.2 to 5.2.4 (see page 95). In order to assess the functional Kok model in this section it is compared to the Ragni model.

In section 5.2 it was noted that the Ragni model does not actually return a rate constant for PSII repair acting on damaged PSII reaction centres (Campbell and Tyystjärvi, 2012). Instead it gives a value which describes how

much the rate of gross photodamage is reduced by repair processes. In the case of no net photodamage the rate of repair from the Ragni model will equal the rate of gross photodamage. Arguably this may be useful information, but it does not actually inform on the rate of PSII repair, and repair values from the Ragni model are not easily converted to rate constants of repair (Campbell and Tyystjärvi, 2012). This is illustrated in Figure 5.6.1, which compares k_r from the functional Kok model to RR from the Ragni model using the data from the present study.

The second criticism of the Ragni model is that by modelling F_v/F_m under net photodamage as a first-order exponential it assumes that eventually all PSII reaction centres will be damaged. Conversely, the functional Kok model assumes that under net photodamage PSII damage and repair eventually reach equilibrium, and the fraction of damaged PSII reaction centres will be asymptotic to some value less than 1. Although measurements of net photodamage appear to suggest the latter (e.g. Aro *et al*., 1993; Campbell and Tyystjärvi, 2012; Patsikka *et al*., 1998; Wu *et al*., 2012) no measurements of sufficient duration could be found to sufficiently test either model.

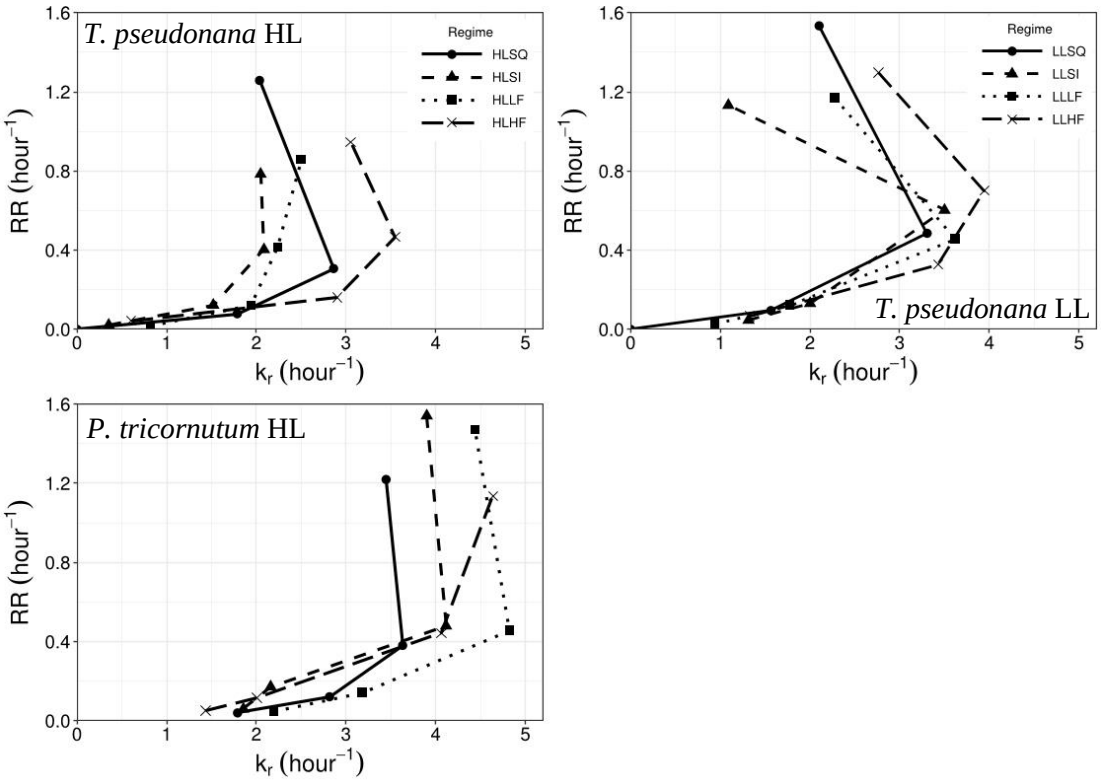

Figure 5.6.1. Comparison of two measures of PSII repair in two diatoms grown under a range of fluctuating and non-fluctuating light regimes.

Thirdly, an underlying assumption of the Ragni model is that at the onset of measurements no PSII reaction centres are damaged. This is unlikely to be the case (Lavaud *et al*., 2016) and in the present study measurements of F_v/F_m often increased during incubation at the lowest irradiance under conditions of net photodamage, indicating that some photodamage was present when samples were initially taken. The functional Kok model was able to accurately model this when the Ragni model was not. Theoretically this could be remedied by allowing samples an extended recovery period in low light or darkness prior to measurements to permit repair of photodamage. However, a prolonged low irradiance recovery period could significantly alter

the acclimation state of the cells with the sample, making measurements irrelevant to the original culture conditions (Anning *et al*., 2000; Harris *et al*., 2009).

One notable advantage of the Ragni model is its comparative simplicity and by not returning a rate constant for repair it also does not carry an assumption of the functional Kok model. Namely, that the total concentration of reaction centres does not change throughout the experiment. Although this is likely to be the case under the conditions found in the present study this assumption may not be met in cultures in the process of acclimating to changes in nutrients (Parkhill *et al*., 2001). Additionally, the functional Kok model carries a mathematical weakness not present in the Ragni model. As k_i decreases values of F_v/F_m predicted by the model are increasingly insensitive to changes in k_r. This led to difficulties in fitting data from the lowest irradiance treatment in which gross photodamage is negligible (Figure 5.3.2) and fitting the functional Kok model occasionally returned excessively large values of k_r. In order to avoid this, it is recommended that the functional Kok model is only used to describe repair in conditions where some gross photodamage is observed. Otherwise k_r should be interpreted with caution.

Figure 5.6.2 shows a comparison between the descriptive power of the Ragni and functional Kok model. Both models were able to describe F_v/F_m under net photodamage relatively well, however the Ragni model tended to overestimate low values of F_v/F_m to a greater degree. The overall sum of squares for residuals for the Ragni model was 0.121, for the functional Kok model it was 0.059 indicating it was a better descriptor of F_v/F_m under net photodamage.

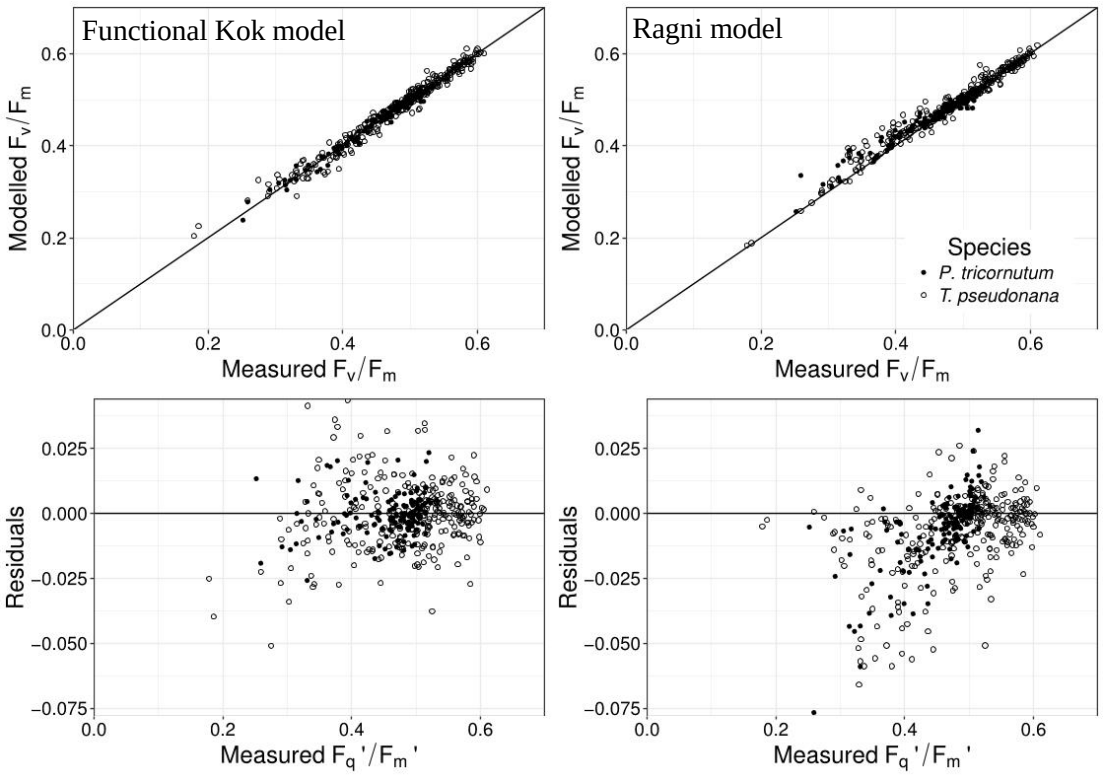

Figure 5.6.2. Comparison between descriptive power of two models of F_v/F_m in two diatoms experiencing net photodamage. Functional Kok model, left, and Ragni model, right. See text (section 3.8) for descriptions of the models. Lines in top plots are 1:1.

Overall the functional Kok model has several theoretical advantages over the Ragni model and gives a better description of the current data.

Therefore, it is concluded that use of the functional Kok model is preferable to the Ragni model.

5.7. Regulation of net photodamage under fluctuating light

PSII repair under HL reported in Figure 5.3.4 can be used to resolve a point of some confusion in the literature. Several studies have reported that higher NPQ capacity reduces the rate of PSII photodamage (Krieger-Liszkay *et al*., 2008; Lavaud *et al*., 2007, 2004, 2002a; Ruban *et al*., 2004). However, if the mechanism of PSII photodamage is by direct excitation of the manganese cluster within PSII, as suggested in section 5.5, a greater capacity for NPQ would not directly prevent it (Onno Feikema *et al*., 2006). This has been used as evidence that the site of photodamage is not the manganese cluster (Vass, 2011). In contrast, several studies have reported that a greater capacity for NPQ does not in fact reduce PSII photodamage (Hakala *et al*., 2005; Jin *et al*., 2003; Olaizola *et al*., 1994; Ragni *et al*., 2010). The key to resolving this issue is the need to distinguish between gross and net photodamage. The studies referenced above which report the dependence of photodamage on NPQ use net photodamage, while those that report the opposite use gross photodamage.

It is also important to note that NPQ can indirectly affect gross photodamage by reducing PSII excitation pressure, but does not directly prevent damage by excitation of the manganese cluster (Hakala *et al*., 2005).

However, the capability of NPQ to mitigate gross photodamage by reducing excitation pressure is relatively small, particularly at high irradiances (Tyystjärvi, 2008). This was demonstrated in the present study, and gross photodamage did not differ greatly between species, despite a considerably greater capacity for NPQ in *P. tricornutum* (Figure 5.3.1). However, k_r was much lower in *T. pseudonana* than in *P. tricornutum*, indicating reduced net photodamage in the species with an enhanced capacity for NPQ. Recently, it has become increasingly apparent that NPQ acts to prevent downregulation of PSII repair process, and does little to prevent photodamage itself (Jin *et al*., 2003; Lavaud *et al*., 2016; Murata *et al*., 2012; Nishiyama *et al*., 2011, 2006; Six *et al*., 2007; Takahashi and Badger, 2011). Present data is consistent with this conclusion.

Greater plasticity of NPQ capacity in *P. tricornutum* enabled this species to alter the rate of PSII repair in response to fluctuating light regimes, resulting in lower net photodamage under higher amplitude light fluctuations. This is hypothesised to reduce net PSII photodamage during high irradiance peaks, enabling *P. tricornutum* to maintain a higher rate of photosynthesis relative to its maximum than *T. pseudonana* throughout light fluctuations within the photoperiod (Lavaud *et al*., 2007). In addition, phytoplankton with a greater capacity for PSII repair have been found to require a smaller pool of RCIIs to maintain a similar concentration of undamaged RCIIs (Lavaud *et al*., 2016). This may confer a reduced energy cost in the synthesis of RCIIs,

enabling greater energy investment in growth. A greater capacity for PSII repair in *P. tricornutum* may therefore contribute to the less negative impact of light fluctuations on growth rate compared with *T. pseudonana*.

NPQ is thought to prevent downregulation of PSII repair by reducing the production of reactive oxygen species (ROS) which inhibit translation of D1 from mRNA (Nishiyama *et al*., 2011; Takahashi and Badger, 2011). Within PSII ROS can be produced by excitation of a reaction centre in which the primary quinone acceptor, Q_A, is already reduced (Krieger-Liszkay, 2005; Krieger-Liszkay *et al*., 2008; Pospíšil, 2009). Therefore production of ROS increases as PSII electron transport become increasingly saturated (Asada, 2006). NPQ reduces the production of ROS by directly competing with photochemical charge separation and subsequent electron transport as a sink for PSII excitation energy (Nishiyama *et al*., 2006; Takahashi and Badger, 2011).

In addition to interspecific differences in k_r, Figure 5.3.4 also shows inhibition of repair under high irradiance, particularly in *T. pseudonana* at LL. Inhibition of PSII repair under high irradiance by ROS has been reported previously (Takahashi and Murata, 2008; Tikkanen *et al*., 2008), however in the current data this is not observed in all cultures. To explain this, it is hypothesised that differences in photoacclimation indirectly affect k_r. Photoacclimation (as discussed in chapter 4) can affect production of ROS by increasing or decreasing the capacity for PSII electron transport (ETR), thereby

altering the PSII excitation pressure at a given irradiance, and changing the fraction of reduced Q_A (Asada, 2006; Murata *et al*., 2007). Differences in the capacity for PSII electron transport in *T. pseudonana* illustrated in Figure 4.3.2 (page 69) can therefore be hypothesised to explain the inhibition of PSII repair under high irradiance at LL observed in Figure 5.3.4. A greater capacity and higher saturation irradiance of ETR in *T. pseudonana* HL cultures would result in lower production of ROS at high irradiance, compared with *T. pseudonana* LL cultures (Murata *et al*., 2007). Since PSII repair is thought to be inhibited by ROS (Nishiyama *et al*., 2011; Takahashi and Badger, 2011), greater inhibition of repair under high irradiance would be expected in *T. pseudonana* LL cultures than in *T. pseudonana* HL cultures. This hypothesis is supported by differences in k_r between *T. pseudonana* HL cultures. Firstly, k_r is highest in under the HLHF regime, in which ETR is also highest. Secondly, among *T. pseudonana* HL cultures, k_r exhibits the greatest inhibition under high irradiance in cultures grown under HLSQ regime, in which ETR is the lowest.

That PSII repair is inhibited under high irradiance invalidates the hypothesis that k_r conforms to Michaelis-Menten kinetics with respect to k_i. In fact, it may be more appropriate to describe k_r with respect to irradiance using a model similar to that of the photosynthesis-irradiance response which includes photoinhibition. For example the model proposed by Platt *et al*. (1980) or Eilers and Peeters (1988). Unfortunately, this could not be tested

with the present data because of the low number of measurements over the range of irradiance explored.

NPQ is hypothesised to reduce inhibition of repair by competing with electron transport as a sink for PSII excitation energy. Based on this hypothesis other processes which compete with PSII electron transport for the deexcitation of absorbed light energy would also modulate production of ROS, and therefore reduce downregulation of PSII repair. In chapter 4 PSII cyclic electron transport was hypothesised to be a significant contributor to variation in alternative electron sinks between cultures grown under different light regimes. Although the mechanism of PSII cyclic electron transport is not entirely clear some evidence suggests it may bypass Q_A and Q_B, and therefore act to reduce ROS production by competing with linear electron transport (Lysenko *et al*., 2016; Onno Feikema *et al*., 2006; Wagner *et al*., 2016). A hypothesis can therefore be presented that acclimation to fluctuating light by increases in alternative electron sinks reduces net photodamage by preventing downregulation of PSII repair by ROS. This hypothesis can also somewhat explain differences in k_r in *T. pseudonana* between light regimes.

5.8. Summary and conclusions

The two species studied here demonstrate differences in the plasticity of NPQ. *P. tricornutum* has previously been demonstrated to have a high plasticity for NPQ compared with other diatoms, and to enhance its capacity

for NPQ in fluctuating light (Lavaud *et al*., 2007). NPQ directly competes with photosynthetic electron transport as an energy sink within PSII. However, the rapid kinetics of its activation and deactivation and control by the transthylakoid proton gradient mean NPQ is only significantly activated under light levels saturating to PSII ETR (Giovagnetti *et al*., 2014; Goss and Jakob, 2010; Lavaud *et al*., 2002a). Thereby minimising the potential reduction of photosynthetic electron transport by NPQ (Derks *et al*., 2015).

NPQ has previously been hypothesised to be a mechanism to reduce photodamage during high irradiance peaks in fluctuating light regimes (Lavaud *et al*., 2007; Lavaud and Lepetit, 2013; Lepetit *et al*., 2017). However, because the target of photoinhibition appears to be largely independent of NPQ (Takahashi and Badger, 2011), acclimation to fluctuating light regimes does not reduce PSII photodamage directly. Rather it is hypothesised to limit the inhibition of PSII repair under high irradiance (Nishiyama *et al*., 2006). Thus, the enhancement and comparatively greater capacity for NPQ in *P. tricornutum* enables it to maintain higher rates of PSII repair than *T. pseudonana* in fluctuating light regimes (Lavaud *et al*., 2016).

Photodamage, and subsequent repair, has recently been found to play a vital role in the control of phytoplankton growth during vertical mixing in the ocean (Alderkamp *et al*., 2010). Depending on physical conditions, vertical mixing of phytoplankton can produce a wide range of light environments. In terms of light environments *T. pseudonana* and *P. tricornutum* can be

characterised as occupying different ecological niches. *P. tricornutum* is an estuarine species whilst *T. pseudonana* is a coastal oceanic species (Lavaud *et al*., 2007). Since estuaries tend to be characterised by rapid mixing and greater light attenuation (caused by higher turbidity) *P. tricornutum* can be expected to experience a light environment that is more rapidly variable, and features higher magnitudes of variability, than the light environment experienced by *T. pseudonana*. It is hypothesised that a higher plasticity and capacity for NPQ in *P. tricornutum* is an adaptation to its ecological niche, allowing it to outcompete *T. pseudonana* in conditions of high light variability by reducing the inhibition of PSII repair during periods of high irradiance (Blommaert *et al*., 2017; Lavaud *et al*., 2007; Lavaud and Lepetit, 2013).

6. Intradiel acclimation to light variability and impacts on estimates of daily photosynthesis

6.1. Introduction

The previous two chapters discussed acclimation of light absorption, the photosynthesis-irradiance response, and photoprotection and damage in fluctuating light regimes as a whole based on measurements made at approximately midday during the photoperiod. Although this gives an understanding of the mode of acclimation to dynamic light it fails to account for variability of photophysiology within the photoperiod itself. In chapter 4 it was acknowledged that the rate constant for photoacclimation is longer than the period of light fluctuations used here, such that cells would be unable to acclimate to individual peaks in irradiance. (Macintyre *et al*., 2000; Nymark *et al*., 2009). However, variability in light harvesting pigments and the photosynthesis irradiance response across the entire photoperiod is well documented in phytoplankton in natural systems, as well as under square-wave illumination in laboratory studies (Harding *et al*., 1981b, 1981a; John *et al*., 2012; Schuback *et al*., 2016; Yoshikawa and Furuya, 2006). This is typically characterised by an increase in chlorophyll specific light absorption, maximum photosynthetic rate (measured as ETR, O_2 evolution, or carbon accumulation) and the initial slope of the photosynthesis-irradiance (P-I) response from

dawn towards approximately midday, and a subsequent decrease to dusk (Harding *et al*., 1981a; Yoshikawa and Furuya, 2006). The xanthophyll pool has also been found to exhibit diurnal variability in natural systems, being maximal around midday (Kudoh *et al*., 2003).

Intradiel variability in photophysiology across the photoperiod has serious implications for estimations of primary productivity. Field measurements of photosynthesis are time consuming and the number of measurements that can be made is limited, as such daily photosynthesis rates may be extrapolated from a single measurement (e.g. Alderkamp *et al*., 2015; Brush *et al*., 2002; Carmack *et al*., 2004). Failure to account for diel variability in the photophysiology of the phytoplankton can result in considerable overestimates or underestimates of daily photosynthesis (Harding *et al*., 1982; Walsby *et al*., 2001; Yoshikawa and Furuya, 2006).

Although some studies have examined intradiel variability of phytoplankton photophysiology to sinusoidal light (Bruyant *et al*., 2005) or more highly fluctuating light regimes (Dimier *et al*., 2009), how changes in light fluctuations impact the magnitude and dynamics of this variability is almost entirely unknown. In the marine environment changes in stratification occur as a result of numerous physical process, and these can significantly affect the amplitude of light variability experienced by phytoplankton (Diehl *et al*., 2002; Huisman *et al*., 2004). Understanding the impact of changes in the light environment on diel variability in the P-I curve is important in order

to assess its impact on the accuracy of estimates of daily photosynthesis rates. For example, Yoshikawa and Furuya (2006) reported that a decline in maximum photosynthetic rate from midday to dusk resulted in daily photosynthesis rates based on dusk measurements of the P-I response considerably underestimating the actual value of daily photosynthesis. However, these measurements were exclusively made during a period of stratification. Increased mixing, and therefore variability in irradiance may significantly alter diel variability in the P-I curve, increasing or reducing the accuracy of estimated daily photosynthesis made based on P-I curves at a single point in the photoperiod (Cullen and Lewis, 1988). One objective of this study was to investigate how intradiel light fluctuations impacted acclimation throughout the photoperiod, and how this may affect estimates of daily photosynthesis based on a single set of measurements. This chapter examines changes in light absorption, the ETR, and NPQ over the course of the photoperiod in *T. pseudonana* and *P. tricornutum* under a sinusoidal and a fluctuating light regime in the context of this objective.

This study, and several others, have documented a reduction in growth rate associated with increased amplitude and variability of light fluctuations under light regimes with comparable light dose (chapter 4, Lavaud *et al*., 2007; Nicklisch, 1998; Nicklisch and Fietz, 2001; Shatwell *et al*., 2012; Wagner *et al*., 2006). Several factors have been hypothesised to be responsible for this. Most often, including in chapter 4 of this study, a reduction in daily

photosynthetic rate as a result of an inability of cells to efficiently utilise light during peaks in irradiance (Litchman, 2000; Shatwell *et al*., 2012). However, alternative hypotheses have been presented, including increased photodamage (Alderkamp *et al*., 2010; Poll *et al*., 2007), greater metabolic costs associated with photoprotection (van Leeuwe *et al*., 2005), and changes in respiration and the molecular composition of cellular biomass (Su *et al*., 2012). The data presented in this chapter provides an opportunity to examine these hypotheses using measurements taken throughout the photoperiod.

6.2. Materials and methods

Measurements were carried out on *T. pseudonana* and *P. tricornutum* grown under high light sinusoidal (HLSI) and high light low fluctuation (HLLF) light regimes as described in chapter 2.

In order to accurately measure daily photosynthesis from electron transport across the photoperiod, photosystem II (PSII) fluorescence induction curves were measured continuously within the cultures themselves. To achieve this the culture vessel had to be mounted on top of the FRRF fluorometer (FastTracka II, Chelsea technologies group). Culture vessels used in previous experiments were enclosed by a water jacket on the bottom and sides to maintain constant temperature. However, the width of the water

jacket on the bottom of the vessel prevented FRRF measurements. In order to take FRRF measurements a different culture vessel was used that lacked the bottom water jacket. This vessel was somewhat thinner than the original vessels for which the light setup was designed. As a result, the distribution of irradiance within the culture was less variable both horizontally and vertically than that presented in Figure 2.5.2 (page 34). Despite the different culture vessel, the volume of cultures was the same as in previous experiments, approximately 500 ml.

Taking FRRF measurements from below prevented mixing using a magnetic stirrer as in previous experiments. Instead cultures were stirred by a metal paddle inserted through a hole in the top of the culture vessel. In order to allow the stirrer to rotate, a gap had to be left in the top of the vessel. This inability to fully seal the vessel led to some instances of contamination with other phytoplankton species, and cultures were regularly examined microscopically to ensure contamination had not occurred. Cultures were inoculated using samples acclimated to the relevant light regime used in previous experiments and were acclimated for a further period of 1 week before measurements. Measurements were then repeated over a period of 3-5 days. When necessary, acclimation and sampling was repeated to obtain a minimum of 3 replicates. As in other experiments, cultures were maintained in exponential growth by dilution with growth media. In order to measure cultures directly using the FRRF technique they had to be kept optically thin.

To this end cultures were diluted following the end of the photoperiod, and again prior to the onset of the photoperiod if necessary for FRRF measurements. To avoid impacting FRRF measurements, cultures were not diluted during the photoperiod. For brevity the onset of the photoperiod is often referred to as dawn, and the end of the photoperiod as dusk.

Samples (~10 ml) were taken at 45-minute intervals for analysis. A portion of the sample was concentrated and used to determine *In vivo* chlorophyll-*a* absorption coefficients as described in section 3.3. The remainder was dark acclimated for 20 minutes and used to measure ETR-irradiance curves using the FRRF method as described in section 3.4. The light steps used in the measurement of the ETR-irradiance response were shortened to 3 minutes so that measurements could be made at 45-minute intervals. The NPQ-irradiance response, as quantified by *NSV*, was also calculated from FRRF measurements as described in section 3.6.

Estimates of daily ETR were calculated from the ETR-irradiance response curves after applying a spectral correction to account for differences in emission spectra between LEDs used to measure ETR, and those used to illuminate cultures. The spectral correction method is described in section 3.6. Daily ETR was then calculated from a single ETR-irradiance response curve, or

by linearly interpolating the parameters of the ETR-irradiance response between measurements.

Single-turnover FRRF measurements of cultures were made at intervals of 60 seconds according to the method described in section 3.4, using a separate FRRF to that used to measure ETR-irradiance response curves, which was positioned below the culture vessel. From these measurements, PSII electron transport rate was calculated using absorption coefficients, spectrally weighted to the spectra of the LEDs used to illuminate cultures and linearly interpolated between measurements made at 45-minute intervals.

To calculate *NSV* across the photoperiod it was necessary to estimate dark acclimated fluorescence measurements. To do this, dark acclimated measurements of F_o and F_m were first interpolated across the photoperiod from those measured during the initial dark step of ETR-irradiance response curves. Then, to account for optical differences between the two FRRFs these were transformed such that the dawn and dusk measurements were consistent with those made within the culture. *NSV* was then calculated based on these estimates of F_o and F_m as described in section 3.6.

The two FRRFs used in this experiment differed in excitation wavelengths. The FRRF used for single turnover measurements had an excitation wavelength of 450nm, while the one used to measure ETR-irradiance response curves had an excitation wavelength of 430nm. This had

no significant impact on the values of *NSV* and ETR since both rely on relative changes in fluorescence rather than absolute fluorescence values.

6.3. Results

Both species exhibited intradiel variability in light absorption coefficients (Figure 6.3.1). Under the HLSI regime a^{chl} increased from dawn to midday and declined in the afternoon before increasing again slightly over the last 1-2 hours of the photoperiod. Under the HLLF regime intradiel variability in a^{chl} was lower than under the HLSI regime. This is most apparent in *P. tricornutum*, in which a^{chl} did not show a distinct trend across the photoperiod.

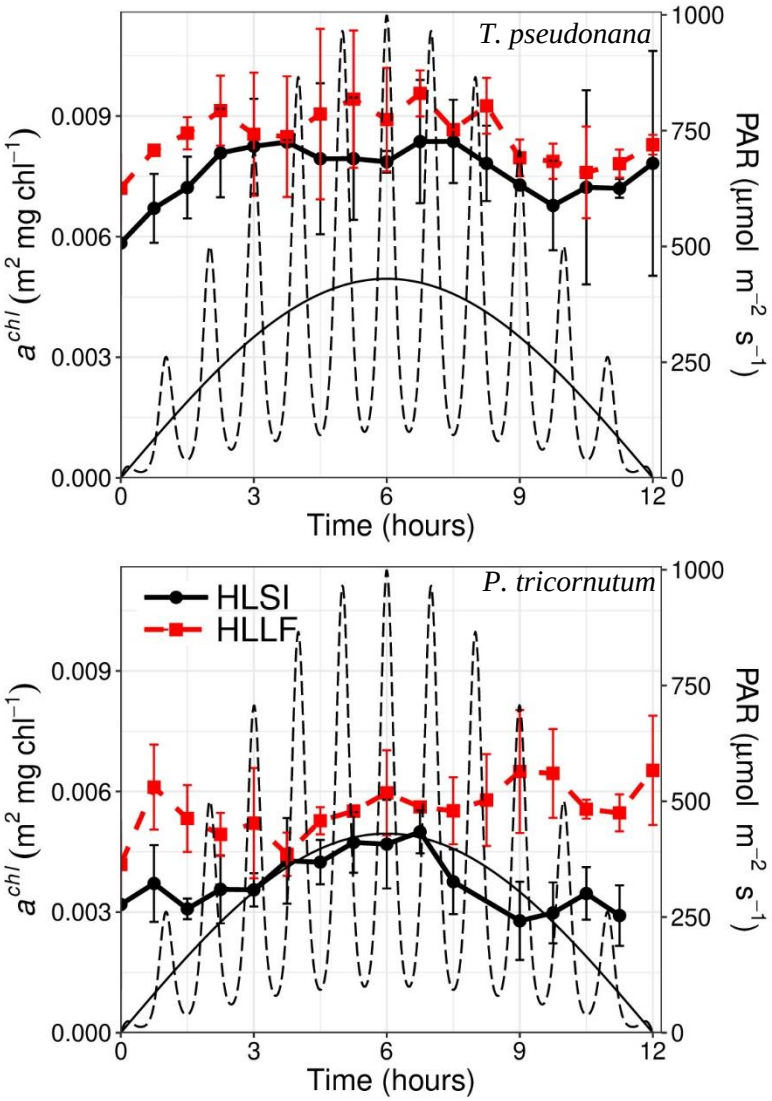

Figure 6.3.1. Chlorophyll-*a* specific absorption coefficients in two diatoms measured over the course of the photoperiod in two variable light regimes. Light regimes are indicated by thin lines. Error bars are 1 standard deviation.

The parameters of the ETR-irradiance relationship showed a similar trend to a^{chl} across the photoperiod (Figures 6.3.2 and 6.3.3). Under the HLSI regime ETR_{max}, I_k, and to a lesser extent α, increased from the onset of the photoperiod to approximately midday, and then decreased towards the end of the photoperiod. ETR_{max} and I_k in *T. pseudonana*, were approximately a factor of 2 greater at midday than at dawn. ETR_{max} was proportionally even

more variable in *P. tricornutum*, being 3.7 times higher at midday than at dawn. The variability in ETR_{max} for *P. tricornutum* under the HLSI regime was largely a result of changes in the light absorption coefficient, rather than changes in PSII operating efficiency. The maximum electron transport rate relative to light absorption $\left(\frac{ETR_{max}}{\bar{a}_{act}^{chl}}\right)$ was less variable than ETR_{max}, increasing by only a factor of 1.6 from dawn to midday in this species (not shown). The same was not true for *T. pseudonana*, in which the maximum electron transport rate relative to light absorption showed variability of a similar magnitude to ETR_{max} (increasing by approximately 1.8 times from dawn to midday versus the 2 times increase in ETR_{max}). This can be seen when comparing a^{chl} (Figure 6.3.1), which varies little in *T. pseudonana* compared with *P. tricornutum*, to ETR_{max} (Figures 6.3.2 and 6.3.3).

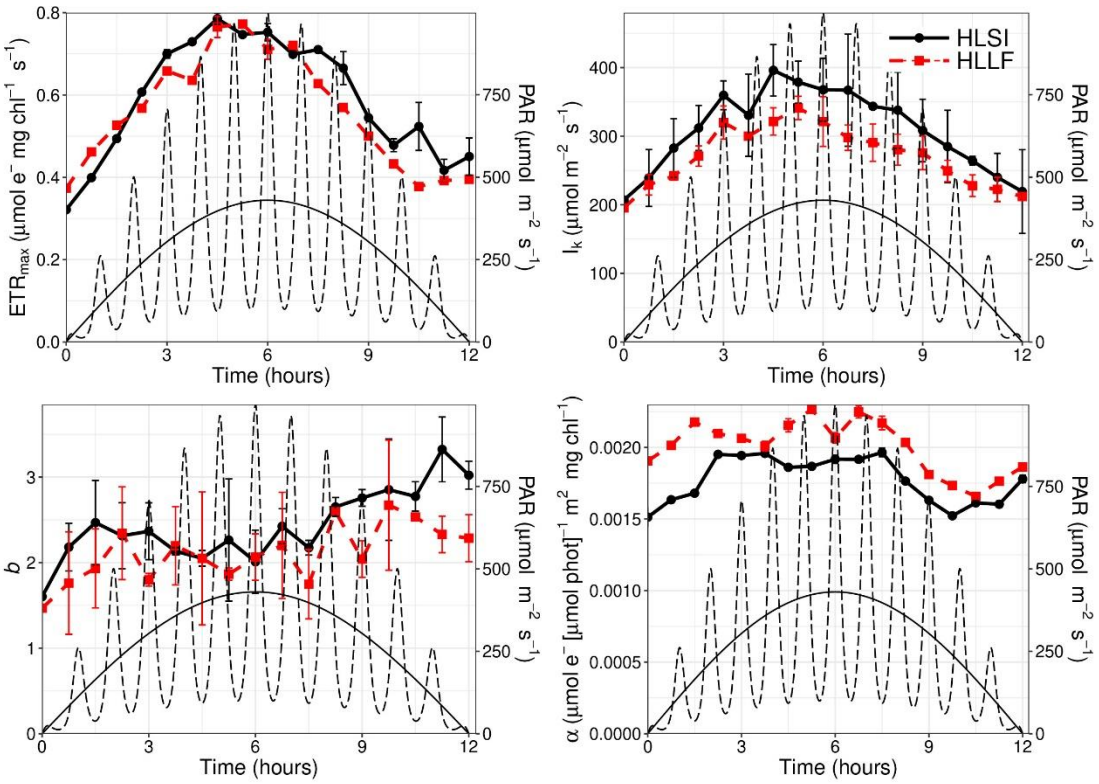

Figure 6.3.2. Parameters of the ETR-irradiance response for *T. pseudonana* measured over the course of the photoperiod in two variable light regimes. Light regimes are indicated by thin lines. Error bars are 1 standard deviation.

In both species, intradiel variability in I_k was less under the HLLF regime than the HLSI regime. Dawn values of I_k in *T. pseudonana* and *P. tricornutum* differed little between light regimes but at midday I_k was noticeably lower under the HLLF regime. Intradiel variability in ETR_{max} in *P. tricornutum* was considerably reduced under the HLLF regime compared with the HLSI regime. This was not solely a result of changes in light absorption, but, rather reflected low variability in both light absorption and PSII operating efficiency. Intradiel variability in ETR_{max} was apparently unaffected by light regime in *T. pseudonana*. In general, for *T. pseudonana* differences in the ETR-irradiance response between HLSI and HLLF were only characterised by

reduced intradiel variability in E_k, while *P. tricornutum* exhibited reduced variability in the ETR-irradiance response as a whole.

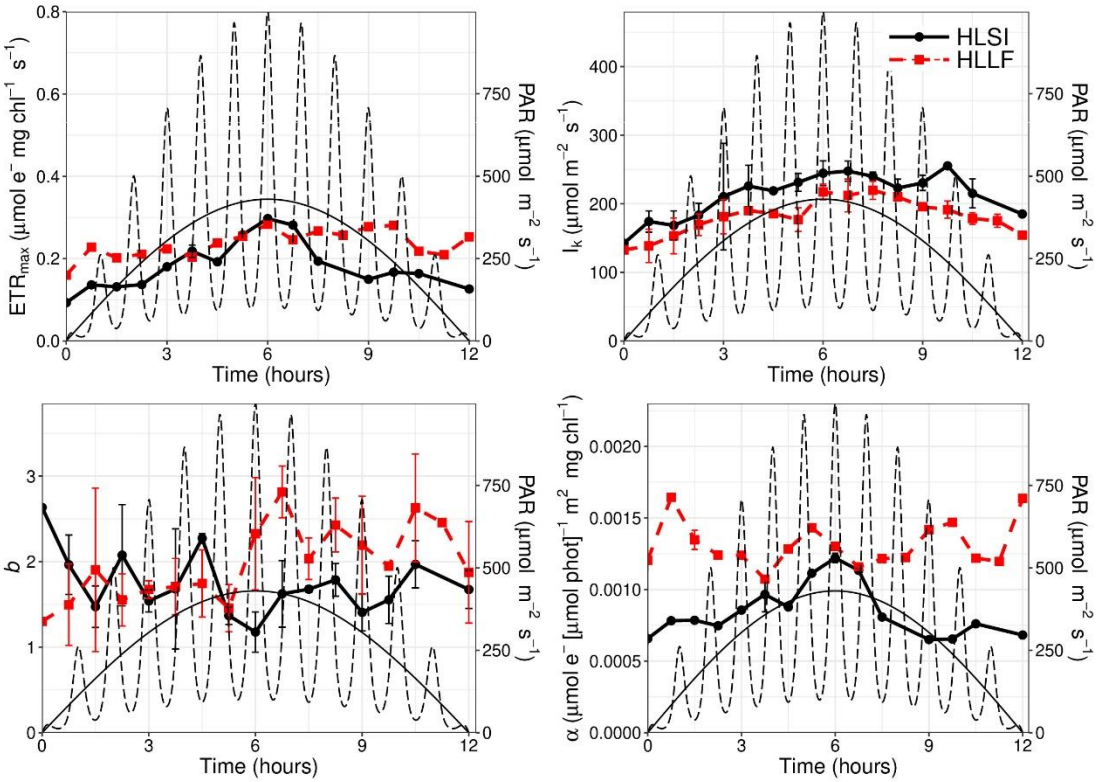

Figure 6.3.3. Parameters of the ETR-irradiance response for *P. tricornutum* measured over the course of the photoperiod in two variable light regimes. Light regimes are indicated by thin lines. Error bars are 1 standard deviation.

The values of ETR calculated from interpolated parameters of the ETR-irradiance relationships across the photoperiod (Figures 6.3.2 and 6.3.3) showed good agreement with measured ETR values at low light levels (Figure 6.3.4). However, at high light levels measured ETR tended to be somewhat higher than the interpolated values, particularly in *T. pseudonana* under the HLLF regime. This may indicate that the irradiance used to calculate ETR from measurements of F_q'/F_m' was somewhat below the actual irradiance. Given the rapid kinetics with which F_q'/F_m' can change following changes in

irradiance (Ihnken *et al*., 2010) this could be a result of variability in irradiance within the culture vessel itself, as opposed to a discrepancy between the supposed and actual mean irradiance. Nevertheless, integrated daily ETR based on measured and interpolated calculations of ETR across the photoperiod do not differ significantly in any of the cultures (Figure 6.3.5, ANOVA and post hoc Tukey HSD).

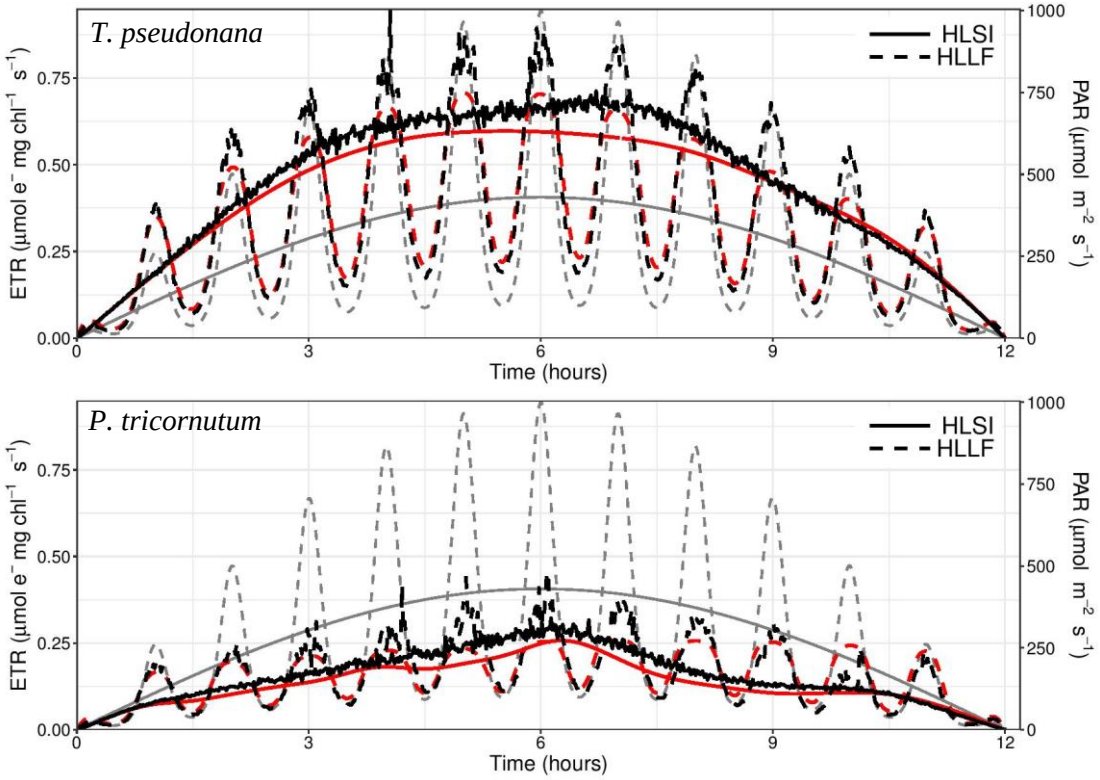

Figure 6.3.4 ETR measured (thick black) and interpolated from parameters fit to the ETR-irradiance relationship measured periodically across the photoperiod (red) in two diatoms grown under two dynamic light regimes. Light regimes are indicated in grey. Measured ETR are means of 3-4 measurements.

In *T. pseudonana* measured daily ETR under the HLLF regime was 78% of that under the HLSI regime (Figure 6.3.5). This difference was highly significant (ANOVA, $F_{1,5}$=68.12, p<0.001). *P. tricornutum* showed the opposite response. Measured daily ETR in this species increased slightly from HLSI to

HLLF (HLLF = 102% of HLSI), although this difference was not statistically significant (ANOVA, $F_{1,5}$=0.17, p<0.696).

Estimates of daily ETR from single fits to the ETR-irradiance response varied wildly in their accuracy depending on the time of day the culture was sampled (Figure 6.3.6). For all cultures the poorest estimates were calculated from the ETR-irradiance response measured in samples taken at dawn. In *T. pseudonana* estimates from samples taken from 4 hours before midday until up to 2 hours after were most accurate, and differed from measured values by <15%. Within this period estimates were most accurate for cultures grown under the HLLF regime, while samples from the HLSI regime tended to overestimate daily ETR. Calculations from curve fits measured towards dawn and dusk increasingly underestimated daily ETR to a degree which was largely independent of light regime. As for *T. pseudonana*, estimated ETR for *P. tricornutum* was most accurate when calculated from samples taken around midday but tended to underestimate daily ETR when calculated from samples taken closer dawn and dusk. However, in *P. tricornutum* ETR estimates were notably more accurate across the photoperiod in cultures grown under the HLLF regime

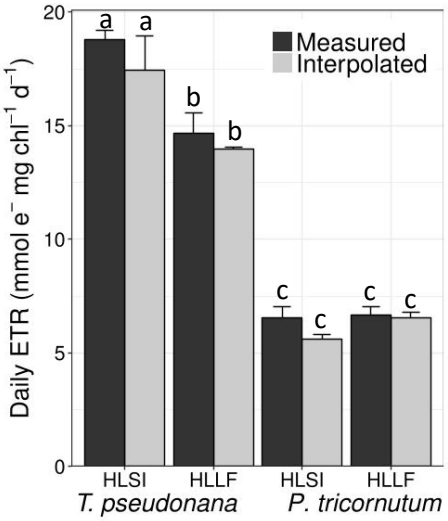

Figure 6.3.5. Integrated daily ETR measured or interpolated from fits to periodically measured ETR-irradiance response curves in two diatoms grown under two dynamic light regimes. Error bars are 1 standard deviation. Letters indicate significance groupings at the 95% confidence level.

than in cultures grown under the HLSI regime. With the exception of two data points, the estimated ETR differed from the measured value by <18% across the photoperiod for *P. tricornutum* under HLLF. Meanwhile, under HLSI 9 of the 15 estimates of daily ETR deviated from the measured value by >18%. The overall greater accuracy of estimated daily ETR in *P. tricornutum* HLLF cultures compared with all other cultures can be illustrated numerically by averaging the absolute values of the percentage deviation reported in Figure 6.3.6. The mean percentage deviation of estimated daily ETR from measured values was 17.0 and 18.0% in *T. pseudonana* grown under HLSI and HLLF respectively, and 20.3 and 10.5% in *P. tricornutum* grown under HLSI and HLLF respectively. Therefore, it can be concluded that increased variability in irradiance had minimal effect on the accuracy of daily ETR estimates in *T. pseudonana* but increased the accuracy of estimates in *P. tricornutum.*

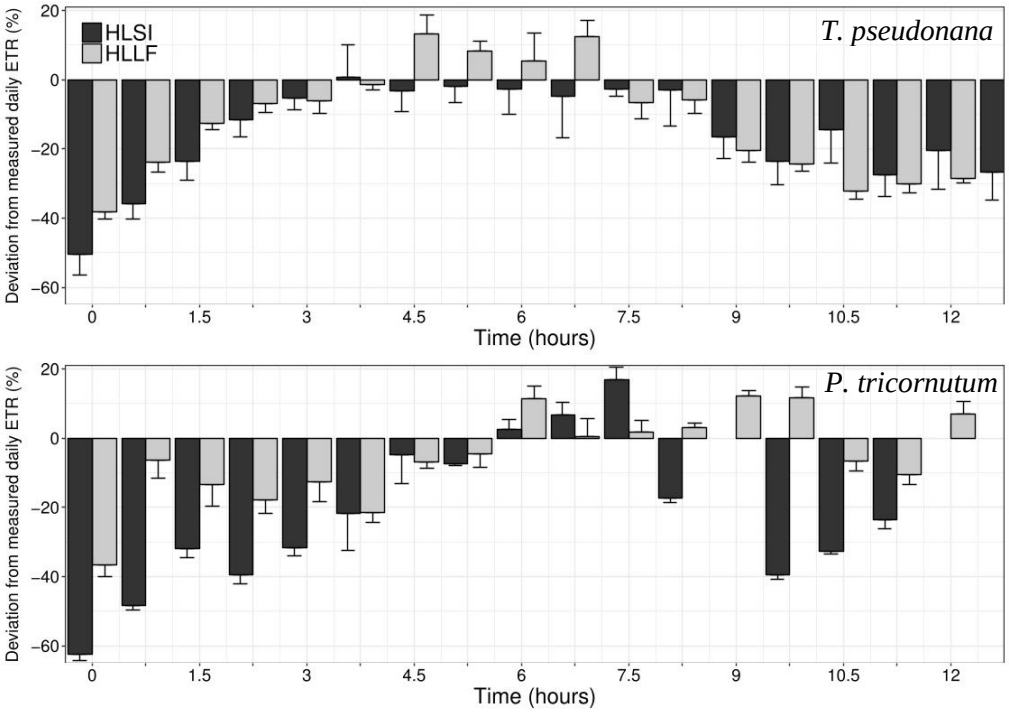

Figure 6.3.6. Estimates of daily ETR from ETR-irradiance curves measured periodically across the photoperiod relative to measured daily ETR. Data are from two diatoms grown under two different dynamic light regimes. Error bars are 1 standard deviation.

As with ETR, the parameters of the *NSV*-irradiance relationship also varied somewhat across the photoperiod in both species (Figures 6.3.7 and 6.3.8). *T. pseudonana* showed a pronounced increase in I_{50} from the onset of the photoperiod to within 1-2 hours of midday, followed by a decrease to dusk. This was also found for *P. tricornutum* to a lesser degree. The minimum NPQ, and maximum capacity for NPQ (NSV_0 and NSV_{max} respectively in Figures 6.3.7 and 6.3.8) were less variable in *T. pseudonana*, than in with *P. tricornutum*. In *P. tricornutum* both NSV_0 and NSV_{max} were substantially higher around midday than at dawn and dusk. Although the values of I_{50}, NSV_0 and NSV_{max} differed between light regimes the variability in these parameters appeared to be minimally affected by light regime in *T.*

pseudonana. The same appears to be true for *P. tricornutum* with the exception of NSV_{max}, which increased to a greater degree, and was more variable, under the HLLF regime than the HLSI regime.

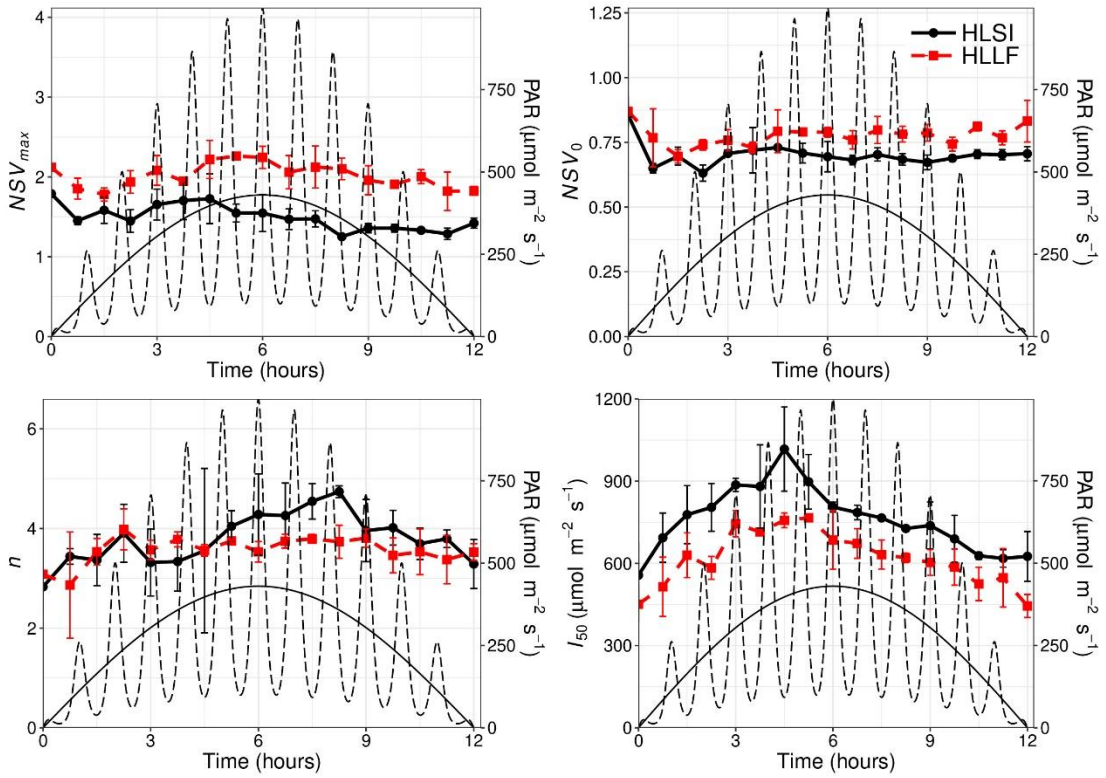

Figure 6.3.7. Parameters of the *NSV*-irradiance response for *T. pseudonana* measured over the course of the photoperiod in two variable light regimes. Light regimes are indicated by thin lines. Error bars are 1 standard deviation.

As would be expected, variability in NPQ over the course of the photoperiod closely followed changes in irradiance (Figure 6.3.9). NPQ was markedly higher in *P tricornutum* than in *T. pseudonana* under both light regimes. Under the HLLF regime NPQ also appeared to be activated at much lower irradiances in *P. tricornutum* than in *T. pseudonana* as NPQ is clearly evident during the second irradiance peak in the former, but not in the latter.

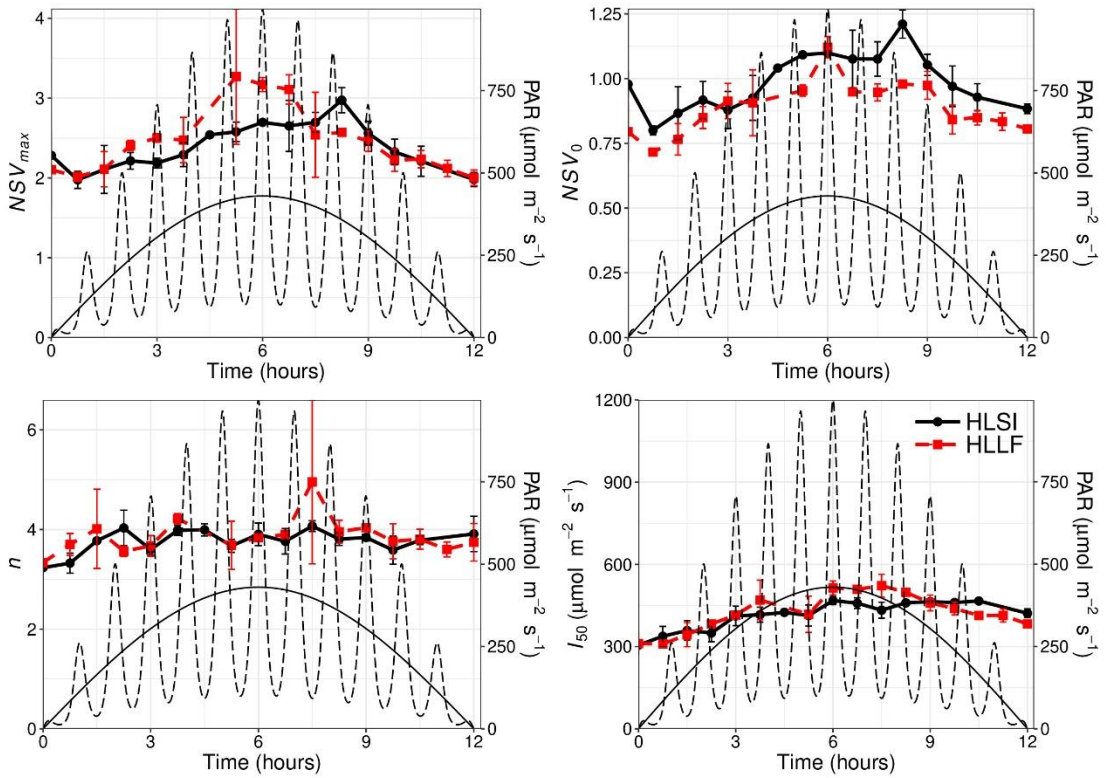

Figure 6.3.8. Parameters of the *NSV*-irradiance response for *P. tricornutum* measured over the course of the photoperiod in two variable light regimes. Light regimes are indicated by thin lines. Error bars are 1 standard deviation.

Overall, the variability in NPQ over the photoperiod was also slightly asymmetrical, being greater prior to midday than after it. In Figure 6.3.9 this is only clear for *P. tricornutum* because of the scale of the axes, but also occurred in *T. pseudonana*.

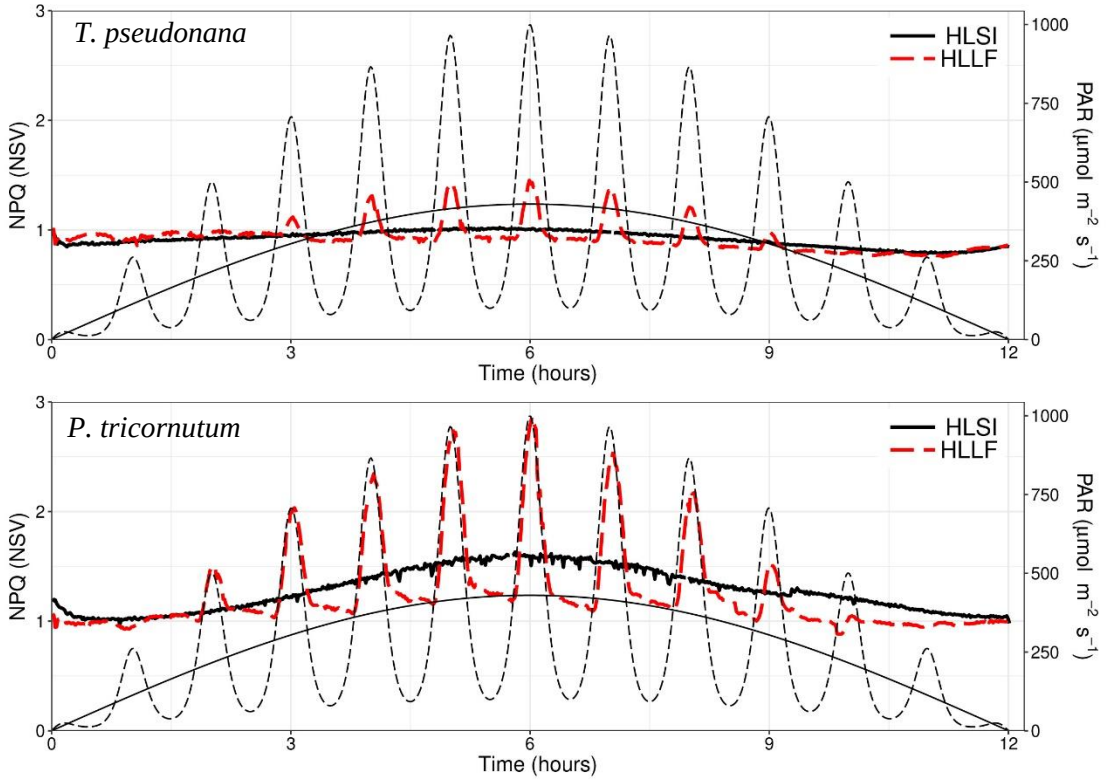

Figure 6.3.9. NPQ across the photoperiod in two diatoms grown under two dynamic light regimes. Light regimes are indicated by thin lines. Values are means of 3-4 measurements.

6.4. Consistency with previously reported data

Chapters 4 and 5 reported data collected at approximately midday. Comparing these with data presented in this chapter shows good agreement with the trend of the data between light regimes and species. ETR-irradiance plots presented in chapter 4 showed a reduction in I_k concurrent with a slight increase in ETR_{max} and α between HLSI and HLLF regimes, while all three parameters were lower in *P. tricornutum* than in T. *pseudonana*. Data from midday samples presented in Figures 6.3.2 and 6.3.3 are consistent with these trends. Parameters of the NPQ-irradiance relationship and measurements of a^{chl} presented in this chapter also show trends consistent with data in

chapters 4 and 5. That said, the absolute values of several of the parameters presented here differ from those reported in previous chapters. This is most apparent in values of I_k and I_{50}, which were lower in this chapter than previously reported. Several factors may contribute to this. As was stated in the methods section of this chapter the culture conditions were different to those used earlier in the study. Not only was irradiance variability within the culture vessel different, but these cultures were mixed by a paddle, rather than the magnetic stirrer bar used in previous experiments. In previous cultures, to prevent the magnetic stirrer from getting stuck a minimum mixing speed had to be maintained which was notably greater than the maximum stirring speed of the paddle used to mix cultures for this part of the study. Differences in the rate of physical mixing can significantly affect growth and photophysiology in diatoms (Leupold *et al*., 2013; Sobczuk *et al*., 2006; Thomas and Gibson, 1990) and this may have contributed to differences between values reported in this chapter and those from previous chapters.

The liner relationship between I_k and I_{50} that was presented in Figure 5.4.1 in Chapter 5 (page 109) is conserved in the data presented in this chapter (Figure 6.4.1). The slope of the liner regression between the two variables is consistent, having a value of 2.26 for data presented in this chapter, compared with 2.2 in Chapter 5. This supports the notion that I_k can be estimated from I_{50} or vice versa (Serôdio and Lavaud, 2011), as well as

illustrating consistency between data presented in this chapter, and those presented in chapters 4 and 5.

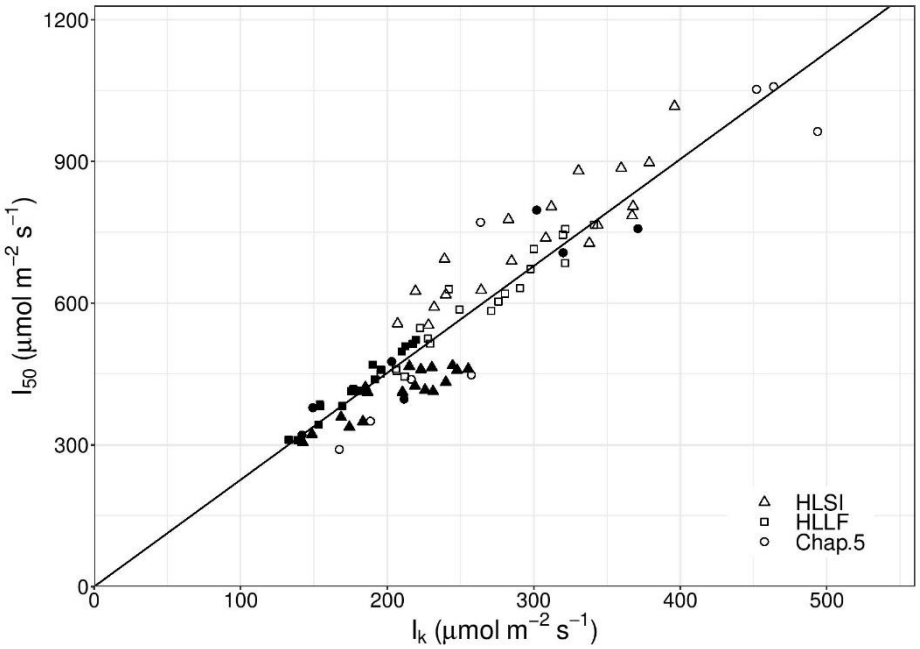

Figure 6.4.1. Relationship between ETR saturation irradiance (I_k) and NPQ saturation irradiance (I_{50}). Filled shapes denote *P. tricornutum*, open shapes *T. pseudonana*. Data presented in this chapter from cultures grown under HLSI and HLLF light regimes, as well as data from 8 light regimes as presented in Chapter 5. Trendline has slope 2.26 and R^2 0.86. Values are means of 3-4 measurements; error bars are omitted to avoid confusion.

Since the trends in measured parameters remain largely consistent with trends reported in previous chapters the effects of light regime on growth rate (reported in chapter 4) can be correctly interpreted in terms of data presented in this chapter, although the absolute values cannot. For instance, calculation of growth efficiency based on daily ETR reported in this chapter, and growth rates presented in chapter 4 would evidently be incorrect.

6.5. Effects of light fluctuations on intradiel variability in the ETR-irradiance response, and consequences for estimating daily photosynthesis

Across the photoperiod changes in the ETR-irradiance relationship, and in a^{chl} under HLSI appeared to reflect photoacclimation to the instantaneous irradiance as described in chapter 4. As irradiance increased, an increase in a^{chl} consistent with a reduction in cellular chlorophyll and subsequent decrease in pigment packaging was observed, as was an increase in ETR_{max} and I_k. This is expected from photoacclimation to the instantaneous irradiance (Behrenfeld *et al*., 2004; Brunet *et al*., 2011; Dubinsky and Stambler, 2009). This was not the case for cultures grown under HLLF, in which photoacclimation across the photoperiod was generally reduced in magnitude compared with that under HLSI. This was particularly evident in *P. tricornutum*, and less so for *T. pseudonana*.

There is some evidence that photoacclimation of a parameter characterising the physiological state of phytoplankton to a shift in irradiance can be described empirically as a first order differential equation (Baklouti *et al*., 2006; Cullen and Lewis, 1988; Raven and Geider, 2003). In this model the rate of change in the parameter is dependent on the rate constant for photoacclimation and the magnitude of the difference between initial and fully acclimated values of the parameter. This is described by Equation 6.5.1 in which Γ is a parameter indicative of photoacclimation to a given irradiance (such as one of the parameters of the P-I response curve). $\Gamma(t)$ denotes the

value of Γ prior to a shift in irradiance and $\Gamma_{acclimated}$ is the value of Γ once it is fully acclimated to the new irradiance. The rate constant of photoacclimation is denoted by τ.

$$\frac{\delta\Gamma}{\delta t} = \tau\left(\Gamma_{acclimated} - \Gamma(t)\right) \qquad \textbf{6.5.1}$$

Evidently, if τ is constant, periodic variability sufficiently more rapid than the rate of photoacclimation would depress photoacclimation, compared with variability in irradiance on longer timescales (Lewis *et al*., 1984). This appears to be case in the present data. Measurements of photoacclimation at a range of times across the photoperiod in response to light variability are scarce in the literature. However, data from van Leeuwe *et al*. (2005) support the hypothesis that rapid intradiel light variability reduces variability in photoacclimation. They showed that the intradiel variability in the maximum yield of photosynthesis in a diatom and a flagellate was higher in a sinusoidal light regime than in fluctuating regime with a 3-hour period. A further increase in intradiel variability was observed when the period of light fluctuations was increased to 1-hour. Similarly, Harding *et al*. (1987) reported minimal intradiel variability in the parameters of the P-I response to light fluctuations on timescales of several minutes to an hour. Further support for this hypothesis comes from field data. Measurements of the parameters of the P-I response in highly stratified waters show significant variability across the photoperiod, consistent with those reported here under the HLSI regime

in both species (Brunet *et al*., 2008; Erga and Skjoldal, 1990; Mercado *et al*., 2006). Meanwhile measurements in turbid estuaries, in which phytoplankton can be expected to experience much greater intradiel irradiance variability, are less variable over the photoperiod (Macintyre and Cullen, 1996).

The hypothesis that the rapid light fluctuations in the HLLF regime depress intradiel variability in photoacclimation can explain differences in the ETR-irradiance response and a^{chl} between HLSI and HLLF light regimes but does not explain the interspecific differences in this effect. Namely, that intradiel variability in photoacclimation is more greatly reduced by light fluctuations in *P. tricornutum* than in *T. pseudonana*. In the empirical model of photoacclimation presented above the rate of photoacclimation is not only dependant on τ, but also on the magnitude of the change in the parameter describing photoacclimation (i.e. the value of $\Gamma_{acclimated} - \Gamma(t)$ in Equation 6.5.1). A lower capacity for photoacclimation in *P. tricornutum* could therefore also reduce the rate of photoacclimation to irradiance shifts and would be expected to enhance the negative effect of light fluctuations on intradiel photoacclimation variability. *P. tricornutum* has previously been reported to have a very low plasticity in photoacclimation of the carbon-specific parameters of the P-I response to different light levels (Geider *et al*., 1985). However, chlorophyll-specific parameters of the P-I relationship in *P. tricornutum*, as are reported in this study, are variable with light intensity because of light dependant changes in the carbon:chlorophyll ratio (Geider *et*

al., 1985). This is therefore unlikely to be the reason for the species-specific response to light fluctuations reported here in the ETR irradiance response.

It is important to note that changes in photoacclimation state across the photoperiod are unlikely to be solely a result of differences in the irradiance. Even under square-wave light regimes parameters of photoacclimation exhibit diel variability as a result of endogenous rhythms and the cell cycle (Bruyant *et al*., 2005; Prezelin, 1992). The magnitude of these variations are known to be species specific (Harding *et al*., 1981a, 1981b)**.** A possible explanation for the species-specific response to light fluctuations is that *T. pseudonana* has more pronounced endogenous variability in photoacclimation than *P. tricornutum.* Therefore, variability in photoacclimation in *T. pseudonana* is less susceptible to the impact of light fluctuations.

Regardless of the cause and mechanism, intradiel variability in photoacclimation clearly has considerable potential impact on calculating daily photosynthesis from measurements taken at a single point in time. This is not just the case for ETR, as reported here, but also for other measurements of photosynthesis and parameters describing photoacclimation which can impact estimates of primary productivity (Harding *et al*., 1982; Mercado *et al*., 2006). Consistent with observations of natural populations, estimating daily photosynthesis from measurements made at approximately midday results in the smallest error in measurements

(Harding *et al*., 1982; Macintyre and Cullen, 1996; Walsby *et al*., 2001; Yoshikawa and Furuya, 2006). Using measurements made towards the extremes of the photoperiod and even outside the photoperiod (Isada *et al*., 2009) can considerably reduce the accuracy of estimates. However, differences between HLSI and HLLF regimes in *P. tricornutum* suggest that this error may be reduced in environments in which cells experience more rapid light variability. It is hypothesised that accounting for intradiel photoacclimation may be less important in estimating daily photosynthesis in more highly mixed environments, as rapid light variability can reduce intradiel photoacclimation, although the magnitude of this impact appears to be species specific. Some support for this hypothesis comes from comparisons between measurements made in a turbid estuary, in which estimated daily photosynthesis was relatively accurate regardless of the time of sampling (Macintyre and Cullen, 1996), with measurements made in stratified shelf seas, in which sampling time had the potential to induce substantial errors in the calculation of daily photosynthesis (Walsby *et al*., 2001; Yoshikawa and Furuya, 2006). Measurements of daily photosynthesis as primary productivity are typically extrapolated from a single measurement that is not necessarily made at a consistent time of day (Alderkamp *et al*., 2015; Brush *et al*., 2002; Carmack *et al*., 2004; Domingues *et al*., 2011). As discussed above, the estimates of daily photosynthesis or primary production extrapolated in this way would be less accurate in more stratified conditions. Depending on the

magnitude of inaccuracies that sampling at different times of day could introduce, this may skew interpretations of the impacts of changes in vertical mixing, for example as a result of seasonality, on primary productivity if unaccounted for (e.g. as in Bouman *et al*., 2010; Domingues *et al*., 2011).

Evidently the light environment is not the only environmental factor that can drive changes in photophysiology across the photoperiod, but it clearly plays an important role (Jouenne *et al*., 2005; Litaker *et al*., 1993).

6.6. Restrictions on growth rate in fluctuating light

In order to measure ETR across the photoperiod cultures were kept dilute and were often diluted twice per day, once after dusk and again before dawn. Growth rates could therefore not be directly measured. As discussed in section 6.4 data presented in this chapter is analysed with reference to growth rates presented in chapter 4, which were measured in separate cultures.

Growth rates of *P. tricornutum* were less negatively affected by increasing amplitude of light fluctuations than those of *T. pseudonana*. Some authors have put forward the hypothesis that the changes in gross photosynthesis caused by a reduction in the efficiency of photosynthetic light utilisation could control phytoplankton growth rate in dynamic light environments (Litchman, 2000; Shatwell *et al*., 2012). Data in this study

suggests this may be the case in some species, but not in others. While *T. pseudonana* incurs a 22% reduction in daily ETR between HLSI and HLLF no such reduction was found for *P. tricornutum*. The equivalent daily ETR between HLSI and HLLF in *P. tricornutum* could be taken to indicate that differences in daily gross photosynthesis do not drive differences in growth rate between these species. However before concluding this an alternate explanation must be addressed. ETR is not necessarily proportional to photosynthetic carbon accumulation, but the two are typically correlated to some extent (Kroom and Thoms, 2006; Suggett *et al*., 2009). In chapter 4 it was reported that alternative electron sinks can drive differences between photosynthetic O_2 evolution and PSII electron transport rate. Light driven oxygen utilisation by the Mehler reaction, PTOX or photorespiration may have substantially reduced O_2 evolution rates from the daily ETR reported here. Although O_2 evolution and possibility for alternative election sinks was not measured for *P. tricornutum* in this study it has been measured in previous studies. Wagner *et al*. (2006) reported that alternative electron sinks comprised a greater fraction of the electrons from PSII photochemistry under a sinusoidal light regime than under a more rapidly fluctuating light regime (akin to the fluctuation amplitude of the HL regimes described in chapter 2). Since measurements of ETR and O_2 evolution increasingly deviate the more light saturated O_2 evolution becomes, this can be linked to the distribution of light dose with respect to irradiance across the photoperiod and the

saturation irradiance for O_2 evolution. Wagner *et al*. (2006) concluded that alternative electron sinks throughout the photoperiod were proportionally greater under a sinusoidal light regime than under a fluctuating light regime of the same maximum irradiance because a greater fraction of the light dose was delivered at irradiances saturating to O_2 evolution in the sinusoidal regime. For *T. pseudonana* in the present data, because of the considerable difference in saturation irradiance for O_2 evolution between the HLSI and HLLF regime the fraction of electrons from PSII photochemistry used in alternative electron sinks is thought to be greater under the HLSI regime. Based on the saturation irradiance for O_2 evolution (Table 4.3.3, page 73) and the distribution of light dose at different irradiances (Figure 2.4.1b, page 31) 93% of the light dose was delivered at irradiances saturating to O_2 evolution under the HLSI regime, but only 70% under HLLF. Although this fails to account for intradiel variability in the saturation irradiance of O_2 evolution, daily ETR can be hypothesised to be overestimating gross photosynthesis, as measured by O_2 evolution, to a greater extent in the HLSI regime than the HLLF regime. Consequently, differences in daily gross photosynthesis alone between variable light regimes cannot explain changes in growth rate, at least in the two diatoms studied here.

Differences in daily ETR may explain interspecific differences in the negative effect of fluctuating light on growth rate. The low intradiel variability in the ETR-irradiance response in *P. tricornutum* under the HLLF regime

enabled this species to exploit peaks in irradiance towards the beginning and the end of the photoperiod better than *T. pseudonana*. A greater reduction in ETR_{max} and α in *T. pseudonana* before and after midday meant that ETR during morning and afternoon irradiance peaks was proportionally lower than midday ETR compared with *P. tricornutum*. For example, integrated ETR during the first irradiance peak (from 0.5 to 1.5 h after dawn) was 34% of ETR during the midday peak (from 5.5 to 6.5 h after dawn) in *T. pseudonana*, compared with 45% in *P. tricornutum*. Consequently, daily ETR in *T. pseudonana* was lower in HLLF cultures than in HLSI cultures but was unaffected by light fluctuations in *P. tricornutum*. Since photosynthesis places a fundamental restriction on growth rate, the observation that daily ETR in *P. tricornutum* is not reduced by increased amplitude of light variability, whereas it is for *T. pseudonana*, may in part explain why growth rate in *P. tricornutum* is less negatively affected by light fluctuations. *P. tricornutum*, being an estuarine species, occupies an ecological niche characterised by high irradiance variability whereas *T. pseudonana* is a coastal and oceanic species, occupying an ecological niche characterised by low irradiance variability (Lavaud *et al*., 2007). It is hypothesised that limited photoacclimation under fluctuating irradiance is an adaptation to high light variability that enables more efficient photosynthetic utilisation of light during short-term peaks in irradiance, whilst avoiding the metabolic cost of photoacclimation. This hypothesis is supported by a modelling study demonstrating that lower

phenotypic plasticity in light harvesting confers a competitive advantage in more rapidly fluctuating light regimes (Stomp *et al*., 2008).

Control by photoinhibition is an alternative hypothesis that has been put forward to explain the reduction of growth rates under higher amplitude light fluctuations (Alderkamp *et al*., 2010; Poll *et al*., 2007). Calculating q_p from FRRF measurements presented in this chapter, it is possible to estimate the rate constants of photodamage and repair based on relationships shown in chapter 5. The rate of gross photodamage (k_i) can be calculated from its linear relationship with $E(1-q_p)$, and the rate constant for repair (k_r) can be estimated from linear interpolation of the relationship between k_i and k_r (see Figures 5.5.2 and 5.3.3 pages 116 and 105 respectively). Assuming an equilibrium between these two processes the impact of photodamage on maximum photochemical efficiency can be found. At equilibrium the functional Kok model of photodamage and repair presented in chapter 5 is described by Equation 6.6.1.

$$k_i RCII_f = k_r RCII_i \qquad \textbf{6.6.1}$$

Since the fraction of inhibited RCIIs ($RCII_i$) is equal to 1 minus the fraction of functional ($RCII_f$) this can be rewritten as Equation 6.6.2. The fraction of functional RCIIs at equilibrium can then be calculated according to Equation 6.6.3.

$$k_i RCII_f = k_r(1 - RCII_f) \qquad \textbf{6.6.2}$$

$$RCII_f = \frac{k_r}{k_i + k_r} \qquad \textbf{6.6.3}$$

The estimated fraction of functional RCIIs across the photoperiod for *T. pseudonana* and *P. tricornutum* is shown in Figure 6.6.1. Clearly the substantially greater capacity for NPQ, and therefore PSII repair, in *P. tricornutum* means this species is far less susceptible to photodamage during the irradiance peaks in the HLLF regime. However, there is little difference between the two species under the HLSI regime. While *P. tricornutum* has a competitive advantage over *T. pseudonana* when it comes to photodamage in highly variable light regimes this is not the case when the variability in irradiance is lower. Differences in photodamage between the two species may therefore also explain why growth of *P. tricornutum* is less negatively affected by increased amplitude of light fluctuations than *T. pseudonana*. Previous studies have linked differences in photoprotective capacity to the dominance of certain species in more dynamic natural environments (Blommaert *et al*., 2017; Kropuenske *et al*., 2009; Lavaud *et al*., 2007; Lavaud and Lepetit, 2013; Mills *et al*., 2010). Present data reinforces this link, further suggesting a role in the capacity for photoprotection in defining phytoplankton ecological niches.

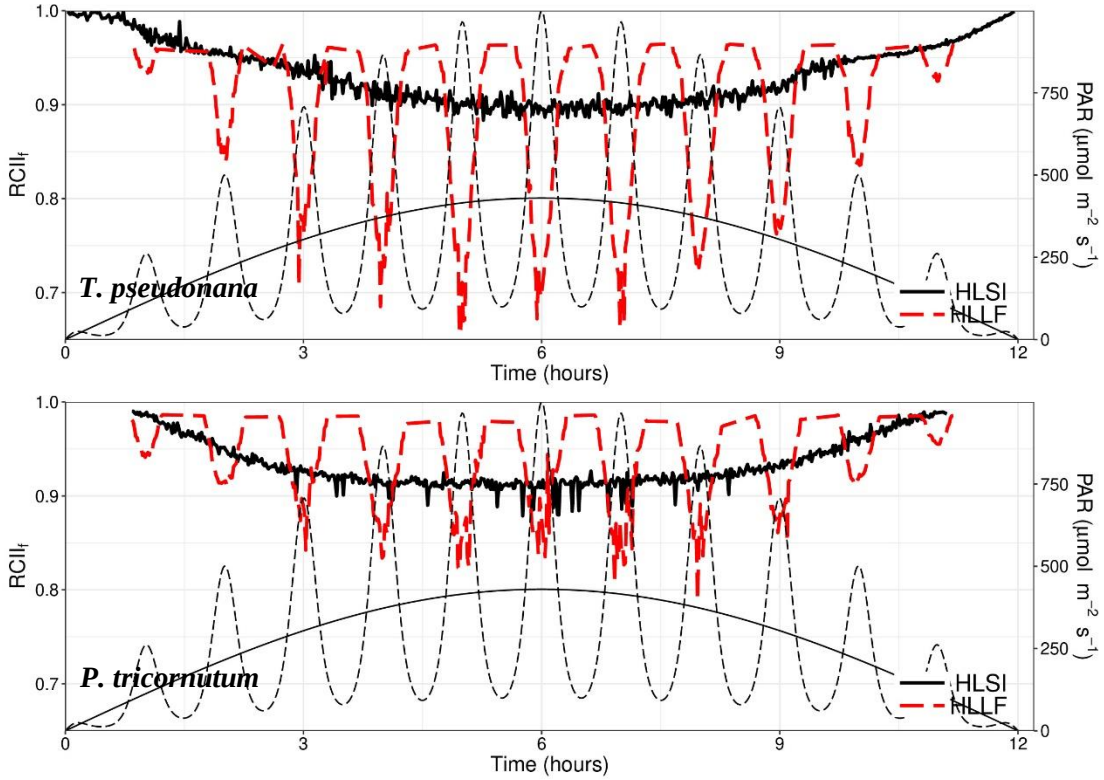

Figure 6.6.1. Estimated fraction of functional PSII reaction centres in two diatoms grown under two dynamic light regimes. Light regimes are indicated by thin lines. Values are means of 3-4 measurements.

Growth rate is not solely dependent on photosynthesis, but photosynthesis does place a fundamental restriction on growth in photoautotrophic organisms (Alderkamp *et al*., 2015; Arrigo *et al*., 2010; Fu *et al*., 2007). Changes in respiration and resource allocation can however impact growth rates independently of gross photosynthesis (Wu *et al*., 2014). The growth rate of *P. tricornutum* is reduced from the HLSI regime to the HLLF regime without a corresponding reduction in daily ETR. In fact, as discussed above, a probable decrease in the fraction of electrons involved in alternative electron sinks between HLSI and HLLF suggests that daily photosynthesis rates measured by O_2 evolution would be higher under the HLLF regime (Wagner *et al*., 2006). Lower growth rates under the HLLF regime indicate a substantial

reduction in the quantum efficiency of growth. Although this may in part be caused by greater photodamage in the HLLF regime other factors may contribute (Raven, 2011). Differences in metabolic costs and molecular composition between phytoplankton species have previously been identified as important factors in determining the quantum efficiency of growth in static and dynamic light regimes (Kunath *et al*., 2012; Su *et al*., 2012). With the exception of a single measurement point (the high standard deviation of which may indicate experimental error) NPQ capacity in *P. tricornutum* is far more variable across the photoperiod in the HLLF regime than in the HLSI regime, increasing to a far greater extent around midday (Figure 6.3.9). Several studies have found that acclimation to rapid changes in irradiance on the timescales used here in the HLLF regime can promote significant *de novo* synthesis of xanthophyll pigments, particularly in species with a high plasticity in NPQ capacity such as *P. tricornutum* (Alderkamp et al., 2011; Lavaud et al., 2004; Olaizola et al., 1994; van de Poll and Buma, 2009). This leads to the hypothesis that in addition to increased photodamage, a greater energetic investment in synthesis of xanthophyll pigments resulted in lower quantum efficiency of growth in *P. tricornutum* grown under the HLLF regime than under the HLSI regime (Alderkamp *et al*., 2011; Dimier *et al*., 2009).

6.7. Summary and conclusions

Examining PSII electron transport, NPQ, and acclimation of *T. pseudonana* and *P. tricornutum* across the photoperiod in two variable light regimes has led to three main conclusions.

Firstly, estimates of daily photosynthesis based on individual samples are significantly impacted by the time of day at which the samples are taken. Samples taken at midday tend to incur less error than samples taken at dawn or dusk, particularly in environments characterised by longer timescales of irradiance variability (Harding *et al*., 1982; Walsby *et al*., 2001; Yoshikawa and Furuya, 2006). The impacts of intradiel light fluctuations across the photoperiod on photoacclimation appear to be species-specific, with intradiel photoacclimation being more affected by increased light fluctuations in some species than others. More rapid light fluctuations tend to depress inter-diel photoacclimation and therefore reduce errors in estimates of daily photosynthesis from single measurements. It may be particularly important to account for this when exploring changes in daily photosynthesis or primary production from periods of low to high stratification.

Secondly, a competitive advantage in dynamic light regimes does not only arise from a greater photoprotective capacity. The lower variability in photoacclimation in *P. tricornutum* compared with *T. pseudonana* is hypothesised to confer a competitive advantage in rapidly variable light

environments. In dynamic light environments photoacclimation is rarely at equilibrium with the incident irradiance (Esposito *et al*., 2009). Continual photoacclimation is not only energetically costly, but also results in little payoff in terms of maximising photosynthesis and minimising photodamage (Stomp *et al*., 2008). Photoprotection is therefore more important than photoacclimation in more variable light environments. Furthermore, differences in both the capacity for photoacclimation and photoprotection may be important in defining ecological niches (Esposito *et al*., 2009; van Leeuwe *et al*., 2005).

Finally, reductions in growth rate within a species associated with increasing amplitude of light fluctuations are unlikely to result solely from differences in gross photosynthesis. Rather, greater photodamage and increased resource allocation to photoprotective mechanisms are more likely to be the cause (Alderkamp *et al*., 2011; Dimier *et al*., 2009; Raven, 2011). Increasing interest in microalgal biofuels has led to substantial research in maximising the rate of growth and biomass accumulation. Several studies have investigated the use of high amplitude variable light environments as a possible mechanism to accomplish this (Bechet *et al*., 2013; Tamburic *et al*., 2014; Yarnold *et al*., 2015). Minimising the energetic cost of photodamage and photoacclimation on phytoplankton growth therefore should be an important target in biofuels research (Wilhelm and Jakob, 2011).

7. Conclusions, implications, and recommendations for future work

7.1. Acclimation to fluctuating light regimes is dominated by photoprotection

Overall, this study found photoacclimation in fluctuating light regimes could not be well described by a single parameter descriptive of the light environment. Of the parameters examined, either the maximum irradiance, or the newly defined parameter, I_{Med}^{D} (which was strongly related to the maximum irradiance) showed the strongest, or second strongest correlation with 5 of the 6 variables used to characterise photoacclimation (R^2 0.56 to 0.81). A summary of the principal findings of this study on the mode of acclimation to increasing light fluctuation amplitude is illustrated in Figure 7.1.1, along with the key differences between the two study species. In general, acclimation to increasing amplitude of light fluctuations was characterised by an apparent reduction in cellular light absorption, an increase in the capacity for photochemical quenching and alternative electron sinks, and greater non-photochemical quenching (NPQ). Under static light regimes these are all characteristic mechanisms to limit photodamage by excess excitation of PSII (photosystem II) and are typical responses to an increase in irradiance (Derks *et al*., 2015; Dubinsky and Stambler, 2009). Several studies have previously reported a similar response in diatoms as a

result of increasing fluctuation amplitude under constant light dose (Boelen *et al*., 2011; Fietz and Nicklisch, 2002; Grouneva *et al*., 2016), or little change in light absorption, photosynthesis-irradiance (P-I) response, and photoprotection between fluctuating light regimes of similar maximum irradiance (Boelen *et al*., 2011; Lepetit *et al*., 2017; van de Poll *et al*., 2010; van Leeuwe *et al*., 2005; Wagner *et al*., 2006). The apparent importance of maximum irradiance in driving acclimation under fluctuating light regimes may indicate that the role of photoreceptors in acclimation is more important than redox signalling in diatoms (Costa *et al*., 2013b; Jaubert *et al*., 2017). This conclusion also provides an experimental counterpart to the finding that phytoplankton populations in vertically mixed environments are acclimated to light intensities above the mean irradiance (Moore *et al*., 2006; Schloss and Ferreyra, 2002). It also calls into question the use of the median irradiance in the mixed layer as an indicator of phytoplankton acclimation state in models (Behrenfeld *et al*., 2016).

Despite the apparent importance of maximum irradiance in driving acclimation to fluctuating light the light dose appears to modulate this response. Data presented here and by others show that differences in growth rate, NPQ, PSII electron transport, and light harvesting between fluctuating light regimes were greater under a higher light dose (Shatwell *et al*., 2012).

When fluctuating light regimes were compared to static regimes, acclimation of *T. pseudonana* and *P. tricornutum* was also found to be mostly

photoprotective with respect to the maximum irradiance. Capacity for photochemical quenching, NPQ, and alternative electron sinks increased between a square-wave regime and fluctuating regimes of the same light dose, and the effective PSII size decreased. As a result, PSII excitation pressure, which was shown to be proportional to photodamage, was much lower in cultures acclimated to fluctuating light regimes than those grown under static light. Very few studies have compared diatom growth and photophysiology under fluctuating light regime to that under static light. Two studies have reported higher chlorophyll specific maximum photosynthesis rates and saturation irradiances for photosynthesis under fluctuating light, as was found here (Fietz and Nicklisch, 2002; Shatwell *et al*., 2012). Additionally, some studies have examined changes in light harvesting between static and fluctuating light regimes and have reported either a minor increase in chlorophyll-*a* specific absorption coefficients under fluctuating light (Fietz and Nicklisch, 2002; Nicklisch, 1998), or little change in cellular pigment content (Hoppe *et al*., 2015). Here, differences in chlorophyll-*a* specific light absorption between fluctuating and constant light were found to be dependent on the amplitude of the fluctuations. Under high amplitude fluctuations chlorophyll-*a* specific light absorption was similar to that under a square-wave of the same dose, but was lower under the two lower amplitude fluctuating light regimes. Most studies comparing acclimation between fluctuating and square-wave light use relatively high fluctuation amplitudes.

This may be the reason why other authors have found little difference in light harvesting between cultures acclimated to square-wave and fluctuating light regimes (Fietz and Nicklisch, 2002; Hoppe *et al*., 2015; Nicklisch, 1998).

Differences in acclimation between square-wave and fluctuating light regimes also appear to be modulated by the light dose. This was found here for the NPQ-irradiance response (particularly in *P. tricornutum*) and the saturation irradiance of PSII electron transport rate (ETR).

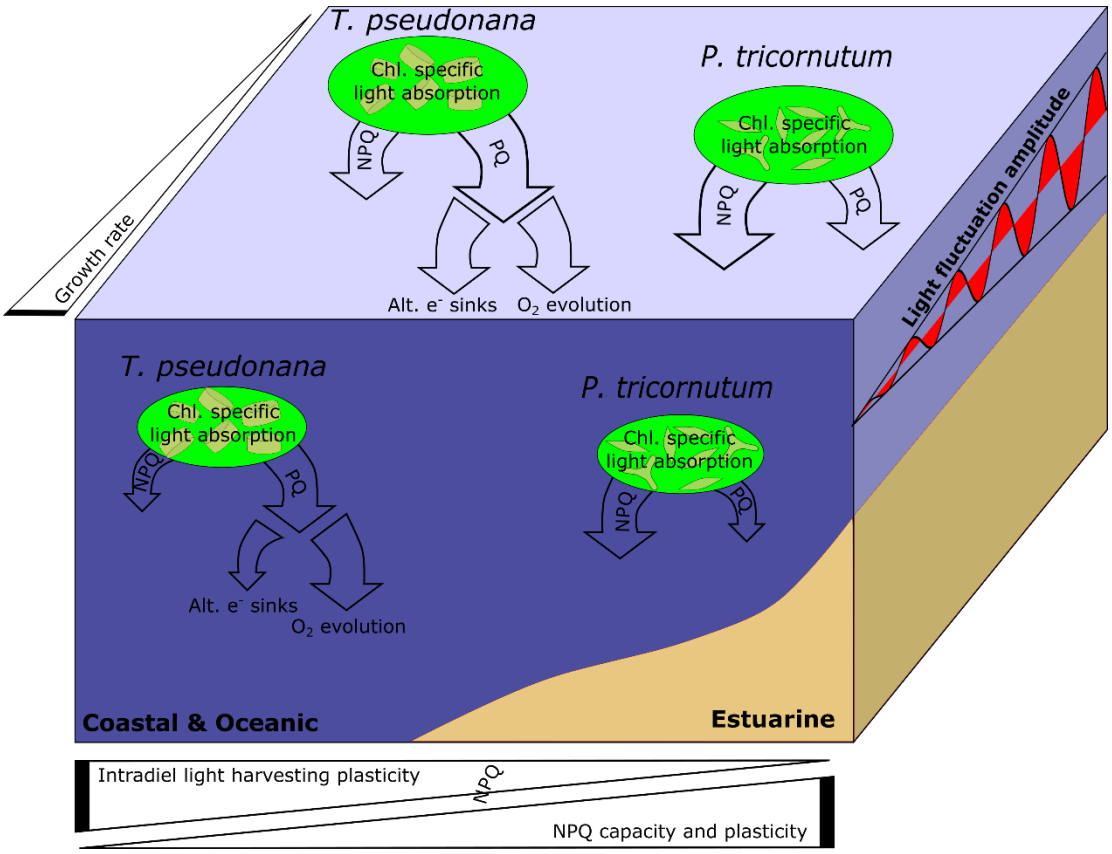

Figure 7.1.1. Illustration of key findings of mode of acclimation to changing light fluctuation amplitude under constant light dose. Interspecific differences relating to ecological niche are also illustrated. Relative size of arrows indicates differences in the magnitude of processes (not to scale)

One implication of the different photophysiology and reduced growth rate under fluctuating light, compared with square-wave light regimes, is that the impacts of other environmental factors on phytoplankton may differ between dynamic and static light environments. This has already been demonstrated in a few studies. Acclimation to fluctuating light has been found to reduce the deleterious effect of ultraviolet light on photosynthesis and primary production compared with acclimation to square-wave light regime, (Guan and Gao, 2008; Xing *et al*., 2015). This is constant with the photoprotective response to light fluctuations reported in the present study. Additionally, compared with square-wave light regimes, fluctuating light has been found to enhance the impact of temperature changes on photophysiology (Xu *et al*., 2016), as well enhancing the negative impact of ocean acidification on light use efficiency (Hoppe *et al*., 2015). These studies illustrate that significant differences in photophysiology between light environments make the application of conclusions from laboratory research conducted under square-wave light regimes, to natural phytoplankton populations, very difficult. It is imperative that the impact of light variability on phytoplankton physiology be understood in order to correctly interpret research outcomes from static light environments in the context of the naturally dynamic marine light environment.

7.2. Growth rate under fluctuating light is reduced by greater photodamage and energy investment in photoprotection

Increasing the amplitude of light fluctuations that occur on timescales of several minutes to a few hours has a typically negative impact on phytoplankton growth rate when the light dose is unchanged (Lavaud *et al*., 2007; Mitrovic *et al*., 2003; Nicklisch, 1998; Nicklisch and Fietz, 2001; Shatwell *et al*., 2012; Wagner *et al*., 2006). This was found to be the case for both *T. pseudonana* and *P. tricornutum*, although the growth rate of *P. tricornutum* was less negatively affected than the growth rate of *T. pseudonana*.

Similar values of daily ETR under a fluctuating and a sinusoidal light regime demonstrated that the lower growth rate of *P. tricornutum* under the fluctuating regime was unlikely to be caused by a reduction in the quantum efficiency of photosynthesis as some studies have hypothesised (Shatwell *et al*., 2012). Instead, greater photodamage, and greater energy investment in mitigating photodamage (e.g. by increasing the capacity for NPQ) are hypothesised to reduce growth rates in fluctuating light regimes (Su *et al*., 2012; van de Poll *et al*., 2011).

Substantial evidence for midday photodamage in natural populations in relatively static mixing environments support the importance of this process in controlling phytoplankton growth and distribution (Brunet *et al*., 2008; Sagert *et al*., 1997; Wu *et al*., 2011; Yue *et al*., 2014; Zhang *et al*., 2008).

However, the role of photodamage in limiting growth in more dynamic irradiance environments, and as a possible factor in shaping phytoplankton distributions, remains relatively poorly researched (Alderkamp *et al*., 2010; van de Poll *et al*., 2011).

7.3. Interspecific differences and ecological niche

T. pseudonana and *P. tricornutum* appear to represent two different ecotypes when it comes to adaptation of photophysiology to fluctuating light. Compared with *P. tricornutum*, *T. pseudonana* is characterised by a higher saturation irradiance, and higher maximum capacity, for chlorophyll-specific ETR, and also has a smaller effective PSII antenna. A higher chlorophyll-*a* specific absorption coefficient in *T. pseudonana* also suggests this species has a lower cellular chlorophyll-*a* content, which is corroborated by previous research (Poulin *et al*., 2018). In general, based on light harvesting and electron transport, *T. pseudonana* appears to be adapted to higher intensity light environments than *P. tricornutum* (Schwaderer *et al*., 2011). Conversely, when considering photoprotection, *T. pseudonana* appears to be adapted to lower light intensity environments than *P. tricornutum*. *T. pseudonana* was found to have a lower capacity and plasticity for NPQ, and consequently experiences greater net photodamage than *P. tricornutum* under high light levels (Lavaud *et al*., 2007). Both of these findings are consistent with

previous research, which has shown that the photosynthetic light utilisation of *T. pseudonana* is adapted to higher light levels than *P. tricornutum* (Burris, 1977; Geider *et al*., 1986, 1985; Kolber *et al*., 1988; Sobrino *et al*., 2008), while *P. tricornutum* has a higher capacity for NPQ (Goss *et al*., 2006; Lavaud *et al*., 2007; Zhu and Green, 2010). Consequently, under square-wave light *T. pseudonana* has been found to outcompete *P. tricornutum* at most light intensities, although the opposite occurs under very low light intensities (Nelson *et al*., 1979; Sharp *et al*., 1979). However, as demonstrated here, the photophysiology of *P. tricornutum* may confer a competitive advantage in dynamic light environments.

This study also presented the apparently novel finding that intradiel variability in light absorption and the ETR-irradiance relationship were more greatly suppressed under higher amplitude light fluctuations in *P. tricornutum* than in *T. pseudonana*. This is thought to have reduced the energy investment in low payoff photoacclimation under fluctuating light (Stomp *et al*., 2008). It also enabled *P. tricornutum* to maintain a daily ETR under a fluctuating light regime comparable to the daily ETR under a sinusoidal regime. In contrast, daily ETR in *T. pseudonana* grown under a fluctuating light regime was only 78% of that in cultures grown under a sinusoidal regime.

Differences in photophysiology between these two species resulted in the growth rate of *P. tricornutum* being less negatively affected by light fluctuations than the growth rate of *T. pseudonana.* The combination of low

light adaptation in light absorption and electron transport, and high light adaptation in photoprotection in *P. tricornutum*, is hypothesised to be an adaptation to dynamic light environments in which cells may spend a large proportion of the photoperiod at low light levels, punctuated by occasional rapid increases to very high light levels. Meanwhile, *T. pseudonana* is hypothesised to be adapted to less variable light environments.

This is consistent with the ecological niche of the two species. *P. tricornutum* is an estuarine species (Lavaud *et al*., 2007; Lavaud and Lepetit, 2013). The high turbidity and turbulence of an estuarine environment means this species experiences a highly variable light environment. *T. pseudonana* is a coastal and oceanic species, and therefore experiences a less variable light environment (Lavaud *et al*., 2007). This data supports the hypothesis that light variability drives species dynamics in mixed environments (Huisman *et al*., 2004; Key *et al*., 2010), as well as the hypothesis that differences in photoprotection may determine ecological niche (Lavaud *et al*., 2007). This study also puts forward the new hypothesis that lower intradiel acclimation of light harvesting and the photosynthesis-irradiance response confers a competitive advantage in dynamic light environments.

7.4. Experimental errors in measurements made in dynamic light environments

This study identified two possible sources of error in measurements of photosynthesis. Both were previously known, but the impact of light variability on them is poorly researched.

Firstly, the relationship between ETR and O_2 evolution in *T. pseudonana* became non-linear as O_2 saturated under fluctuating light regimes. Under a square-wave regime the relationship remained linear. This has also been reported for *P. tricornutum* and is hypothesised to be caused primarily by an increase in cyclic electron transport around PSII (Wagner *et al*., 2016, 2006). In recent years the use of variable fluorescence to measure PSII ETR and estimate photosynthesis and primary productivity in aquatic ecosystems has become increasingly popular. Compared with measurements of gas exchange, which require samples to be incubated for a period of time in a contained environment, fluorescence measurements can be made near-instantaneously *in situ*, and can capture a greater spatial and temporal resolution (Suggett *et al*., 2010). Since the FRRF method exclusively measures PSII photochemistry, a series of exchange rates need to be used to convert this measurement into an estimate of O_2 evolution or carbon assimilation (Suggett *et al*., 2009). These exchange rates are often parameterised from laboratory studies using square-wave light regimes (Melrose *et al*., 2006; Suggett *et al*., 2009), and as such may fail to capture the apparent decoupling

between PSII ETR and O_2 evolution observed under dynamic light regimes (Wagner *et al*., 2006). This could result in a substantial overestimation of photosynthetic O_2 evolution and should be considered when using variable fluorescence to estimate photosynthesis in dynamically illuminated phytoplankton populations.

Secondly, acclimation across the photoperiod is known to impact measured parameters of the photosynthesis-irradiance response throughout the day. This can lead to errors in estimating daily photosynthesis in natural systems from measurements taken at a single time of day (Harding *et al*., 1982). In this study it was found that variability in the ETR-irradiance response was higher in cultures grown under a sinusoidal light regime, than in cultures grown under a more highly fluctuating regime. This difference was species-specific, and greater in *P. tricornutum* than in *T. pseudonana*. As a result of these differences between light regimes, estimates of daily ETR from samples taken at a single time of day incurred on average 10% less error in cultures of *P. tricornutum* grown under a more highly fluctuating light regime. This may indicate daily photosynthesis or ETR estimated from single samples is more accurate in environments with greater vertical mixing, than in more stratified environments. Under both light regimes the error was minimised by using midday measurements

7.5. Recommendations for future work

It remains unclear what aspects of the light environment are important factors in driving acclimation and photosynthesis of phytoplankton. This is a particular point of interest in order to refine predictions of photoacclimation and photosynthesis to changing environments. Current models of photosynthesis and primary production may be based on the assumption that a single parameter of the light environment is sufficient to predict photoacclimation (Behrenfeld *et al*., 2016; Graff *et al*., 2016). The present study indicates this may not be correct. In recent decades global climate change has caused worldwide changes in ocean stratification and vertical mixing, and these changes are predicted to continue in the future (Behrenfeld *et al*., 2006; Saba *et al*., 2016). To understand and predict the responses of phytoplankton to such changes, an understanding of which aspects of the light environment are most important in driving acclimation is vital.

To date, much of the laboratory research on acclimation of phytoplankton to dynamic light has involved predictable light environments such as those used in this study. However, these are highly unrealistic and fail to capture the true variability in light intensity experienced by phytoplankton in aquatic environments. Phytoplankton acclimation and photosynthesis needs to be studied under more stochastic light regimes in order to better relate laboratory experiments using predictable light regimes to responses of natural phytoplankton populations.

This study aimed to examine how phytoplankton respond to changes in irradiance comparable with those caused by vertical mixing, but did not take into account depth-dependant variability in light spectra (Morel and Maritorena, 2001). Photosynthetic light absorption, photoreceptors that may be involved in photoacclimation, and the proposed mechanism of PSII photodamage are all wavelength dependant (Costa *et al*., 2013b; Havurinne and Tyystjärvi, 2017; Markager and Warwick, 2001). Variability in light quality in dynamic light environments can therefore be expected to impact photosynthesis, photoacclimation and photodamage in phytoplankton. Thus far, some research has investigated the impact of ultraviolet radiation on phytoplankton (Bertoni *et al*., 2011; Bouchard *et al*., 2005; Janknegt *et al*., 2009), but the effects of spectral variability in the context of vertical mixing remain largely unknown.

Finally, a distinct species-specific response was observed between growth and acclimation of the two diatoms studied here in response to light fluctuations. Other authors have reported similar species-specific responses both among and between phytoplankton groups (Lavaud *et al*., 2007; Litchman, 2000; Su *et al*., 2012). To understand how light variability can drive species distributions and diversity the impact of light variability on a wider range of species needs to be assessed. This could also lead to a greater understanding of the processes and mechanisms responsible for determining phytoplankton distributions and diversity in the ocean.

8. References

Alderkamp, A.-C., De Baar, H.J.W., Visser, R.J.W., Arrigo, K.R., 2010. Can photoinhibition control phytoplankton abundance in deeply mixed water columns of the Southern Ocean? Limnol. Oceanogr. 55, 1248–1264. doi:10.4319/lo.2010.55.3.1248

Alderkamp, A.-C., Garcon, V., de Baar, H.J.W., Arrigo, K.R., 2011. Short-term photoacclimation effects on photoinhibition of phytoplankton in the Drake Passage (Southern Ocean). Deep. Res. Part I Oceanogr. Res. Pap. 58, 943–955. doi:10.1016/j.dsr.2011.07.001

Alderkamp, A.-C., Kulk, G., Buma, A.G.J., Visser, R.J.W., Van Dijken, G.L., Mills, M.M., Arrigo, K.R., 2012. the Effect of Iron Limitation on the Photophysiology of *Phaeocystis Antarctica* (Prymnesiophyceae) and *Fragilariopsis Cylindrus* (Bacillariophyceae) Under Dynamic Irradiance1. J. Phycol. 48, 45–59. doi:10.1111/j.1529-8817.2011.01098.x

Alderkamp, A.-C., van Dijken, G.L., Lowry, K.E., Connelly, T.L., Lagerström, M., Sherrell, R.M., Haskins, C., Rogalsky, E., Schofield, O., Stammerjohn, S.E., Yager, P.L., Arrigo, K.R., 2015. Fe availability drives phytoplankton photosynthesis rates during spring bloom in the Amundsen Sea Polynya, Antarctica. Elem. Sci. Anthr. 3, 000043. doi:10.12952/journal.elementa.000043

Anning, T., Macintyre, H.L., Pratt, S.M., Sammes, P.J., Gibb, S., Geider, R.J., 2000. Photoacclimation in the marine diatom *Skeletonema costatum*. Limnol. Oceanogr. 45, 1807–1817. doi:10.4319/lo.2000.45.8.1807

Aro, E.-M., Virgin, I., Andersson, B., 1993. Photoinhibition of Photosystem II. Inactivation, protein damage and turnover. Biochim. Biophys. Acta - Bioenerg. 1143, 113–134.

Arrigo, K.R., Mills, M.M., Kropuenske, L.R., Van Dijken, G.L., Alderkamp, A.-C., Robinson, D.H., 2010. Photophysiology in two major southern ocean phytoplankton taxa: Photosynthesis and growth of *Phaeocystis antarctica* and *Fragilariopsis cylindrus* under different irradiance levels. Integr. Comp. Biol. 50, 950–966. doi:10.1093/icb/icq021

Asada, K., 2006. Production and Scavenging of Reactive Oxygen Species in Chloroplasts and Their Functions. Plant Physiol. 141, 391–396. doi:10.1104/pp.106.082040

Baker, N.R., Oxborough, K., 2004. Photosynthetic Productivity, in: Papageorgiou, G.C., Govindjee (Eds.), Chlorophyll a Fluorescence: A Signature of Photosynthesis. Springer, Dordrecht, pp. 66–82.

Baker, N.R., 2008. Chlorophyll fluorescence: a probe of photosynthesis in vivo. Annu. Rev. Plant Biol. 59, 89–113. doi:10.1146/annurev.arplant.59.032607.092759

Baklouti, M., Diaz, F., Pinazo, C., Faure, V., Quéguiner, B., 2006. Investigation of mechanistic formulations depicting phytoplankton dynamics for models of marine pelagic ecosystems and description of a new model. Prog. Oceanogr. 71, 1–33. doi:10.1016/j.pocean.2006.05.002

Bannister, T.T., 1979. Quantitative description of steady state, nutrient-saturated algal growth, including adaptation. Limnol. Oceanogr. 24, 76–96. doi:10.4319/lo.1979.24.1.0076

Barnett, A., Méléder, V., Blommaert, L., Lepetit, B., Gaudin, P., Vyverman, W., Sabbe, K., Dupuy, C., Lavaud, J., 2015. Growth form defines physiological photoprotective capacity in intertidal benthic diatoms. ISME J. 9, 32–45. doi:10.1038/ismej.2014.105

Baroli, I., Melis, A., 1998. Photoinhibitory damage is modulated by the rate of photosynthesis and by the photosystem II light-harvesting chlorophyll antenna size. Planta 205, 288–296. doi:10.1007/s004250050323

Baroli, I., Melis, A., 1996. Photoinhibition and repair in *Dunaliella salina* acclimated to different growth irradiances. Planta 198, 640–646.

Bates, S.S., Platt, T., 1984. Fluorescence induction as a measure of photosynthetic capacity in marine phytoplankton: response of *Thalassiosira pseudonana* (Bacillariophyceae) and *Dunaliella tertiolecta* (Chlorophyceae). Mar. Ecol. Prog. Ser. 18, 67–77.

Bechet, Q., Shilton, A., Guieysse, B., 2013. Modeling the effects of light and temperature on algae growth: State of the art and critical assessment for productivity prediction during outdoor cultivation. Biotechnol. Adv. 31, 1648–1663. doi:10.1016/j.biotechadv.2013.08.014

Behrenfeld, M.J., Marañón, E., Siegel, D.A., Hooker, S.B., 2002. Photoacclimation and nutrient-based model of light-saturated photosynthesis for quantifying oceanic primary production. Mar. Ecol. Prog. Ser. 228, 103–117. doi:10.3354/meps228103

Behrenfeld, M.J., O'Malley, R.T., Boss, E.S., Westberry, T.K., Graff, J.R., Halsey, K.H., Milligan, A.J., Siegel, D.A., Brown, M.B., 2016. Revaluating ocean warming impacts on global phytoplankton. Nat. Clim. Chang. 6, 323–330. doi:10.1038/nclimate2838

Behrenfeld, M.J., O'Malley, R.T., Siegel, D.A., McClain, C.R., Sarmiento, J.L., Feldman, G.C., Milligan, A.J., Falkowski, P.G., Letelier, R.M., Boss, E.S., 2006. Climate-driven trends in contemporary ocean productivity. Nature 444, 752–755. doi:10.1038/nature05317

Behrenfeld, M.J., Prasil, O., Babin, M., Bruyant, F., 2004. In search of a physiological basis for covariations in light-limited and light-saturated photosynthesis. J. Phycol. 40, 4–25. doi:10.1046/j.1529-8817.2004.03083.x

Behrenfeld, M.J., Randerson, J.T., McClain, C.R., Feldman, G.C., Los, S.O., Tucker, C.J., Falkowski, P.G., Field, C.B., Frouin, R., Esaias, W.E., Kolber, D.D., Pollack, N.H., 2001. Biospheric primary production during an ENSO transition. Science 291, 2594–2597. doi:10.1126/science.1055071

Bellacicco, M., Volpe, G., Colella, S., Pitarch, J., Santoleri, R., 2016. Influence of photoacclimation on the phytoplankton seasonal cycle in the Mediterranean Sea as seen by satellite. Remote Sens. Environ. 184, 595–604. doi:10.1016/j.rse.2016.08.004

Bennoun, P., 2002. The present model for chlororespiration. Photosynth. Res. 73, 273–277.

Berges, J.A., Franklin, D.J., Harrison, P.J., 2001. Evolution of an artificial seawater medium: Improvements in enriched seawater, artificial water over the last two decades. J. Phycol. 37, 1138–1145. doi:10.1046/j.1529-8817.2001.01052.x

Bertoni, R., Jeffrey, W.H., Pujo-Pay, M., Oriol, L., Conan, P., Joux, F., 2011. Influence of water mixing on the inhibitory effect of UV radiation on primary and bacterial production in Mediterranean coastal water. Aquat. Sci. 73, 377–387. doi:10.1007/s00027-011-0185-8

Blache, U., Jakob, T., Su, W., Wilhelm, C., 2011. The impact of cell-specific absorption properties on the correlation of electron transport rates measured by chlorophyll fluorescence and photosynthetic oxygen production in planktonic algae. Plant Physiol. Biochem. 49, 801–808.

Blauw, A.N., Benincà, E., Laane, R.W.P.M., Greenwood, N., Huisman, J., 2012. Dancing with the Tides: Fluctuations of Coastal Phytoplankton Orchestrated by Different Oscillatory Modes of the Tidal Cycle. PLoS One 7. doi:10.1371/journal.pone.0049319

Blommaert, L., Huysman, M.J.J., Vyverman, W., Lavaud, J., Sabbe, K., 2017. Contrasting NPQ dynamics and xanthophyll cycling in a motile and a non-motile intertidal benthic diatom. Limnol. Oceanogr. 62, 1466–1479. doi:10.1002/lno.10511

Boelen, P., van de Poll, W.H., van der Strate, H.J., Neven, I.A., Beardall, J., Buma, A.G.J., 2011. Neither elevated nor reduced CO2 affects the photophysiological performance of the marine Antarctic diatom Chaetoceros brevis. J. Exp. Mar. Bio. Ecol. 406, 38–45. doi:10.1016/j.jembe.2011.06.012

Bouchard, J.N., Campbell, D.A., Roy, S., 2005. Effects of UV-B radiation on the D1 protein repair cycle of natural phytoplankton communities from three latitudes (Canada, Brazil, and Argentina). J. Phycol. 41, 273–286. doi:10.1111/j.1529-8817.2005.04126.x

Bouman, H.A., Nakane, T., Oka, K., Nakata, K., Kurita, K., Sathyendranath, S., Platt, T., 2010. Environmental controls on phytoplankton production in coastal ecosystems: A case study from Tokyo Bay. Estuar. Coast. Shelf Sci. 87, 63–72. doi:10.1016/j.ecss.2009.12.014

Bricaud, A., Babin, M., Claustre, H., Ras, J., Tièche, F., 2010. Light absorption properties and absorption budget of Southeast Pacific waters. J. Geophys. Res. Ocean. 115, 1–19. doi:10.1029/2009JC005517

Brunet, C., Casotti, R., Vantrepotte, V., 2008. Phytoplankton diel and vertical variability in photobiological responses at a coastal station in the Mediterranean Sea. J. Plankton Res. 30, 645–654. doi:10.1093/plankt/fbn028

Brunet, C., Johnsen, G., Lavaud, J., Roy, S., 2011. Pigments and photoacclimation, in: Roy, S., Llewellyn, C.A., Egeland, E.S., Johnsen, G. (Eds.), Phytoplankton Pigments: Characterization, Chemotaxonomy and Applications in Oceanography. Cambridge University Press, pp. 445–471.

Brush, M.J., Brawley, J.W., Nixon, S.W., Kremer, J.N., 2002. Modeling phytoplankton production: Problems with the Eppley curve and an empirical alternative. Mar. Ecol. Prog. Ser. 238, 31–45. doi:10.3354/meps238031

Bruyant, F., Babin, M., Genty, B., Prasil, O., Behrenfeld, M.J., Claustre, H., Bricaud, A., Garczarek, L., Holtzendorff, J., Koblizek, M., Dousova, H., Partensky, F., 2005. Diel variations in the photosynthetic parameters of *Prochlorococcus* strain PCC 9511: Combined effects of light and cell cycle. Limnol. Oceanogr. 50, 850–863. doi:10.4319/lo.2005.50.3.0850

Burris, J.E., 1977. Photosynthesis, photorespiration, and dark respiration in eight species of algae. Mar. Biol. 39, 371–379. doi:10.1007/BF00391940

Campbell, D.A., Tyystjärvi, E., 2012. Parameterization of photosystem II photoinactivation and repair. Biochim. Biophys. Acta - Bioenerg. 1817, 258–265. doi:10.1016/j.bbabio.2011.04.010

Cardol, P., Forti, G., Finazzi, G., 2011. Regulation of electron transport in microalgae. Biochim. Biophys. Acta - Bioenerg. 1807, 912–918. doi:10.1016/j.bbabio.2010.12.004

Carmack, E.C., Macdonald, R.W., Jasper, S., 2004. Phytoplankton productivity on the Canadian Shelf of the Beaufort Sea. Mar. Ecol. Prog. Ser. 277, 37–50. doi:10.1109/JCN.2008.6389856

Carpenter, E.J., Subramaniam, A., Capone, D.G., 2004. Biomass and primary productivity of the cyanobacterium *Trichodesmium* spp. in the tropical N Atlantic ocean. Deep. Res. Part I Oceanogr. Res. Pap. 51, 173–203. doi:10.1016/j.dsr.2003.10.006

Claquin, P., Kromkamp, J.C., Martin-Jezequel, V., 2004. Relationship between photosynthetic metabolism and cell cycle in a synchronized culture of the marine alga *Cylindrotheca fusiformis* (Bacillariophyceae). Eur. J. Phycol. 39, 33–41. doi:10.1080/0967026032000157165

Costa, B.S., Jungandreas, A., Jakob, T., Weisheit, W., Mittag, M., Wilhelm, C., 2013a. Blue light is essential for high light acclimation photoprotection in the diatom *Phaeodactylum tricornutum*. J. Exp. Bot. 64, 483–493. doi:10.1093/jxb/err313

Costa, B.S., Sachse, M., Jungandreas, A., Bartulos, C.R., Gruber, A., Jakob, T., Kroth, P.G., Wilhelm, C., 2013b. Aureochrome 1a Is Involved in the Photoacclimation of the Diatom *Phaeodactylum tricornutum*. PLoS One 8. doi:10.1371/journal.pone.0074451

Cruz, S., Goss, R., Wilhelm, C., Leegood, R., Horton, P., Jakob, T., 2011. Impact of chlororespiration on non-photochemical quenching of chlorophyll fluorescence and on the regulation of the diadinoxanthin cycle in the diatom *Thalassiosira pseudonana*. J. Exp. Bot. 62, 509–519. doi:10.1093/jxb/erq284

Cullen, J.J., Lewis, M.R., 1988. The kinetics of algal photoadaptation in the context of vertical mixing. J. Plankton Res. 10, 1039–1063. doi:10.1093/plankt/10.5.1039

Curien, G., Flori, S., Villanova, V., Magneschi, L., Giustini, C., Forti, G., Matringe, M.,

Petroutsos, D., Kuntz, M., Finazzi, G., 2016. The Water to Water Cycles in Microalgae. Plant Cell Physiol. 57, 1354–1363. doi:10.1093/pcp/pcw048

Dau, H., Haumann, M., 2008. The manganese complex of photosystem II in its reaction cycle-Basic framework and possible realization at the atomic level. Coord. Chem. Rev. 252, 273–295. doi:10.1016/j.ccr.2007.09.001

Depauw, F.A., Rogato, A., D'Alcalá, M.R., Falciatore, A., 2012. Exploring the molecular basis of responses to light in marine diatoms. J. Exp. Bot. 63, 1575–1591. doi:10.1093/jxb/ers005

Dera, J., Stramski, D., 1993. Focusing of sunlight by sea surface waves : new results from the Black Sea. Oceanologia 34, 13–25.

Derks, A., Schaven, K., Bruce, D., 2015. Diverse mechanisms for photoprotection in photosynthesis. Dynamic regulation of photosystem II excitation in response to rapid environmental change. Biochim. Biophys. Acta - Bioenerg. 1847, 468–485. doi:10.1016/j.bbabio.2015.02.008

Diehl, S., Berger, S., Ptacnik, R., Wild, A., 2002. Phytoplankton, Light, and Nutrients in a Gradient of Mixing Depths: Field Experiments. Ecology 83, 399–411. doi:10.1890/0012-9658(2002)083[0386:PLANIA]2.0.CO;2

Dijkman, N.A., Kroom, B.M.A., 2002. Indications for chlororespiration in relation to light regime in the marine diatom *Thalassiosira weissflogii*. J. Photochem. Photobiol. B Biol. 66, 179–187. doi:10.1016/S1011-1344(02)00236-1

Dimier, C., Brunet, C., Geider, R., Raven, J., 2009. Growth and photoregulation dynamics of the picoeukaryote Pelagomonas calceolata in fluctuating light. Limnol. Oceanogr. 54, 823–836. doi:10.4319/lo.2009.54.3.0823

Ditullio, G.R., Geesey, M.E., Jones, D.R., Daly, K.L., Campbell, L., Smith, W., 2003. Phytoplankton assemblage structure and primary productivity along 170°W in the South Pacific Ocean. Mar. Ecol. Prog. Ser. 255, 55–80. doi:10.3354/meps255055

Domingues, R.B., Anselmo, T.P., Barbosa, A.B., Sommer, U., Galvão, H.M., 2011. Light as a driver of phytoplankton growth and production in the freshwater tidal zone of a turbid estuary. Estuar. Coast. Shelf Sci. 91, 526–535. doi:10.1016/j.ecss.2010.12.008

Dubinsky, Z., Stambler, N., 2009. Photoacclimation processes in phytoplankton: mechanisms, consequences, and applications. Aquat. Microb. Ecol. 56, 163–176. doi:10.3354/ame01345

Ducklow, H.W., Steinberg, D.K., Buesseler, K.O., 2001. Upper ocean carbon export and the biological pump. Oceanography 14, 50–58. doi:10.5670/oceanog.2001.06

Durnford, D.G., Falkowski, P.G., 1997. Chloroplast redox regulation of nuclear transcription during photoacclimation. Photosynth. Res. 53, 229–241. doi:10.1023/A

Eilers, P.H.C., Peeters, J.C.H., 1988. A model for the relationship between light intensity and the rate of photosynthesis in phytoplankton. Ecol. Modell. 42, 199–215. doi:10.1016/0304-3800(88)90057-9

Elterman, P., 1970. Integrating Cavity Spectroscopy. Appl. Opt. 9, 2140–2142.

Erga, S.R., Skjoldal, H.R., 1990. Diel variations in photosynthetic activity of summer phytoplankton in Lindiispollene, western Norway. Mar. Ecol. Prog. Ser. 65, 73–85.

Escoubas, J.-M., Lomas, M., LaRoche, J., Falkowski, P.G., 1995. Light intensity regulation of cab gene transcription is signaled by the redox state of the plastoquinone pool. Proc. Natl. Acadamy Sci. USA 92, 10237–10241.

Esposito, S., Botte, V., Iudicone, D., Ribera d'Alcala', M., 2009. Numerical analysis of cumulative impact of phytoplankton photoresponses to light variation on carbon assimilation. J. Theor. Biol. 261, 361–371. doi:10.1016/j.jtbi.2009.07.032

Falkowski, P.G., 1994. The role of phytoplankton photosynthesis in global biogeochemical cycles. Photosynth. Res. 39, 235–258. doi:10.1007/BF00014586

Falkowski, P.G., 1984. Physiological responses of phytoplankton to natural light regimes. J.

Plankton Res. 6, 295–307. doi:10.1093/plankt/6.2.295

Falkowski, P.G., Chen, Y.-B., 2003. Photoacclimation of light harvesting systems in eukaryotic algae, in: Green, B.R., Parson, W.W. (Eds.), Light-Harvesting Antennas in Photosynthesis. Springer, Dordrecht, pp. 423–447.

Falkowski, P.G., Dubinsky, Z., Wyman, K., 1985. Growth-irradiance relationships in phytoplankton. Limnol. Oceanogr. 30, 311–321.

Falkowski, P.G., LaRoche, J., 1991. Acclimation to spectral irradiance in algae. J. Phycol. 27, 8–14.

Falkowski, P.G., Owens, T.G., 1980. Light-shade adaptation. Plant Physiol. 66, 592–595. doi:10.1007/978-1-4684-3890-1_6

Falkowski, P.G., Raven, J.A., 2007. Aquatic Photosynthesis, Second Edi. ed. Princeton University Press.

Falkowski, P.G., Sholes, R.J., Boyle, E., Canadell, J., Canfield, D.E., Elser, J., Gruber, N., Hibbard, K., Hogberg, P., Linder, S., Mackenzie, F.T., Moore III, B., Pedersen, T., Rosenthal, Y., Seitzinger, S., Smetacek, V., Steffen, W., 2000. The global carbon cicle: a test of our knowledge of earth as a system. Science 290, 291–296.

Field, C.B., Behrenfeld, M.J., Randerson, J.T., Falkowski, P.G., 1998. Primary Production of the Biosphere: Integrating Terrestrial and Oceanic Components. Science 281, 237–240.

Fietz, S., Nicklisch, A., 2002. Acclimation of the diatom *Stephanodiscus neoastraea* and the cyanobacterium *Planktothrix agardhii* to simulated natural light fluctuations. Photosynth. Res. 72, 95–106. doi:10.1023/A:1016052726149

Flameling, I.A., Kromkamp, J., 1997. Photoacclimation of *Scenedesmus protuberans* (Chlorophyceae) to fluctuating irradiances simulating vertical mixing. J. Plankton Res. 19, 1011–1024.

Flöder, S., Urabe, J., Kawabata, Z., 2002. The influence of fluctuating light intensities on species composition and diversity of natural phytoplankton communities. Oecologia 133, 395–401. doi:10.1007/s00442-002-1048-8

Forsythe, W.C., Rykiel, E.J., Stahl, R.S., Wu, H., Schoolfield, R.M., 1995. A model comparison for daylength as a function of latitude and day of year. Ecol. Modell. 80, 87–95. doi:10.1016/0304-3800(94)00034-F

Foyer, C.H., Neukermans, J., Queval, G., Noctor, G., Harbinson, J., 2012. Photosynthetic control of electron transport and the regulation of gene expression. J. Exp. Bot. 63, 1637–1661. doi:10.1093/jxb/ers013

Fry, E.S., Kattawar, G.W., Pope, R.M., 1992. Integrating cavity absorption meter. Appl. Opt. 31, 2055–2056.

Fu, F., Warner, M.E., Zhang, Y., Feng, Y., Hutchins, D.A., 2007. Effects of increased temperature and CO2 on photosynthesis, growth, and elemental ratios in marine *Synechococcus* and *Prochlorococcus* (cyanobacteria). J. Phycol. 43, 485–496. doi:10.1111/j.1529-8817.2007.00355.x

Fujiki, T., Taguchi, S., 2002. Variability in chlorophyll a specific absorption coefficient in marine phytoplankton as a function of cell size and irradiance. J. Plankton Res. 24, 859–874. doi:10.1093/plankt/24.9.859

Garcia-Mendoza, E., Matthijs, H.C.P., Schubert, H., Mur, L.R., 2002. Non-photochemical quenching of chlorophyll fluorescence in *Chlorella fusca* acclimated to constant and dynamic light conditions. Photosynth. Res. 74, 303–315. doi:10.1023/A

Geider, R.J., Osborne, B.A., Raven, J.A., 1986. Growth, Photosynthesis and Maintenance Metabolic Cost in the Diatom *Phaeodactylum tricornutum* At Very Low Light Levels. J. Phycol. 22, 39–48. doi:10.1111/j.1529-8817.1986.tb02513.x

Geider, R.J., Osborne, B.A., Raven, J.A., 1985. Light dependence of growth and photosynthesis in *Phaeodactylum tricornutum* (Bacillariophyceae). J. Phycol. 21.

Genty, B., Briantais, J.-M., Baker, N.R., 1989. The relationship between the quantum yield of

photosynthetic electron transport and quenching of chlorophyll fluorescence. Biochim. Biophys. Acta 990, 87–92.

Gervais, F., Riebesell, U., Gorbunov, M.Y., 2002. Changes in primary productivity and chlorophyll a in response to iron fertilization in the Southern Polar Frontal Zone. Limnol. Oceanogr. 47, 1324–1335. doi:10.4319/lo.2002.47.5.1324

Gilbert, M., Domin, A., Becker, A., Wilhelm, C., 2000. Estimation of Primary Productivity by Chlorophyll a in vivo Fluorescence in Freshwater Phytoplankton. Photosynthetica 38, 111–126.

Giovagnetti, V., Flori, S., Tramontano, F., Lavaud, J., Brunet, C., 2014. The velocity of light intensity increase modulates the photoprotective response in coastal diatoms. PLoS One 9, 1–12. doi:10.1371/journal.pone.0103782

Gorbunov, M.Y., Kolber, Z.S., Lesser, M.P., Falkowski, P.G., 2001. Photosynthesis and photoprotection in symbiotic corals 46, 75–85.

Goss, R., Ann Pinto, E., Wilhelm, C., Richter, M., 2006. The importance of a highly active and ΔpH-regulated diatoxanthin epoxidase for the regulation of the PS II antenna function in diadinoxanthin cycle containing algae. J. Plant Physiol. 163, 1008–1021. doi:10.1016/j.jplph.2005.09.008

Goss, R., Jakob, T., 2010. Regulation and function of xanthophyll cycle-dependent photoprotection in algae. Photosynth. Res. 106, 103–122.

Graff, J.R., Behrenfeld, M.J., 2018. Photoacclimation Responses in Subarctic Atlantic Phytoplankton Following a Natural Mixing-Restratification Event. Front. Mar. Sci. 5, 1–11. doi:10.3389/fmars.2018.00209

Graff, J.R., Westberry, T.K., Milligan, A.J., Brown, M.B., Dall'Olmo, G., Reifel, K.M., Behrenfeld, M.J., 2016. Photoacclimation of natural phytoplankton communities. Mar. Ecol. Prog. Ser. 542, 51–62. doi:10.3354/meps11539

Granger, J., Sigman, D.M., Needoba, J.A., Harrison, P.J., 2004. Coupled nitrogen and oxygen isotope fractionation of nitrate during assimilation by cultures of marine phytoplankton. Limnol. Oceanogr. 49, 1763–1773.

Gray, G.R., Savitch, L. V., Ivanov, A.G., Huner, N.P.A., 1996. Photosystem II excitation pressure and development of resistance to photoinhibition. Plant Physiol. 110, 61–71.

Grouneva, I., Jakob, T., Wilhelm, C., Goss, R., 2009. The regulation of xanthophyll cycle activity and of non-photochemical fluorescence quenching by two alternative electron flows in the diatoms *Phaeodactylum tricornutum* and *Cyclotella meneghiniana*. Biochim. Biophys. Acta - Bioenerg. 1787, 929–938. doi:10.1016/j.bbabio.2009.02.004

Grouneva, I., Muth-Pawlak, D., Battchikova, N., Aro, E.-M., 2016. Changes in Relative Thylakoid Protein Abundance Induced by Fluctuating Light in the Diatom *Thalassiosira pseudonana*. J. Proteome Res. 15, 1649–1658. doi:10.1021/acs.jproteome.6b00124

Gruber, N., 2004. The dynamics of the marine nitrogen cycle and its influence on atmospheric CO 2 variations, in: Follows, M., Oguz, T. (Eds.), The Ocean Carbon Cycle and Climate. Springer, Dordrecht, pp. 97–148. doi:10.1007/978-1-4020-2087-2

Guan, W., Gao, K., 2008. Light histories influence the impacts of solar ultraviolet radiation on photosynthesis and growth in a marine diatom, Skeletonema costatum. J. Photochem. Photobiol. B Biol. 91, 151–156. doi:10.1016/j.jphotobiol.2008.03.004

Guillard, R.R.L., 1975. Culture of phytoplankton for feeding marine invertebrates, in: Smith, W.L., Chanley, M.H. (Eds.), Culture of Marine Invertebrate Animals. Plenum Press, New York, USA, pp. 26–60.

Guillard, R.R.L., Ryther, H.J., 1962. Studies of marine planktonic diatoms: I. *Cyclotella nana* Hustedt, and *Detonula confervacea* (Cleve) Gran. Can. J. Microbiol. 8, 229–239.

Hakala, M., Tuominen, I., Keränen, M., Tyystjärvi, T., Tyystjärvi, E., 2005. Evidence for the role of the oxygen-evolving manganese complex in photoinhibition of Photosystem II. Biochim. Biophys. Acta - Bioenerg. 1706, 68–80. doi:10.1016/j.bbabio.2004.09.001

Harding, L.W., Fisher Jr., T.R., Tyler, M.A., 1987. Adaptive Responses of Photosynthesis in Phytoplankton: Specificity to Time-Scale of Change in Light. Biol. Oceanogr. 4, 403–437.

Harding, L.W., Meeson, B.W., Prézelin, B.B., Sweeney, B.M., 1981a. Diel periodicity of photosynthesis in marine phytoplankton. Mar. Biol. 61, 95–105. doi:10.1007/BF00386649

Harding, L.W., Prézelin, B.B., Sweeney, B.M., Cox, J.L., 1982. Primary production as influenced by diel periodicity of phytoplankton photosynthesis. Mar. Biol. 67, 179–186. doi:10.1007/BF00401283

Harding, L.W., Prézelin, B.B., Sweeney, B.M., Cox, J.L., 1981b. Diel Oscillations in the Photosynthesis-Irradiance Relationship of a Planktonic Marine Diatom. J. Phycol. doi:10.1111/j.0022-3646.1981.00389.x

Harris, G.N., Scanlan, D.J., Geider, R.J., 2009. Responses of *Emiliania huxleyi* (Prymnesiophyceae) to step changes in photon flux density. Eur. J. Phycol. 44, 31–48. doi:10.1080/09670260802233460

Harvey, E.L., Menden-Deuer, S., 2012. Predator-Induced Fleeing Behaviors in Phytoplankton: A New Mechanism for Harmful Algal Bloom Formation? PLoS One 7. doi:10.1371/journal.pone.0046438

Havelkova-Dousova, H., Prasil, O., Behrenfeld, M.J., 2004. Photoacclimation of *Dunaliella tertiolecta* (Chlorophyceae) under fluctuating irradiance. Photosynthetica 42, 273–281.

Havurinne, V., Tyystjärvi, E., 2017. Action spectrum of photoinhibition in the diatom *Phaeodactylum tricornutum*. Plant Cell Physiol. 58, 2217–2225. doi:10.1093/pcp/pcx156

Hobson, L.A., McQuoid, M.R., 2001. Pelagic diatom assemblages are good indicators of mixed water intrusions into Saanich Inlet, a stratified fjord in Vancouver Island. Mar. Geol. 174, 125–138.

Hoppe, C.J.M., Holtz, L., Trimborn, S., Rost, B., 2015. Ocean acidification decreases the light-use efficiency in an Antarctic diatom under dynamic but not constant light. New Phytol. 207, 159–171.

Huisman, J., Sharples, J., Stroom, J.M., Visser, P.M., Kardinaal, W.E.A., Verspagen, J.M.H., Sommeijer, B., 2004. Changes in turbulent mixing shift competition for light between phytoplankton species. Ecology 85, 2960–2970.

Hüner, N.P.A., Bode, R., Dahal, K., Busch, F.A., Possmayer, M., Szyszka, B., Rosso, D., Ensminger, I., Krol, M., Ivanov, A.G., Maxwell, D.P., 2013. Shedding some light on cold acclimation, cold adaptation, and phenotypic plasticity 1. Botany 91, 127–136.

Huner, N.P.A., Oquistb, G., Sarhanc, F., 1998. Energy balance and acclimation to light and cold. Trends Plant Sci. 3, 224–230.

Hurry, V., Anderson, J.M., Badger, M.R., Price, G.D., 1996. Reduced levels of cytochrome b6/f in transgenic tobacco increases the excitation pressure on photosystem II without increasing sensitivity to photoinhibition in vivo. Photosynth. Res. 50, 159–169.

Ibelings, B.W., Kroom, B.M.A., Mur, L.R., 1994. Acclimation of photosystem II in a cyanobacterium and a eukaryotic green alga to high and fluctuating photosynthetic photon flux densities, simulating light regimes induced by mixing in lakes. New Phytol. 128, 407–424. doi:10.1111/j.1469-8137.1994.tb02987.x

Ihnken, S., Eggert, A., Beardall, J., 2010. Exposure times in rapid light curves affect photosynthetic parameters in algae. Aquat. Bot. 93, 185–194. doi:10.1016/j.aquabot.2010.07.002

Interlandi, S.J., 2002. Nutrient-toxicant interactions in natural and constructed phytoplankton communities: results of experiments in semi-continuous and batch culture. Aquat. Toxicol. 61, 35–51.

Isada, T., Kuwata, A., Saito, H., Ono, T., Ishii, M., Yoshikawa-Inoue, H., Suzuki, K., 2009.

Photosynthetic features and primary productivity of phytoplankton in the Oyashio and Kuroshio-Oyashio transition regions of the northwest Pacific. J. Plankton Res. 31, 1009–1025. doi:10.1093/plankt/fbp050

Jakob, T., Goss, R., Wilhelm, C., 2001. Unusual pH-dependence of diadinoxanthin de-epoxidase activation causes chlororespiratory induced accumulation of diatoxanthin in the diatom *Phaeodactylum tricornutum*. J. Plant Physiol. 158, 383–390. doi:10.1078/0176-1617-00288

Janknegt, P.J., Graaff, C.M. de, van de Poll, W.H., Visser, R.J.W., Helbling, E.W., Buma, A.G.J., 2009. Antioxidative Responses of Two Marine Microalgae During Acclimation to Static and Fluctuating Natural UV Radiation. Photochem. Photobiol. Sci. 85, 1336–1345.

Janssen, M., Kuijpers, T.C., Veldhoen, B., Ternbach, M.B., Tramper, J., Mur, L.R., Wijffels, R.H., 1999. Specific growth rate of *Chlamydomonas reinhardtii* and *Chlorella sorokiniana* under medium duration light/dark cycles: 13–87 s. Mar. Bioprocess Eng. 35, 323–333.

Järvi, S., Gollan, P.J., Aro, E.-M., 2013. Understanding the roles of the thylakoid lumen in photosynthesis regulation. Front. Plant Sci. 4, 1–14. doi:10.3389/fpls.2013.00434

Jaubert, M., Bouly, J.-P., D'Alcalà, M.R., Falciatore, A., 2017. Light sensing and responses in marine microalgae. Curr. Opin. Plant Biol. 37, 70–77.

Javorfi, T., Erostyak, J., Gal, J., Buzady, A., Menczel, L., Garab, G., Razi Naqvi, K., 2006. Quantitative spectrophotometry using integrating cavities. J. Photochem. Photobiol. B Biol. 82, 127–131. doi:10.1016/j.jphotobiol.2005.10.002

Jin, E., Yokthongwattana, K., Polle, J.E.W., Melis, A., 2003. Role of the Reversible Xanthophyll Cycle in the Photosystem II Damage and Repair Cycle in *Dunaliella salina*. Plant Physiol. 132, 352–364. doi:10.1104/pp.102.019620.The

John, D.E., Lopez-Diaz, J.M., Cabrera, A., Santiago, N.A., Corredor, J.E., Bronk, D.A., Paul, J.H., 2012. A day in the life in the dynamic marine environment: How nutrients shape diel patterns of phytoplankton photosynthesis and carbon fixation gene expression in the Mississippi and Orinoco River plumes. Hydrobiologia 679, 155–173. doi:10.1007/s10750-011-0862-6

Jones, C.T., Craig, S.E., Barnett, A.B., Macintyre, H.L., Cullen, J., 2014. Curvature in models of the photosynthesis-irradiance response. J. Phycol. 50, 341–355.

Jouenne, F., Lefebvre, S., Véron, B., Lagadeuc, Y., 2005. Biological and physicochemical factors controlling short-term variability in phytoplankton primary production and photosynthetic parameters in a macrotidal ecosystem (eastern English Channel). Estuar. Coast. Shelf Sci. 65, 421–439. doi:10.1016/j.ecss.2005.05.023

Kana, T.M., 1992. Relationship between photosynthetic oxygen cycling and carbon assimilation in *Synechococcus* WH7803 (cyanophyta). J. Phycol. 28, 304–308.

Key, T., McCarthy, A., Campbell, D.A., Six, C., Roy, S., Finkel, Z. V., 2010. Cell size trade-offs govern light exploitation strategies in marine phytoplankton. Environ. Microbiol. 12, 95–104. doi:10.1111/j.1462-2920.2009.02046.x

Klein, S.A., Hartmann, D.L., 1993. The seasonal cycle of low stratiform clouds. J. Clim. 6, 1587–1606.

Kliphuis, A.M.J., de Winter, L., Vejrazka, C., Martens, D.E., Janssen, M., Wijffels, R.H., 2010. Photosynthetic efficiency of *Chlorella sorokiniana* in a turbulently mixed short light-path photobioreactor. Biotechnol. Prog. 26, 687–696.

Köhler, J., 1997. in Situ Growth Rates of Phytoplankton Under Conditions of Simulated Turbulence. J. Plankton Res. 19, 849–862. doi:10.1093/plankt/19.7.849

Köhler, J., Schmitt, M., Krumbeck, H., Kapfer, M., 2001. Effects of UV on carbon assimilation of phytoplankton. Environ. Res. 63, 294–309. doi:10.1007/PL00001356

Kok, B., 1956. On the inhibition of photosynthesis by intense light. Biochim. Biophys. Acta

21, 234–244.

Kolber, Z.S., Prasil, O., Falkowski, P.G., 1998. Measurements of variable chlorophyll fuorescence using fast repetition rate techniques: defning methodology and experimental protocols. Biochim. Biophys. Acta 1367, 88–106.

Kolber, Z.S., Prasil, O., Falkowski, P.G., 1998. Measurements of variable chlorophyll fuorescence using fast repetition rate techniques: defning methodology and experimental protocols. Biochim. Biophys. Acta 1367, 88–106.

Krieger-Liszkay, A., 2005. Singlet oxygen production in photosynthesis. J. Exp. Bot. 56, 337–346. doi:10.1093/jxb/erh237

Krieger-Liszkay, A., Fufezan, C., Trebst, A., 2008. Singlet oxygen production in photosystem II and related protection mechanism. Photosynth. Res. 98, 551–564. doi:10.1007/s11120-008-9349-3

Kromkamp, J., Limbeek, M., 1993. Effect of short-term variation in irradiance on light harvesting and photosynthesis of the marine diatom Skeletonemu costaturn: a laboratory study simulating vertical mixing. J. Gen. Microbiol. 139, 2277–2284.

Kromkamp, J.C., Forster, R.M., 2003. The use of variable fluorescence measurements in aquatic ecosystems: Differences between multiple and single turnover measuring protocols and suggested terminology. Eur. J. Phycol. 38, 103–112. doi:10.1080/0967026031000094094

Kroom, B.M.A., Thoms, S., 2006. From electron to biomass: A mechanistic model to describe phytoplankton photosynthesis and steady-state growth rates. J. Phycol. 42, 593–609. doi:10.1111/j.1529-8817.2006.00221.x

Kropuenske, L.R., Mills, M.M., Van Dijken, G.L., Robinson, D.H., Welschmeyer, N.A., Arrigo, K.R., 2009. Photophysiology in two major Southern Ocean phytoplankton taxa: Photoprotection in *Phaeocystis antarctica* and *Fragilariopsis cylindrus*. Limnol. Oceanogr. 54, 1176–1196. doi:10.1093/icb/icq021

Kudoh, S., Imura, S., Kashino, Y., 2003. Xanthophyll-cycle of ice algae on the sea ice bottom in Saroma Ko lagoon , Hokkaido , Japan. Polar Biosci. 16, 86–97.

Kunath, C., Jakob, T., Wilhelm, C., 2012. Different phycobilin antenna organisations affect the balance between light use and growth rate in the cyanobacterium *Microcystis aeruginosa* and in the cryptophyte *Cryptomonas ovata*. Photosynth. Res. 111, 173–183. doi:10.1007/s11120-011-9715-4

Lauria, M. Lou, Purdie, D.A., Sharples, J., 1999. Contrasting phytoplankton distributions controlled by tidal turbulence in an estuary. J. Mar. Syst. 21, 189–197.

Lavaud, J., Goss, R., 2014. The peculair features of non-photochemical fluorescence quenching in diatoms and brown algae, in: Demmig-Adams, B., Garab, G., Adams III, W. (Eds.), Non-Photochemical Quenching and Energy Dissipation in Plants, Algae and Cyanobacteria, Advances in Photosynthesis and Respiration. Springer Netherlands, Dordrecht, pp. 421–443. doi:10.1007/978-94-017-9032-1

Lavaud, J., Kroth, P.G., 2006. In diatoms, the transthylakoid proton gradient regulates the photoprotective non-photochemical fluorescence quenching beyond its control on the xanthophyll cycle. Plant Cell Physiol. 47, 1010–1016. doi:10.1093/pcp/pcj058

Lavaud, J., Lepetit, B., 2013. An explanation for the inter-species variability of the photoprotective non-photochemical chlorophyll fluorescence quenching in diatoms. Biochim. Biophys. Acta - Bioenerg. 1827, 294–302. doi:10.1016/j.bbabio.2012.11.012

Lavaud, J., Rousseau, B., Etienne, A., 2004. General features of photoprotection by energy dissipation in planktonic diatoms (Bacillariophyceae). J. Phycol. 40, 130–137. doi:10.1046/j.1529-8817.2004.03026.x

Lavaud, J., Rousseau, B., van Gorkom, H.J., Etienne, A.-L., 2002a. Influence of the diadinoxanthin pool size on photoprotection in the marine planktonic diatom *Phaeodactylum tricornutum*. Plant Physiol. 129, 1398–1406. doi:10.1104/pp.002014

Lavaud, J., Six, C., Campbell, D.A., 2016. Photosystem II repair in marine diatoms with contrasting photophysiologies. Photosynth. Res. 127, 189–199. doi:10.1007/s11120-015-0172-3

Lavaud, J., Strzepek, R.F., Kroth, P.G., 2007. Photoprotection capacity differs among diatoms: Possible consequences on the spatial distribution of diatoms related to fluctuations in the underwater light climate. Limnol. Oceanogr. 52, 1188–1194.

Lavaud, J., van Gorkom, H.J., Etienne, A.-L., 2002b. Photosystem II electron transfer cycle and chlororespiration in planktonic diatoms. Photosynth. Res. 74, 51–59. doi:10.1023/A

Lavergne, J., Trissl, H.W., 1995. Theory of fluorescence induction in photosystem II: derivation of analytical expressions in a model including exciton-radical-pair equilibrium and restricted energy transfer between photosynthetic units. Biophys. J. 68, 2474–92. doi:10.1016/S0006-3495(95)80429-7

Lazier, J.R.N., Mann, K.H., 1989. Turbulence and the diffusive layers around small organisms. Deep. Res. Part I Oceanogr. Res. Pap. 36, 1721–1733.

Lefebvre, S., Mouget, J., Loret, P., Rosa, P., Tremblin, G., 2007. Comparison between fluorimetry and oximetry techniques to measure photosynthesis in the diatom *Skeletonema costatum* cultivated under simulated seasonal conditions. J. Photochem. Photobiol. B Biol. 86, 131–139. doi:10.1016/j.jphotobiol.2006.08.012

Lemos, R.T., Sanso, B., 2006. Spatio-temporal variability of ocean temperature in the Portugal Current System. J. Geophys. Res. Ocean. 111, 1–14. doi:10.1029/2005JC003051

Lepetit, B., Gélin, G., Lepetit, M., Sturm, S., Vugrinec, S., Rogato, A., Kroth, P.G., Falciatore, A., Lavaud, J., 2017. The diatom *Phaeodactylum tricornutum* adjusts nonphotochemical fluorescence quenching capacity in response to dynamic light via fine-tuned Lhcx and xanthophyll cycle pigment synthesis. New Phytol. 214, 205–218. doi:10.1111/nph.14337

Lepetit, B., Goss, R., Jakob, T., Wilhelm, C., 2012. Molecular dynamics of the diatom thylakoid membrane under different light conditions. Photosynth. Res. 111, 245–257. doi:10.1007/s11120-011-9633-5

Leupold, M., Hindersin, S., Gust, G., Kerner, M., Hanelt, D., 2013. Influence of mixing and shear stress on *Chlorella vulgaris*, *Scenedesmus obliquus*, and *Chlamydomonas reinhardtii*. J. Appl. Phycol. 25, 485–495. doi:10.1007/s10811-012-9882-5

Lewis, K.M., Arntsen, A.E., Coupel, P., Joy-Warren, H., Lowry, K.E., Matsuoka, A., Mills, M.M., van Dijken, G.L., Selz, V., Arrigo, K.R., 2018. Photoacclimation of Arctic Ocean phytoplankton to shifting light and nutrient limitation. Limnol. Oceanogr. doi:10.1002/lno.11039

Lewis, M., Cullen, J., Piatt, T., 1984. Relationships between vertical mixing and photoadaptation of phytoplankton: similarity criteria. Mar. Ecol. Prog. Ser. 15, 141–149. doi:10.3354/meps015141

Li, X.-P., Muller-Moule, P., Gilmore, A.M., Niyogi, K.K., 2002. PsbS-dependent enhancement of feedback de-excitation protects photosystem II from photoinhibition. Proc. Natl. Acadamy Sci. USA 99, 15222–15227. doi:10.1073/pnas.232447699

Litaker, W., Duke, C.S., Kenney, B.E., Ramus, J., 1993. Short-term environmental variability and phytoplankton abundance in a shallow tidal estuary. II. Spring and fall. Mar. Ecol. Prog. Ser. 94, 141–154. doi:10.3354/meps094141

Litchman, E., 2003. Competition and coexistence of phytoplankton under fluctuating light: experiments with two cyanobacteria. Aquat. Microb. Ecol. 31, 241–248. doi:10.3354/ame031241

Litchman, E., 2000. Growth rates of phytoplankton under fluctuating light. Freshw. Biol. 44, 223–235.

Litchman, E., 1998. Population and community responses of phytoplankton to fluctuating light. Oecologia 117, 247–257.

Litchman, E., Klausmeier, C.A., Bossard, P., 2004. Phytoplankton nutrient competition under dynamic light regimes. Limnol. Oceanogr. 49, 1457–1462.

Long, S.P., Humphries, S., Falkowski, P.G., 1994. Photoinhibition of photosynthesis in nature. Annu. Rev. Plant Physiol. Plant Mol. Biol. 45, 633–662.

Losh, J.L., Young, J.N., Morel, F.M.M., 2013. Rubisco is a small fraction of total protein in marine phytoplankton. New Phytol. 198, 52–58. doi:10.1111/nph.12143

Lysenko, V., Guo, Y., Chugueva, O., 2016. Cyclic Electron Transport Around Photosystem II: Mechanisms and Methods of Study. Am. J. Plant Physiol. 12, 1–9. doi:10.3923/ajpp.2017.1.9

Macintyre, H.L., Cullen, J.J., 1996. Primary production by suspended and benthic microalgae in a turbid estuary: Time-scales of variability in San Antonio Bay, Texas. Mar. Ecol. Prog. Ser. 145, 245–268. doi:10.3354/meps145245

Macintyre, H.L., Kana, T.M., Anning, T., Geider, R.J., 2002. Photoacclimation of photosynthesis irradiance response curves and photosynthetic pigments in microalgae and cyanobacteria. J. Phycol. 38, 17–38.

Macintyre, H.L., Kana, T.M., Geider, R.J., 2000. The effect of water motion on short-term rates of photosynthesis by marine phytoplankton. Trends Plant Sci. 5, 12–17.

Mallin, M.A., Paerl, H.W., 1992. Effects of variable irradiance on phytoplankton productivity in shallow estuaries. Limnol. Oceanogr. 37, 54–62. doi:10.4319/lo.1992.37.1.0054

Markager, S., Warwick, V.F., 2001. Light absorption by phytoplankton: development of a matching parameter for algal photosynthesis under different spectral regimes. J. Plankton Res. 23, 1373–1384. doi:10.1093/plankt/23.12.1373

Marra, J., 1978. Phytoplankton Photosynthetic Response to Vertical Movement in a Mixed Layer. Mar. Biol. 208, 203–208.

Maxwell, D.P., Falk, S., Huner, N.P.A., 1995. Photosystem II Excitation Pressure and Development of Resistance to Photoinhibition (I. Light-Harvesting Complex II Abundance and Zeaxanthin Content in *Chlorella vulgaris*). Plant Physiol. 107, 687–694. doi:10.1104/pp.107.3.687

McKew, B.A., Davey, P., Finch, S.J., Hopkins, J., Lefebvre, S.C., Metodiev, M. V, Oxborough, K., Raines, C.A., Lawson, T., Geider, R.J., 2013. The trade-off between the light-harvesting and photoprotective functions of fucoxanthin-chlorophyll proteins dominates light acclimation in Emiliania huxleyi (clone CCMP 1516). New Phytol. 200, 74–85.

Mejdoul, R., Taqi, M., 2012. The Mean Hourly Global Radiation Prediction Models Investigation in Two Different Climate Regions in Morocco. Int. J. Renew. Energy Res. 2, 608–617.

Melis, A., 1999. Photosystem-II damage and repair cycle in chloroplasts: what modulates the rate of photodamage in vivo? Trends Plant Sci. 4, 130–135.

Melrose, D.C., Oviatt, C.A., O'Reilly, J.E., Berman, M.S., 2006. Comparisons of fast repetition rate fluorescence estimated primary production and14C uptake by phytoplankton. Mar. Ecol. Prog. Ser. 311, 37–46. doi:10.3354/meps311037

Mercado, J.M., Ramírez, T., Cortés, D., Sebastián, M., Reul, A., Bautista, B., 2006. Diurnal changes in the bio-optical properties of the phytoplankton in the Alborán Sea (Mediterranean Sea). Estuar. Coast. Shelf Sci. 69, 459–470. doi:10.1016/j.ecss.2006.05.019

Mills, M.M., Kropuenske, L.R., Dijken, G.L. Van, Alderkamp, A., Berg, G.M., Robinson, D.H., Welschmeyer, N.A., Arrigo, K.R., 2010. Photophysiology in two major southern ocean phytoplankton taxa: Photosynthesis and growth of *Phaeocystis antarctica* (prymnesiophyceae) and *Fragilariopsis cylindrus* (bacillariophyceae) under simulated mixed-layer irradiance. J. Phycol. 46, 1114–1127. doi:10.1111/j.1529-8817.2010.00923.x

Miloslavina, Y., Grouneva, I., Lambrev, P.H., Lepetit, B., Goss, R., Wilhelm, C., Holzwarth, A.R., 2009. Ultrafast fluorescence study on the location and mechanism of non-photochemical quenching in diatoms. Biochim. Biophys. Acta - Bioenerg. 1787, 1189–1197. doi:10.1016/j.bbabio.2009.05.012

Mitchell, J.G., Okubo, A., Fuhrman, J.A., 1985. Microzones surrounding phytoplankton form the basis for a stratified marine microbial ecosystem. Nature 316, 58–59.

Mitrovic, S.M., Howden, C.G., Bowling, L.C., Buckney, R.T., 2003. Unusual allometry between in situ growth of freshwater phytoplankton under static and fluctuating light environments: Possible implications for dominance. J. Plankton Res. 25, 517–526. doi:10.1093/plankt/25.5.517

Moisan, T.A., Mitchell, B.G., 1999. Photophysiological acclimation of *Phaeocystis antarctica* Karsten under light limitation. Limnol. Oceanogr. 44, 247–258. doi:10.4319/lo.1999.44.2.0247

Moore, C.M., Suggett, D.J., Hickman, A.E., Kim, Y.-N., Tweddle, J.F., Sharples, J., Geider, R.J., Holligan, P.M., 2006. Phytoplankton photoacclimation and photoadaptation in response to environmental gradients in a shelf sea. Limnol. Oceanogr. 51, 936–949.

Morel, A., Maritorena, S., 2001. Bio-optical properties of oceanic waters: A reappraisal. J. Geophys. Res. Ocean. 106, 7163–7180. doi:10.1029/2000JC000319

Moreno-Ostos, E., Cruz-Pizarro, L., Basanta, A., George, D.G., 2009. The influence of wind-induced mixing on the vertical distribution of buoyant and sinking phytoplankton species. Aquat. Ecol. 43, 271–284. doi:10.1007/s10452-008-9167-x

Mouget, J., Legendre, L., Noiie, J. De, 1995. Long-term acclimatization of Scenedesmus bicellularis to high- frequency intermittent lighting (100 Hz), II. Photosynthetic pigments , carboxylating enzymes and biochemical composition. J. Plankton Res. 17, 875–890.

Muller, P., Li, X., Niyogi, K.K., 2001. Non-photochemical quenching. A response to excess light energy. Plant Physiol. 125, 1558–1566.

Murata, N., Allakhverdiev, S.I., Nishiyama, Y., 2012. The mechanism of photoinhibition in vivo: Re-evaluation of the roles of catalase, α-tocopherol, non-photochemical quenching, and electron transport. Biochim. Biophys. Acta - Bioenerg. 1817, 1127–1133. doi:10.1016/j.bbabio.2012.02.020

Murata, N., Takahashi, S., Nishiyama, Y., Allakhverdiev, S.I., 2007. Photoinhibition of photosystem II under environmental stress. Biochim. Biophys. Acta 1767, 414–421. doi:10.1016/j.bbabio.2006.11.019

Nawrocki, W.J., Buchert, F., Joliot, P., Rappaport, F., Bailleul, B., Wollman, F.-A., 2018. Chlororespiration controls growth under intermittent light. Plant Physiol. doi:doi:10.1104/pp.18.01213

NDong, C., Anzellotti, D., Ibrahim, R.K., Huner, N.P.A., Sarhan, F., 2003. Daphnetin methylation by a novel O-methyltransferase is associated with cold acclimation and photosystem II excitation pressure in rye. J. Biol. Chem. 278, 6854–6861. doi:10.1074/jbc.M209439200

Nedbal, L., Tichy, V., Xiong, F., Grobbelaar, J.U., 1996. Microscopic green algae and cyanobacteria in high-frequency intermittent light. J. Appl. Phycol. 8, 325–333.

Nelson, D.M., D'Elia, C.F., Guillard, R.R.L., 1979. Growth and competition of the marine diatoms *Phaeodactylum tricornutum* and *Thalassiosira pseudonana*. II. Light limitation. Mar. Biol. 50, 313–318. doi:10.1007/BF00387007

Nelson, N.B., Prézelin, B.B., 1993. Calibration of an integrating sphere for determining the absorption coefficient of scattering suspensions. Appl. Opt. 32, 6710–7. doi:10.1364/AO.32.006710

Nicklisch, A., 1998. Growth and light absorption of some planktonic cyanobacteria, diatoms and Chlorophyceae under simulated natural light fluctuations. J. Plankton Res. 20, 105–119.

Nicklisch, A., Fietz, S., 2001. The influence of light fluctuations on growth and photosynthesis of *Stephanodiscus neoastraea* (diatom) and *Planktothrix agardhii* (cyanobacterium). Arch. fur Hydrobiol. 151, 141–156.

Nicklisch, A., Shatwell, T., Köhler, J., 2008. Analysis and modelling of the interactive effects of temperature and light on phytoplankton growth and relevance for the spring bloom. J. Plankton Res. 30, 75–91. doi:10.1093/plankt/fbm099

Nishino, S., Kikuchi, T., Yamamoto-Kawai, M., Kawaguchi, Y., Hirawake, T., Itoh, M., 2011. Enhancement/reduction of biological pump depends on ocean circulation in the sea-ice reduction regions of the Arctic Ocean. J. Oceanogr. 67, 305–314. doi:10.1007/s10872-011-0030-7

Nishiyama, Y., Allakhverdiev, S.I., Murata, N., 2011. Protein synthesis is the primary target of reactive oxygen species in the photoinhibition of photosystem II. Physiol. Plant. 142, 35–46. doi:10.1111/j.1399-3054.2011.01457.x

Nishiyama, Y., Allakhverdiev, S.I., Murata, N., 2006. A new paradigm for the action of reactive oxygen species in the photoinhibition of photosystem II. Biochim. Biophys. Acta - Bioenerg. 1757, 742–749. doi:10.1016/j.bbabio.2006.05.013

Nixon, P.J., Michoux, F., Yu, J., Boehm, M., Komenda, J., 2010. Recent advances in understanding the assembly and repair of photosystem II. Ann. Bot. 106, 1–16. doi:10.1093/aob/mcq059

Nymark, M., Valle, K.C., Brembu, T., Hancke, K., Winge, P., Andresen, K., Johnsen, G., Bones, A.M., 2009. An integrated analysis of molecular acclimation to high light in the marine diatom *Phaeodactylum tricornutum*. PLoS One 4. doi:10.1371/journal.pone.0007743

O'Brien, K.R., Burford, M.A., Brookes, J.D., 2009. Effects of light history on primary productivity in a phytoplankton community dominated by the toxic cyanobacterium *Cylindrospermopsis raciborskii*. Freshw. Biol. 54, 272–282.

Oelze, M.-L., Kandlbinder, A., Dietz, K.-J., 2008. Redox regulation and overreduction control in the photosynthesizing cell: Complexity in redox regulatory networks. Biochim. Biophys. Acta 1780, 1261–1272.

Ogbonna, J.C., Yada, H., Tanaka, H., 1995. Effect of cell movement by random mixing between the surface and bottom of photobioreactors on algal productivity. J. Ferment. Bioeng. 79, 152–157. doi:10.1016/0922-338X(95)94083-4

Olaizola, M., Roche, J. La, Kolber, Z., Falkowski, P.G., 1994. Non-photochemical fluorescence quenching and the diadinoxanthin cycle in a marine diatom. Photosynth. Res. 41, 357–370. doi:10.1007/BF00023370

Onno Feikema, W., Marosvölgyi, M.A., Lavaud, J., van Gorkom, H.J., 2006. Cyclic electron transfer in photosystem II in the marine diatom *Phaeodactylum tricornutum*. Biochim. Biophys. Acta - Bioenerg. 1757, 829–834. doi:10.1016/j.bbabio.2006.06.003

Oxborough, K., Baker, N.R., 1997. Resolving chlorophyll a fluorescence images of photosynthetic efficiency into photochemical and non-photochemical components – calculation of qP and Fv'/Fm' without measuring Fo'. Photosynth. Res. 54, 135–142.

Parkhill, J.-P., Maillet, G., Cullen, J.J., 2001. Fluorescence-based maximal quantum yield for psii as a diagnostic of nutrient stress. J. Phycol. 37, 517–529.

Passow, U., Carlson, C.A., 2012. The biological pump in a high CO2 world. Mar. Ecol. Prog. Ser. 470, 249–271. doi:10.3354/meps09985

Patsikka, E., Aro, E.-M., Tyystjärvi, E., 1998. Increase in the Quantum Yield of Photoinhibition Contributes to Copper Toxicity in Vivo. Plant Physiol. 117, 619–627. doi:10.1104/pp.117.2.619

Paytan, A., McLaughlin, K., 2007. The oceanic phosphorus cycle. Chem. Rev. 107, 563–576. doi:10.1021/cr0503613

Perutz, M.F., 1989. Mechanisms of cooperativity and allosteric regulation in proteins. Q.

Rev. Biophys. 22, 139–237. doi:10.1017/S0033583500003826

Petrou, K., Doblin, M.A., Ralph, P.J., 2011. Heterogeneity in the photoprotective capacity of three Antarctic diatoms during short-term changes in salinity and temperature. Mar. Biol. 158, 1029–1041. doi:10.1007/s00227-011-1628-4

Platt, T., Gallegos, C.L., Harrison, W.G., 1980. Photoinhibition of photosynthesis in natural assemblages of marine phytoplankton. J. Mar. Res. 38, 103–111.

Poll, W.H. Van De, Visser, R.J.W., Buma, A.G.J., 2007. Acclimation to a dynamic irradiance excessive irradiance of regime changes sensitivity Emiliania and Thalassiosira huxleyi weissflogii. Limnol. Oceanogr. 52, 1430–1438.

Pospíšil, P., 2009. Production of reactive oxygen species by photosystem II. Biochim. Biophys. Acta - Bioenerg. 1787, 1151–1160. doi:10.1016/j.bbabio.2009.05.005

Poulin, C., Antoine, D., Huot, Y., 2018. Diurnal variations of the optical properties of phytoplankton in a laboratory experiment and their implication for using inherent optical properties to measure biomass. Opt. Express 26, 711. doi:10.1364/OE.26.000711

Prezelin, B.B., 1992. Diel periodicity in phytoplankton productivity. Hydrobiologia 238, 1–35. doi:10.1007/BF00048771

Ragni, M., Airs, R.L., Hennige, S., Suggett, D.J., Warner, M.E., Geider, R.J., 2010. PSII photoinhibition and photorepair in *Symbiodinium* (Pyrrhophyta) differs between thermally tolerant and sensitive phylotypes. Mar. Ecol. Prog. Ser. 406, 57–70. doi:10.3354/meps08571

Ragni, M., Airs, R.L., Leonardos, N., Geider, R.J., 2008. Photoinhibition of PSII in *Emiliania huxleyi* (Haptophyta) under high light stress: The roles of photoacclimation, photoprotection, and photorepair. J. Phycol. 44, 670–683. doi:10.1111/j.1529-8817.2008.00524.x

Rascher, U., Nedbal, L., 2006. Dynamics of photosynthesis in fluctuating light. Curr. Opin. Plant Biol. 9, 671–678.

Raven, J.A., 2011. The cost of photoinhibition. Physiol. Plant. 142, 87–104. doi:10.1111/j.1399-3054.2011.01465.x

Raven, J.A., Geider, R.J., 2003. Adaptation, acclimation and regulation in algal photosynthesis., in: Raven, J.A., Larkum, A.W.D., Douglas, S.E. (Eds.), Photosynthesis of Algae. Dordrecht, pp. 385–412.

Riebesell, U., Schulz, K.G., Bellerby, R.G.J., Botros, M., Fritsche, P., Meyerhöfer, M., Neill, C., Nondal, G., Oschlies, A., Wohlers, J., Zöllner, E., 2007. Enhanced biological carbon consumption in a high CO2 ocean. Nature 450, 545–548. doi:10.1038/nature06267

Ritchie, R.J., 2006. Consistent sets of spectrophotometric chlorophyll equations for acetone, methanol and ethanol solvents. Photosynth. Res. 89, 27–41. doi:10.1007/s11120-006-9065-9

Roháček, K., Bertrand, M., Moreau, B., Jacquette, B., Caplat, C., Morant-Manceau, A., Schoefs, B., 2014. Relaxation of the non-photochemical chlorophyll fluorescence quenching in diatoms: Kinetics, components and mechanisms. Philos. Trans. R. Soc. B Biol. Sci. 369. doi:10.1098/rstb.2013.0241

Ross, O.N., Geider, R.J., Piera, J., 2011. Modelling the effect of vertical mixing on bottle incubations for determining in situ phytoplankton dynamics. II. Primary production. Mar. Ecol. Prog. Ser. 435, 33–45. doi:10.3354/meps09194

Ross, O.N., Sharples, J., 2007. Phytoplankton motility and the competition for nutrients in the thermocline. Mar. Ecol. Prog. Ser. 347, 21–38. doi:10.3354/meps06999

Ross, O.N., Sharples, J., 2004. Recipe for 1-D Lagrangian particle tracking models in space-varying diffusivity. Limnol. Oceanogr. Methods 2, 289–302.

Ruban, A. V, Lavaud, J., Rousseau, B., Guglielmi, G., Horton, P., Etienne, A.-L., 2004. The super-excess energy dissipation in diatom algae: comparative analysis with higher plants. Photosynth. Res. 82, 165–175.

Saba, V.S., Griffies, S.M., Anderson, W.G., Winton, M., Alexander, M.A., Delworth, T.L., Hare, J.A., Harrison, M.J., Rosati, A., Vecchi, G.A., Zhang, R., 2016. Enhanced warming of the Northwest Atlantic Ocean under climate change. J. Geophys. Res. Ocean. 121, 118–132. doi:10.1002/2015JC011346.Received

Sagert, S., Forster, R.M., Feuerpfeil, P., Schubert, H., 1997. Daily course of photosynthesis and photoinhibition in *chondrus crispus* (rhodophyta) from different shore levels. Eur. J. Phycol. 32, 363–371. doi:10.1080/09670269710001737299

Schloss, I.R., Ferreyra, G.A., 2002. Primary production, light and vertical mixing in Potter Cove, a shallow bay in the maritime Antarctic. Polar Biol. 25, 41–48. doi:10.1007/s003000100309

Schonknecht, G., Neimanis, S., Katona, E., Gerst, U., Heber, U., 1995. Relationship between photosynthetic electron transport and pH gradient across the thylakoid membrane in intact leaves. Proc. Natl. Acadamy Sci. USA 92, 12185–12189. doi:10.1073/pnas.92.26.12185

Schuback, N., Flecken, M., Maldonado, M.T., Tortell, P.D., 2016. Diurnal variation in the coupling of photosynthetic electron transport and carbon fixation in iron-limited phytoplankton in the NE subarctic Pacific. Biogeosciences 13, 1019–1035. doi:10.5194/bg-13-1019-2016

Schwaderer, A.S., Yoshiyama, K., De Tezanos Pinto, P., Swenson, N.G., Klausmeier, C.A., Litchman, E., 2011. Eco-evolutionary differences in light utilization traits and distributions of freshwater phytoplankton. Limnol. Oceanogr. 56, 589–598. doi:10.4319/lo.2011.56.2.0589

Serôdio, J., Lavaud, J., 2011. A model for describing the light response of the nonphotochemical quenching of chlorophyll fluorescence. Photosynth. Res. 108, 61–76. doi:10.1007/s11120-011-9654-0

Sharp, J.H., Underhill, P.A., Hughes, D.J., 1979. Interaction (Allelopathy) Between Marine Diatoms: *Thalassiosira Pseudonana* and *Phaeodactylum tricornutum*. J. Phycol. doi:10.1111/j.1529-8817.1979.tb00705.x

Shatwell, T., Nicklisch, A., Köhler, J., 2012. Temperature and photoperiod effects on phytoplankton growing under simulated mixed layer light fluctuations. Limnol. Oceanogr. 57, 541–553. doi:10.4319/lo.2012.57.2.0541

Siegel, D.A., Behrenfeld, M.J., Maritorena, S., McClain, C.R., Antoine, D., Bailey, S.W., Bontempi, P.S., Boss, E.S., Dierssen, H.M., Doney, S.C., Eplee, R.E., Evans, R.H., Feldman, G.C., Fields, E., Franz, B.A., Kuring, N.A., Mengelt, C., Nelson, N.B., Patt, F.S., Robinson, W.D., Sarmiento, J.L., Swan, C.M., Werdell, P.J., Westberry, T.K., Wilding, J.G., Yoder, J.A., 2013. Regional to global assessments of phytoplankton dynamics from the SeaWiFS mission. Remote Sens. Environ. 135, 77–91. doi:10.1016/j.rse.2013.03.025

Six, C., Finkel, Z. V., Irwin, A.J., Campbell, D.A., 2007. Light variability illuminates niche-partitioning among marine picocyanobacteria. PLoS One 2. doi:10.1371/journal.pone.0001341

Six, C., Finkel, Z. V., Rodriguez, F., Marie, D., Partensky, F., Campbell, D.A., 2008. Contrasting photoacclimation costs in ecotypes of the marine eukaryotic picoplankter *Ostreococcus*. Limnol. Oceanogr. 53, 255–265. doi:10.4319/lo.2008.53.1.0255

Sobczuk, T.M., Camacho, F.G., Grima, E.M., Chisti, Y., 2006. Effects of agitation on the microalgae *Phaeodactylum tricornutum* and *Porphyridium cruentum*. Bioprocess Biosyst. Eng. 28, 243–250. doi:10.1007/s00449-005-0030-3

Sobrino, C., Ward, M.L., Neale, P.J., 2008. Acclimation to elevated carbon dioxide and ultraviolet radiation in the diatom 53, 1–49.

Soitamo, A., Havurinne, V., Tyystjärvi, E., 2017. Photoinhibition in marine picocyanobacteria. Physiol. Plant. 161, 97–108. doi:10.1111/ppl.12571

Staehr, P.A., Sand-Jensen, K.A.J., 2006. Seasonal changes in temperature and nutrient

control of photosynthesis, respiration and growth of natural phytoplankton communities. Freshw. Biol. 51, 249–262.

Stomp, M., van Dijk, M.A., van Overzee, H.M.J., Wortel, M.T., Sigon, C.A.M., Egas, M., Hoogveld, H., Gons, H.J., Huisman, J., 2008. The Timescale of Phenotypic Plasticity and Its Impact on Competition in Fluctuating Environments. Am. Nat. 172, E169–E185. doi:10.1086/591680

Stramska, M., Dickey, T.D., 1998. Short-term variability of the underwater light field in the oligotrophic ocean in response to surface waves and clouds. Deep. Res. Part I Oceanogr. Res. Pap. 45, 1393–1410. doi:10.1016/S0967-0637(98)00020-X

Stramski, D., Legendre, L., 1992. Laboratory simulation of light-focussing by water-surface waves. Mar. Biol. 114, 341–348.

Stramski, D., Piskozub, J., 2003. Estimation of scattering error in spectrophotometric measurements of light absorption by aquatic particles from three-dimensional radiative transfer simulations. Appl. Opt. 42, 3634–3646. doi:10.1364/AO.42.003634

Stramski, D., Rosenberg, G., Legendre, L., 1993. Photosynthetic and optical properties of the marine chlorophyte *Dunaliella tertiolecta* grown under fluctuating light caused by surface-wave focussing. Mar. Biol. 115, 363–372.

Su, W., Jakob, T., Wilhelm, C., 2012. The impact of nonphotochemical quenching of fluorescence on the photon balance in diatoms under dynamic light conditions. J. Phycol. 48, 336–346. doi:10.1111/j.1529-8817.2012.01128.x

Suggett, D.J., Le Floc'H, E., Harris, G.N., Leonardos, N., Geider, R.J., 2007. Different strategies of photoacclimation by two strains of *Emiliania huxleyi* (Haptophyta). J. Phycol. 43, 1209–1222. doi:10.1111/j.1529-8817.2007.00406.x

Suggett, D.J., Macintyre, H.L., Geider, R.J., 2004. Evaluation of biophysical and optical determinations of light absorption by photosystem II in phytoplankton. Limnol. Oceanogr. Methods 2, 316–332.

Suggett, D.J., Macintyre, H.L., Kana, T.M., Geider, R.J., 2009. Comparing electron transport with gas exchange: Parameterising exchange rates between alternative photosynthetic currencies for eukaryotic phytoplankton. Aquat. Microb. Ecol. 56, 147–162. doi:10.3354/ame01303

Suggett, D.J., Moore, C.M., Geider, R.J., 2010. Estimating aquatic productivity from active fluorescence measurements, in: Chlorophyll a Fluorescence in Aquatic Sciences: Methods and Applications. Springer, Dordrecht, pp. 103–127.

Suggett, D.J., Oxborough, K., Baker, N.R., MacIntyre, H.L., Kana, T.M., Geider, R.J., 2003. Fast repetition rate and pulse amplitude modulation chlorophyll a fluorescence measurements for assessment of photosynthetic electron transport in marine phytoplankton. Eur. J. Phycol. 38, 371–384. doi:10.1080/0967026031000161265 5

Takahashi, F., Yamagata, D., Ishikawa, M., Fukamatsu, Y., Ogura, Y., Kasahara, M., Kiyosue, T., Kikuyama, M., Wada, M., Kataoka, H., 2007. AUREOCHROME, a photoreceptor required for photomorphogenesis in stramenopiles. Proc. Natl. Acadamy Sci. USA 104, 19625–19630. doi:10.1073/pnas.0707692104

Takahashi, S., Badger, M.R., 2011. Photoprotection in plants: A new light on photosystem II damage. Trends Plant Sci. 16, 53–60. doi:10.1016/j.tplants.2010.10.001

Takahashi, S., Murata, N., 2008. How do environmental stresses accelerate photoinhibition? Trends Plant Sci. 13, 178–182. doi:10.1016/j.tplants.2008.01.005

Talmy, D., Blackford, J., Hardman-Mountford, N.J., Dumbrell, A.J., Geider, R.J., 2013. An optimality model of photoadaptation in contrasting aquatic light regimes. Limnol. Oceanogr. 58, 1802–1818. doi:10.4319/lo.2013.58.5.0000

Tamburic, B., Guruprasad, S., Radford, D.T., Szabó, M., Lilley, R.M.C., Larkum, A.W.D., Franklin, J.B., Kramer, D.M., Blackburn, S.I., Raven, J.A., Schliep, M., Ralph, P.J., 2014. The effect of diel temperature and light cycles on the growth of *Nannochloropsis oculata* in a photobioreactor matrix. PLoS One 9. doi:10.1371/journal.pone.0086047

Thomas, W.H., Gibson, C.H., 1990. Effects of small-scale turbulence on microalgae. J. Appl. Phycol. 2, 71–77. doi:10.1007/BF02179771

Tikkanen, M., Nurmi, M., Kangasjärvi, S., Aro, E.-M., 2008. Core protein phosphorylation facilitates the repair of photodamaged photosystem II at high light. Biochim. Biophys. Acta - Bioenerg. 1777, 1432–1437. doi:10.1016/j.bbabio.2008.08.004

Tilstone, G., Smyth, T., Poulton, A., Hutson, R., 2009. Measured and remotely sensed estimates of primary production in the Atlantic Ocean from 1998 to 2005. Deep Sea Res. Part II Top. Stud. Oceanogr. 56, 918–930. doi:10.1016/j.dsr2.2008.10.034

Ting, C.S., Owens, T.G., 1994. The effects of excess irradiance on photosynthesis in the marine diatom (*Phaeodactylum tricornutum*). Plant Physiol. 106, 763–770.

Trissl, H.W., 2002. Theory of Fluorescence Induction: An introduction.

Tyystjärvi, E., 2008. Photoinhibition of Photosystem II and photodamage of the oxygen evolving manganese cluster. Coord. Chem. Rev. 252, 361–376. doi:10.1016/j.ccr.2007.08.021

Tyystjärvi, E., Maenpaa, P., Aro, E.-M., 1994. Mathematical modelling of photoinhibition and Photosystem II repair cycle. I. Photoinhibition and D1 protein degradation in vitro and in the absence of chloroplast protein synthesis in vivo. Photosynth. Res. 41, 439–449.

Uitz, J., Claustre, H., Gentili, B., Stramski, D., 2010. Phytoplankton class-specific primary production in the world's oceans: Seasonal and interannual variability from satellite observations. Global Biogeochem. Cycles 24, 1–19. doi:10.1029/2009GB003680

van de Poll, W.H., Buma, A.G.J., 2009. Does ultraviolet radiation affect the xanthophyll cycle in marine phytoplankton? Photochem. Photobiol. Sci. 8, 1295–1301. doi:10.1039/b904501e

van de Poll, W.H., Buma, A.G.J., Visser, R.J.W., Janknegt, P.J., Villafane, V.E., Helbing, E.W., 2010. Xanthophyll cycle activity and photosynthesis of *Dunaliella tertiolecta* (Chlorophyceae) and *Thalassiosira weissflogii* (Bacillariophyceae) during fluctuating solar radiation. Phycologia 49, 249–259. doi:10.2216/08-83.1

van de Poll, W.H., Lagunas, M., de Vries, T., Visser, R.J.W., Buma, A.G.J., 2011. Non-photochemical quenching of chlorophyll fluorescence and xanthophyll cycle responses after excess PAR and UVR in *Chaetoceros brevis*, *Phaeocystis antarctica* and coastal Antarctic phytoplankton. Mar. Ecol. Prog. Ser. 426, 119–131. doi:10.3354/meps09000

van Leeuwe, M.A., Van Sikkelerus, B., Gieskes, W.W.C., Stefels, J., 2005. Taxon-specific differences in photoacclimation to fluctuating irradiance in an Antarctic diatom and a green flagellate. Mar. Ecol. Prog. Ser. 288, 9–19.

van Thor, J.J., Mullineaux, C.W., Matthijs, H.C.P., Hellingwerf, K.J., 1998. Light harvesting and state transitions in cyanobacteria. Bot. Acta 111, 430–443. doi:10.1111/j.1438-8677.1998.tb00731.x

Vass, I., 2011. Role of charge recombination processes in photodamage and photoprotection of the photosystem II complex. Physiol. Plant. 142, 6–16. doi:10.1111/j.1399-3054.2011.01454.x

Vass, I., Aro, E.-M., 2007. Photoinhibition of photosynthetic electron transport, in: Renger, G. (Ed.), Primary Processes of Photosynthesis: Principles and Apparatus, Part 1. The Royal Society of Chemistry, Cambridge, pp. 393–425.

Vass, I., Styring, S., Hundal, T., Koivuniemi, A., Aro, E.-M., Andersson, B., 1992. Reversible and irreversible intermediates during photoinhibition of photosystem II: Stable reduced QA species promote chlorophyll triplet formation. Proc. Natl. Acadamy Sci. USA 89, 1408–1412.

Veal, C.J., Carmi, M., Dishon, G., Sharon, Y., Michael, K., Tchernov, D., Hoegh-Guldberg, O., Fine, M., 2010. Shallow-water wave lensing in coral reefs: a physical and biological case study. J. Exp. Biol. 213, 4304–4312. doi:10.1242/jeb.044941

Wagner, H., Jakob, T., Lavaud, J., Wilhelm, C., 2016. Photosystem II cycle activity and alternative electron transport in the diatom *Phaeodactylum tricornutum* under dynamic light conditions and nitrogen limitation. Photosynth. Res. 128, 151–161. doi:10.1007/s11120-015-0209-7

Wagner, H., Jakob, T., Wilhelm, C., 2006. Balancing the energy flow from captured light to biomass under fluctuating light conditions. New Phytol. 169, 95–108.

Walsby, A.E., Dubinsky, Z., Kromkamp, J.C., Lehmann, C., Schanz, F., 2001. The effects of diel changes in photosynthetic coefficients and depth of 63, 326–349.

Westberry, T., Behrenfeld, M.J., Siegel, D.A., Boss, E., 2008. Carbon-based primary productivity modeling with vertically resolved photoacclimation. Global Biogeochem. Cycles 22, 1–18. doi:10.1029/2007GB003078

Whitney, F.A., 2011. Nutrient variability in the mixed layer of the subarctic Pacific Ocean, 1987–2010. J. Oceanogr. 67, 481.

Wilhelm, C., Jakob, T., 2011. From photons to biomass and biofuels: Evaluation of different strategies for the improvement of algal biotechnology based on comparative energy balances. Appl. Microbiol. Biotechnol. 92, 909–919. doi:10.1007/s00253-011-3627-2

Williams, P.J.B., Heinmann, K.R., Mara, J., Purdie, D.A., 1983. Comparison of 14C and O2 measurements of phytoplankton production in oligotrophic waters. Nature 305, 49–50.

Wu, H., Roy, S., Alami, M., Green, B.R., Campbell, D.A., 2012. Photosystem II photoinactivation, repair, and protection in marine centric diatoms. Plant Physiol. 160, 464–76. doi:10.1104/pp.112.203067

Wu, X., Kong, F., Zhang, M., 2011. Photoinhibition of colonial and unicellular *Microcystis* cells in a summer bloom in Lake Taihu. Limnology 12, 55–61. doi:10.1007/s10201-010-0321-5

Wu, Y., Campbell, D.A., Irwin, A.J., Suggett, D.J., Finkel, Z. V., 2014. Ocean acidification enhances the growth rate of larger diatoms. Limnol. Oceanogr. 59, 1027–1034. doi:10.4319/lo.2014.59.3.1027

Xing, T., Gao, K., Beardall, J., 2015. Response of growth and photosynthesis of *Emiliania huxleyi* to visible and UV irradiances under different light regimes. Photochem. Photobiol. 91, 343–349. doi:10.1111/php.12403

Xu, X., Liu, J., Shi, Q., Mei, H., Zhao, Y., Wu, H., 2016. Ocean warming alters photosynthetic responses of diatom *Phaeodactylum tricornutum* to fluctuating irradiance. Phycologia 55, 126–133. doi:10.2216/15-64.1

Yarnold, J., Ross, I.L., Hankamer, B., 2015. Photoacclimation and productivity of *Chlamydomonas reinhardtii* grown in fluctuating light regimes which simulate outdoor algal culture conditions. Algal Res. 13, 182–194. doi:10.1016/j.algal.2015.11.001

Yoshikawa, T., Furuya, K., 2006. Effects of diurnal variations in phytoplankton photosynthesis obtained from natural fluorescence. Mar. Biol. 150, 299–311. doi:10.1007/s00227-006-0331-3

Yue, D., Peng, Y., Qian, X., Xiao, L., 2014. Spatial and seasonal patterns of size-fractionated phytoplankton growth in Lake Taihu. J. Plankton Res. 36, 709–721. doi:10.1093/plankt/fbt131

Zhang, M., Kong, F., Wu, X., Xing, P., 2008. Different photochemical responses of phytoplankters from the large shallow Taihu Lake of subtropical China in relation to light and mixing. Hydrobiologia 603, 267–278. doi:10.1007/s10750-008-9277-4

Zhu, S.H., Green, B.R., 2010. Photoprotection in the diatom *Thalassiosira pseudonana*: Role of LI818-like proteins in response to high light stress. Biochim. Biophys. Acta - Bioenerg. 1797, 1449–1457. doi:10.1016/j.bbabio.2010.04.003